



City Research Online

City, University of London Institutional Repository

Citation: Gebremichael, Y. (2000). Highly Birefringent Fibre Based Polarisation Modulated Ellipsometry and Sensor Applications. (Unpublished Doctoral thesis, City, University of London)

This is the accepted version of the paper.

This version of the publication may differ from the final published version.

Permanent repository link: <https://openaccess.city.ac.uk/id/eprint/30898/>

Link to published version:

Copyright: City Research Online aims to make research outputs of City, University of London available to a wider audience. Copyright and Moral Rights remain with the author(s) and/or copyright holders. URLs from City Research Online may be freely distributed and linked to.

Reuse: Copies of full items can be used for personal research or study, educational, or not-for-profit purposes without prior permission or charge. Provided that the authors, title and full bibliographic details are credited, a hyperlink and/or URL is given for the original metadata page and the content is not changed in any way.

City Research Online:

<http://openaccess.city.ac.uk/>

publications@city.ac.uk

Highly Birefringent Fibre based Polarisation Modulated Ellipsometry and Sensor Applications

By

Yonas Meressi Gebremichael

A thesis submitted for the degree of
Doctor of Philosophy

City University

Department of Electrical, Electronic and information Engineering

December 2000

Table of contents.....	i
List of figures and tables.....	vi
Acknowledgements.....	x
Declaration.....	xi
Abstract.....	xii

Chapter 1

Introduction to optics and Sensor Technology

1.0 Introduction.....	1
1.1 Polarised light as a measuring tool.....	4
1.2 Aims and objectives.....	4
1.3 Thesis structure.....	5
Reference.....	7

Chapter 2

Electromagnetic Waves: Theory of Polarisation and Ellipsometry

Abstract.....	8
2.0 Introduction.....	9
2.1 Polarisation of light.....	10
2.2 Ellipsometry.....	12
2.3 Mathematical description of polarised light.....	13
2.4 Interaction of light with matter.....	16
2.4.1 Reflection by ambient-substrate boundary system.....	17
2.4.2 Reflection by ambient-film-substrate system.....	20
2.5 Summary.....	23
Reference.....	24

Chapter 3

History of Ellipsometry and polarisation control

Abstract.....	26
3.0 Introduction.....	27
3.1 Instrumentation and optical elements.....	27
3.1.1 Linear polariser.....	28
3.1.2 Retarder.....	28
3.1.3 Optical sample.....	29
3.1.4 Analyser.....	29
3.1.5 Light source.....	29
3.1.6 Photodetector.....	29
3.2 Null ellipsometer.....	30
3.3 Automated ellipsometers.....	31
3.3.1 Automatic null instruments.....	32
3.3.2 Automatic photometric ellipsometers.....	34
3.3.2.1 The rotating analyser ellipsometer.....	34
3.3.2.2 Polarisation modulated ellipsometry	34
3.4 The future of ellipsometry.....	37
3.5 The need for an all fibre ellipsometer.....	37
3.6 Polarisation state control and polarisation modulation.....	38
3.7 Polarisation maintaining behaviour in single mode fibres.....	39
3.8 Summary.....	43
Reference.....	44

Chapter 4

HiBi Fibre polarisation modulated ellipsometry

Abstract.....	46
4.0 Introduction.....	47

4.1 Experimental configuration.....	48
4.2 Mathematical analysis and measurement technique	49
4.3 The PCMCSA arrangement.....	49
4.4 experimental analysis of the PCMCSA system.....	54
4.4.1 Calibration.....	54
4.4.2 Azimuthal alignment.....	55
4.4.3 Signal analysis.....	56
4.5 Ellipsometric parameters and system calibration.....	61
4.6 Determination of optical parameters of samples with a HiBi PME.....	63
4.6.1 Two phase system.....	64
4.6.2 Experimental results.....	65
4.6.2.1 Non absorbing sample: Air-glass interface.....	65
4.6.2.2 Absorbing ample: Air-silver interface.....	67
4.7 Summary.....	69
Reference.....	70

Chapter 5

Ellipsometer for following dynamic film growth and sensor applications

Abstract.....	71
5.0 Introduction.....	72
5.1 Sol-gel based thin film measurement.....	73
5.1.1 Experimental condition.....	73
5.1.1.1 Film preparation.....	73
5.1.1.2 ψ and Δ measurement.....	74
5.2 Thin film based sensor system.....	76
5.2.1 Temperature effects.....	77
5.2.2 Humidity effects.....	79
5.3 Dynamic oil film thickness measurements.....	81

5.3.1 experimental configuration.....	82
5.3.2 Results and discussion.....	83
5.4 Summary.....	87
Reference.....	89

Chapter 6

Sources of errors in PME

Abstract.....	91
6.0 Introduction.....	92
6.1 Azimuth angle errors.....	94
6.1.1 Polariser misalignment.....	95
6.1.2 Analyser misalignment.....	96
6.2 Quarter wave plates: component imperfection and azimuthal misalignment.....	98
6.2.1 Azimuth errors.....	98
6.2.2 Component imperfection.....	101
6.3 Other sources of errors.....	104
6.4 Summary.....	105
Reference.....	107

Chapter 7

A High Birefringence fibre polarisation modulated scheme:

A new configuration for ellipsometric measurements

Abstract.....	108
7.0 Introduction.....	109
7.1 Theoretical analysis.....	113
7.2 Experimental alignment procedure.....	116
7.3 Theoretical analysis and calibration.....	118
7.4 Lock-in phase bias control and feedback compensation.....	120

7.5 Measurement technique.....	126
7.6 Signal processing.....	127
7.7 System performance and calibration.....	129
7.8 Measurement results.....	131
7.8.1 ψ and Δ measurements on a two phase system.....	131
7.8.2 ψ and Δ measurements on a three phase system.....	133
7.9 Summary.....	135
Reference.....	136

Chapter 8

Conclusions and future work

8.0 Summary of achievements.....	138
8.1 Future work.....	142
Reference.....	145
Appendix A.....	146
Appendix B.....	147
List of publications.....	149

List of Figures and Tables

- Figure 2.1: Examples of polarised light.
- Figure 2.2: The principle of reflection ellipsometry.
- Figure 2.3: Elliptical light.
- Figure 2.4: Incident and transmitted polarisation states at the input and output of a polarising element, M.
- Figure 2.5: Reflection and refraction of light at a boundary between two media.
- Figure 2.6: Reflection and transmission of a plane wave by an ambient-film-substrate system. Where d , is the film thickness, ϕ_0 is the angle of incidence at the ambient-film boundary, ϕ_1 and ϕ_2 are angles of refraction at the film and substrate interface.
- Figure 3.1: Basic ellipsometric set up. P is linear polariser, R is a retarder, A is analyser and S is a sample.
- Figure 3.2: Schematic diagram of a null ellipsometer. L, Light source; P, polariser; C, compensator; S, sample; A, analyser; PD photo-detector.
- Figure 3.3: Schematic Classification of Automatic ellipsometers. (after Azzam et al. 1977).
- Figure 3.4: Examples of polarisation preserving fibre core structures.
- Figure 3.5: Polarisation state azimuth control using a single highly birefringent monomode fibre. L, Ar⁺ laser; PZT piezo electric transducer; F, HiBi fibre; $\lambda/4$, QWP. (After Tatam et al. 1986).
- Figure 4.1: Experimental configuration of the ellipsometer. A helium neon laser, HeNe, a linear polarizer, P, QWP, Q, HiBi fibre, HB, fibre stretcher, M, signal generator, OS, glass reflector, GS, sample, S, linear analyzer, A and a photodetector, PD.
- Figure 4.2: Periodic polarisation evolution of the light beam at the output of the fibre.
- Figure 4.4: Shows signal fringes, where ‘_’ is the detection signal and ‘...’, is the reference signal.

- Figure 4.4: Illustrating the beat pattern and high frequency fluctuation resulting from coherent interference of the main signal and back reflection signal.
- Figure 4.5: detected signal with high frequency components from a fibre cut at 90° end face.
- Figure 4.6: Illustrating the reduction of high frequency components after the fibre end is cut at an angle.
- Figure 4.7: Illustrating the effect of beat pattern resulting from back reflection. The simulated data shows that the amplitudes of the fringes on either side of the turning point are unequal.
- Figure 4.8: Repeatability in the measurement of ψ and Δ over time.
- Figure 4.9: Two phase system.
- Figure 4.10: ψ and $\cos(\Delta)$ measurements for a Bk7 glass sample.
- Figure 4.11: Measurement of ψ for an air/silver interface at various angles of incidence.
- Figure 4.12: Measurement of Δ for an air/silver interface at various angles of incidence.
- Figure 5.1: ψ Measurements of three sol-gel films of different thickness on silica substrate at various angles of incidence.
- Figure 5.2: Δ Measurements of three sol-gel films of different thickness on silica substrate at various angles of incidence.
- Figure 5.3: Variation of, ψ of the thin film on exposure to temperatures up to 90° over a period of 1 minute.
- Figure 5.4: Variation of, Δ of the thin film on exposure to temperatures up to 90° over a period of 1 minute.
- Figure 5.5: Variation of ψ , as the sol-gel film is exposed to humidity.
- Figure 5.6: Variation of $\cos(\Delta)$, as the sol-gel film is exposed to humidity.
- Figure 5.7: Experimental set up of the Hi-Bi ellipsometer. P, polarizing prism, Q, quarter wave plate, L, Lens, M, fibre stretcher, HiBi, birefringent fibre, GS, glass, A_r and A_a , analyzers, S, sample, PD, photodetector.
- Figure 5.8: variation of ψ with time as the oil spreads on water surface. The oil sample here is MOBIL lubricant oil.

- Figure 5.9: variation of $\cos(\Delta)$ with time as the oil spreads on water surface. The oil sample here is MOBIL lubricant oil.
- Figure 5.10: Variation of Δ with the spread of transmission oil film, as the oil film thickness varies with time. Smooth curve is measured data Δ_m . Dotted curve is calculated, Δ_c data.
- Figure 5.11: Variation of ψ with the spread of transmission oil film, as the oil film thickness varies with time. Smooth curve is measured data ψ_m . Dotted curve is calculated, ψ_c data.
- Figure 6.1: The PCMCSA arrangement. Where all the components are labelled as described before.
- Table 6.1: Ideal component specification and alignment. Where P is the polariser, QWP1 and QWP2 are quarter wave plates, M is the modulator. A_a and A_r are analysers and S is a sample.
- Figure 6.2: ψ and Δ errors resulting from a small azimuthal error on the polariser, P, at the input of the fibre.
- Figure 6.3: ψ and Δ errors resulting from a small azimuthal error on the analyser, A_a , at the detection arm.
- Figure 6.4: ψ and Δ errors resulting from a small azimuthal error on the analyser, A_r , at the reference arm.
- Figure 6.5: Ellipticity resulting from a small azimuthal error on the QWP at the input of the fibre.
- Figure 6.6: ψ and Δ errors resulting from a small azimuthal error on the QWP at the input of the fibre.
- Figure 6.7: Ellipticity resulting from a small azimuthal error on the QWP at the output of the fibre.
- Figure 6.8: ψ and Δ errors resulting from a small azimuthal error on the QWP at the output of the fibre.
- Figure 6.9: Ellipticity resulting from retardance error of an imperfect QWP at the input of the fibre.
- Figure 6.10: Ellipticity resulting from retardance error of an imperfect QWP at the output of the fibre.
- Figure 6.11: Δ errors introduced by an imperfect QWP at the input of the fibre with various retardance tolerance levels.

- Figure 7.1: The PMSA experimental configuration with no QWPs. P_{45} , A_{45} : polarisers at 45° respect to the fibre eigen axis; L, lens.
- Figure 7.2: Experimental configuration of the ellipsometer. A helium neon laser, He-Ne, a linear polariser, P, HiBi fibre, HB, fibre stretcher, M, phase compensator, PC, signal generator, OS, lock-in detection, LD, glass reflector, GS, sample, S and linear analyser, A.
- Figure 7.3: A free running interferometric signal and a dc error signal.
- Figure 7.4: A stabilised interferometric signal with a 0V dc error signal.
- Figure 7.5: Experimental configuration of a HiBi fibre based ellipsometer with no quarter wave plate. P_{45} , A_{45} , are polarisers at 45° to the fibre eigen axes, M is a fibre modulator, S is a sample and PD is a photodiode.
- Figure 7.6: Repeatability of Δ and ψ measurements taken over a period of 20 days.
- Figure 7.7: Ellipsometric angles, ψ and Δ as functions of incidence angles for reflection at an air/glass interface.
- Figure 7.8: Ellipsometric angles, ψ and Δ as functions of incidence angles for reflection at an air/silicon interface.
- Figure 7.9: ψ Measurements of three sol-gel films on silica substrate with various thickness at various angles of incidence.
- Figure 7.10: Δ Measurements of three sol-gel films on silica substrate with various thickness at various angles of incidence.

Acknowledgements

Grateful acknowledgement is made to my supervisors Professors A.W. Palmer and K.T.V. Grattan for their supervision and in particular professor Grattan for his reviewing my publications.

The author would also like to thank Dr. K. Weir (Imperial college, London) for his helpful discussions in the early part of the work.

Recognition must also be made to my colleague G. Tedeschi for his involvement in the final stages of the work and putting up with me in the dark labs for long hours. I would also like to express my appreciation to the entire research students and staff in the Optical Measurement Instrumentation group, secretaries and technicians in the department, in particular Mr. R. Valsler for his help in making optical and mechanical accessories needed during the entire period of the work.

I'm also grateful for the financial support provided by Engineering and Physical Sciences Research Council.

Most of all, my deepest gratitude is dedicated to my dad, mum, brothers and sisters for their unconditional guidance love and support.

Declaration

The Author hereby grants power of discretion to the University Librarian to allow the thesis to be copied in whole or in part with out further reference to the author. This permission covers single copies made for study purposes, subject to normal conditions of acknowledgement.

Abstract

This work discusses polarisation modulated HiBi fibre based ellipsometry. The polarisation of light is discussed with mathematical representation of polarised light and propagation of polarised light through optical components. Such mathematical representation allows convenient analysis of the interaction of light with matter.

The history and evolution ellipsometry as a measuring tool through various optical configurations is reviewed. This gives an insight in to the existing ellipsometric configurations and point out important features such as operation procedure, type of modulation, resolution and speed of measurement, optical components used and application limitations etc. The review concludes polarisation modulation as being an obvious choice for fast real time ellipsometric applications.

High birefringent (HiBi) fibre based polarisation modulated ellipsometry is discussed in which rotating polarisation is generated by stretching a HiBi fibre. Mathematical analysis of the optical set up is given using Muller and Jones matrix methods.

The performance of the system is studied thoroughly and applied for refractive index and film thickness measurements both on bulk (absorbing or non-absorbing) optical samples. The potential for sensor use is also demonstrated with dynamic measurements carried out on oil films and sol-gel based films.

The system is simulated to identify sources of errors and their effect of the ellipsometric parameters, ψ and Δ . The conclusions drawn from the error analysis identify the quarter wave plates as being major sources of errors due to azimuth misalignmant and component imperfection. This finding lead to an alternative approach for the ellipsometric configuration.

A modified ellipsometric configuration that does not employ any use of quarter wave plates is introduced. The new configuration enables a measurement technique that is simpler (ratio of intensities) and more accurate with faster data update rates.

Polarisation modulation again involves stretching a HiBi fibre longitudinally. The output beam is a phase-generated carrier and is analysed with Bessel functions. Lock-in amplifier feedback control system is implemented to control the polarisation. The new configuration is applied for ellipsometric measurements and results obtained are presented and discussed.

The main advantages of this system include improved accuracy, more compact system with smaller number of optical components and thus cheaper system. The ease of signal processing as simple ratio of intensities is also an important advantage for high bandwidth measurements.

Starting with polarisation theory of light, the thesis discusses the present state of ellipsometry and its limited application arising mainly due to the bulky nature of existing systems and mechanically moving nature of operation. This also limits the bandwidth of the measurement. An all fibre ellipsometer should overcome most of the limitations of existing ellipsometers and with a wider scope of application.

Chapter 1

Introduction to Optics and Sensor Technology

1.0 Introduction

Application of light in communication and measurement has been known for over a century. In these systems, air was originally used as a medium of light transmission and the eye did optical detection while a movement such as by the human hand did signal modulation. Such simple optical system left much to be desired for. A breakthrough came when Kao and Hockham in 1966 demonstrated that light could be transmitted in thin, flexible fibre guides [1]. This discovery which led to the birth of the possibility of guiding light through a confined space over a long distance thereby eliminating the uncertainties of atmospheric transmission was an important step in the early form of optical communication.

Early work carried out in confining light transmission into a small space such as a glass tube was not so successful with losses of $\sim 10^5$ dB/Km [2]. With such huge potential application for high bandwidth communication evident at that stage, research continued to bring down the transmission loss to a level less than 20dB/Km,

which was seen as an economic barrier to fibre optic communication as opposed to the well established conventional metallic transmission lines for communication applications. This led to the world-wide interest on optical fibres as transmission line for optical communications. During this period, the high sensitivity of optical fibres to external perturbations such as, pressure, microbends, temperature etc became evident, and research continued to reduce these effects and produce a signal carrying fibre immune to such external effects. At the same time, the observation of the sensitivity of optical fibres to external perturbations led to the application of optical fibres as sensing devices. This grew particularly with the growth of optical communications industry in the production of low loss optical fibres, development of high power lasers, modulated laser diodes, integrated optical devices as well as light detectors [3][4]. The use of optical fibres in sensing applications has many advantages [5][6]. Primarily, they possess the advantage of being immune to electromagnetic interference. The result is noise free transmission and can operate in electrically hazardous environment. The highly directional nature of the fibre means that, fibre sensors become important in sensing applications such as chemically corrosive environments, hazardous atmospheres or medical applications, where conventional metallic or electrical sensors, are impractical.

In sensor applications, in addition to being a transmission medium, the fibre is more importantly used as transducer or a modulation unit.

The transduction advantages over conventional electrical counterparts in sensor applications such as described above may be summarised as follows:

1. **Remote sensor:** The sensing head can be easily directed to a remote measurement point via a low loss fibre.

2. **Immunity to electromagnetic interference:** since optical materials are non-conductive, safety and noise problems associated with electrical sensors are irrelevant.
3. **Safety:** Most fibre sensing heads are passive and do not employ electrical power directly for their operation. And thus introduce no danger of electrical sparking in hazardous environments.
4. **Compact and small size:** The sensor head can be made as small as the diameter of the fibre and few millimetres long.
5. **Sensitivity and bandwidth:** High-resolution measurements can be obtained with a possibility of addressing a large number of measurands.

Thus optical measurement techniques offer various advantages. The measurement technique can be non-contact and non-evasive which is important in applications where the substrate under measurement has to be preserved from damage or contamination during measurement process.

Measurement technique in most optical sensors among variety of methods is based on measuring the intensity change, phase change, polarisation change or wavelength shift measurements upon the interaction of the light or the sensor head with the measurand. Broadly, fibre optic sensors may be classified as intrinsic or extrinsic sensors based on the role of the fibre on the measurement technique. In intrinsic fibre sensors, the physical parameter to be sensed modulates the characteristics of the fibre, and thus the fibre is used as a sensor head. In this case the properties of the guided light, such as intensity, phase, polarisation (e.g. current sensor) or spectral content (e.g. Bragg grating) is modulated by the measurand. Another family of sensors is the extrinsic sensor. In this case the fibre either acts as a mere means of guiding the light to and

from the sensor head or the fibre may also act as a modulator guiding a modulated light to and from the sensor head (e.g. interferometry and polarimetry).

1.1 Polarised light as a measuring tool

Polarised light carries valuable information about where the light has been and the various physical parameters, which have been acting upon it [7]. A variety of physical phenomena influence the state of polarisation of light. Chemical interactions, molecular structures, mechanical stress all impose changes in the polarisation state of an optical beam, thus applications relying on the study of polarisation state of light cover a vast range of engineering, medical, physical, agricultural and various industrial processes. Ellipsometry is an important application of polarised light. The technique involves measuring the change in the polarisation of light upon interaction with a material. Such measurement allows characterising important optical properties of the material. The science of ellipsometry is the subject of the thesis.

1.2 Aims and objectives

In summary, the objectives of the work presented in this thesis can be outlined as:

- To review the present state of ellipsometry and its application in optical measurement.
- To evaluate the potential use of HiBi fibre ellipsometer as a compact non-mechanically moving ellipsometer.
- To test the system as a device for thin film measurement applications.
- To study the system performance and identify sources of errors for further improvement.

- To devise an alternative approach for the design of the fibre ellipsometer as a simplified, compact, improved accuracy and high bandwidth system.
- To report and discuss the results of the work.

1.3 Thesis structure and outline

The thesis is structured so as to give a step-by-step development of the theory of polarisation-based measurements for ellipsometric application. In doing so various ellipsometric configurations are reviewed.

Chapter 2 reviews the electromagnetic nature of light and the theory of polarisation of light needed to describe polarisation based measurements. Mathematical description of polarised light, the fundamental equation of ellipsometry and the mathematics behind the inversion of measured ellipsometric parameters into optical properties of samples are introduced. Chapter 3 discusses the evolution of ellipsometry as a measuring tool over the years. In this Chapter, various ellipsometric configurations that exist commercially as well as laboratory prototypes are described. This Chapter concludes with techniques of polarisation control as a basis for the work in Chapter 4. Chapter 4 introduces the main subject of this thesis; Fibre based Polarisation Modulated Ellipsometry (FPME). Experimental configuration as well as the performance of FPME is discussed in great detail. This Chapter concludes with ellipsometric measurement results on bulk substrates. In Chapter 5, we encounter the use of FPME as a dynamic thin film sensor. Measurement of Dynamic film thickness changes used to highlight the potential use of the FPME in *in situ* time domain measurements. Chapter 6 looks at sources of errors in the FPME described thus far. This Chapter does not seek to investigate a detailed error analysis of all possible error

sources. It does however look at the subject of measurement errors in an attempt to make the FPME more compact and simple. Chapter 7 starts with critical analysis of the FPME dealt with in the previous chapters based on the conclusions obtained from Chapter 6. A modified version of the FPME described in Chapter 7, with fewer number of optical components and improved signal processing technique is introduced and analysed. The new FPME is used for measurement applications. The results of the measurement are presented. A final conclusion of the work reported in this thesis is given in Chapter 8 with a review of the system performance levels obtained and also a comparison with commercial ellipsometers. The thesis concludes with some suggestions for future work.

Reference

1. Bishnu, P.P. (1992) "*Fundamentals of Fibre optics in telecommunications and sensor systems*" (John Wiley & Sons Inc).
2. Culshaw, B. (1984) "*Optical fibre sensing and signal processing*" (Peter Peregrinus Ltd).
3. Grattan, K. T. V. & Meggit, B. T. (1995) "*Optical fibre sensor technology*" (Chapman & Hall).
4. Hoss, R. J. & Lacy, E. A. () "*Fibre Optics*" (Prentice Hall International).
5. Wolfbeis, O. S. (1991) "*Fibre optic chemical sensors and biosensors*" Vol. 1 (Boca. Raton, Fla: CRC Press), p. 10-113.
6. Seitz, W. (1984) "*Chemical sensors based on fibre optics*", Anal. Chem. 56, p. 427-429.
7. Vasicek, A. (1960) "*Optics of thin films*" (North-Holland Publishing Co. Amsterdam)

Chapter 2

Electromagnetic waves: Theory of polarisation and Ellipsometry

Abstract

Light is electromagnetic in nature and can be described as a vector wave. Such transverse vector waves possess a common property, the vector field of disturbance vibrates in a certain orientation. The directional vibration of transverse waves is termed its *state of polarisation*. In this chapter the electromagnetic wave nature of light and the concept of polarisation of the light is introduced. Mathematical methods for describing polarised light and its interaction with optical elements are developed with particular reference to ellipsometric measurements. Mathematical determination of optical properties of samples from ellipsometric measurements is also discussed.

2.0 Introduction

Electromagnetic waves are transverse waves with both electric field strength, \mathbf{E} and magnetic field, \mathbf{H} , which are perpendicular to each other and normal to the wave propagation direction. Light waves, being electromagnetic waves, can be analysed by electric or magnetic field vectors. In a generalised manner, the orientational characteristics of one of these carriers of field, observed at a fixed point in space and time, defines the polarisation of the same wave [1][2]. In the particular case of light, it is generally accepted that the electric field strength, \mathbf{E} is chosen for optical study purposes. This is based on the fact that when light interacts with matter, the force exerted on the electrons by the electric field is much greater than that exerted by magnetic field of the wave [3]. Thus, throughout this thesis and for the purpose of ellipsometric studies, the polarisation of light will be defined as the direction of vibration of the electric field, $\mathbf{E}(\mathbf{r},t)$ observed at a fixed point in space, \mathbf{r} , with time, t . The periodic nature of the vibration of light at the tip of the electric vector as defined by electromagnetic theory traces out a geometrical shape looking towards the source. The locus of such geometrical shape a fixed point in space and time defines the state of polarisation of light. In general, the vibration direction traces out an elliptical shape, the locus could also be circular or linear, and thus light is generally elliptically polarised with circular or linear polarisations being special cases.

2.1 Polarisation of Light

Most of the light we encounter every day is a chaotic mixture of light waves vibrating in all directions. Such a combination is known as "unpolarised" light [4]. In such natural or unpolarised light, the radiation is emitted by molecules, which are randomly excited. A beam of unpolarised light, if observed over a short time interval, appears to be elliptically polarised but the type of polarisation changes continually. In other words, the electric vector traces out an ellipse whose size, eccentricity and orientation gradually change, consequently each new ellipse is completely unrelated to the original one. Thus in any experiment which requires a longer period of observation, one measures the average effect of a large variety of different polarisations. Some light sources generate a polarised light, in general however polarised light is obtained by passing the light beam through a polarising optical element or by causing the beam to make a reflection at a specific angle called Brewster angle [5].

A plane polarised light (constant plane of vibration) can be resolved into two orthogonal optical disturbances, E_x and E_y , which are resultant components along x and y axes [5]. This may be expressed as:

$$E_x(z, t) = E_{x0} e^{j(\omega t - 2\pi z/\lambda)} \quad (2.1)$$

$$E_y(z, t) = E_{y0} e^{j(\omega t - 2\pi z/\lambda + \varepsilon)} \quad (2.2)$$

Where ε is the relative phase difference between the two waves, E_x and E_y , both of which are travelling in the z direction. E_{x0} and E_{y0} are amplitudes of the x and y vibrations at $z = 0$. ω is the angular frequency and λ is the wavelength. The resultant optical disturbance is given by:

$$E(z,t) = E_x(z,t) + E_y(z,t) \quad (2.3)$$

If the two waves are considered to have the same phase, i.e. ϵ is zero or an integral multiple of $\pm 2\pi$, the resultant wave is *linearly polarised* light beam with a fixed amplitude and constant polarisation angle. Another case of particular interest is when both the component waves are 90° out of phase and have equal amplitudes. When these two waves are combined, the tip of the resultant electric vector traces a circle, and the light beam is referred to as *circularly polarised*. If the phase difference is other than 0° or 90° , the resultant electric vector will both rotate and also change its magnitude as well. The end point of the electric vector will trace out an ellipse. Such light is *elliptically polarised*.

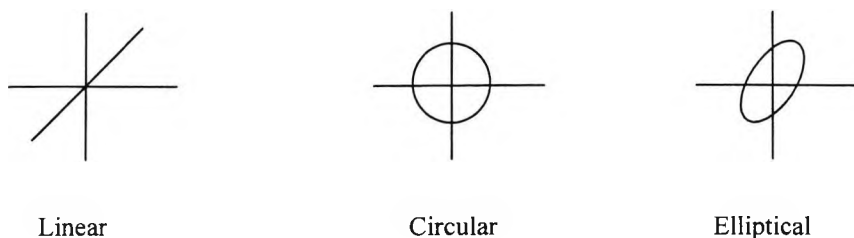


Fig. 2.1 Examples polarised light

In practice, there are several ways to obtain elliptically polarised light. Of primary interest in polarimetry is the fact that when linearly polarised light interacts with an optical surface, there is a change in amplitude as well as a shift in the phases of both the normal polarisation states. This change, in general, is not the same for both components; hence the resultant light will be elliptically polarised. The change of polarisation that the incident light suffers among other things is a function of the optical properties of the substrate [3]. This is the basis of *ellipsometry*, which is the subject of this thesis.

2.2 Ellipsometry

Ellipsometry [3][6][7] is a sensitive optical technique for determining the optical properties of surfaces and thin films. If linearly polarised light of a known orientation is reflected at oblique incidence from a surface then the reflected light is elliptically polarised. The shape and orientation of the ellipse depend on the angle of incidence, the direction of the polarisation of the incident light, and the reflection properties of the surface. An ellipsometer measures the changes in the polarisation state of light when it is reflected from a sample. If the sample undergoes a change, for example a thin film on the surface changes its thickness, then its reflection properties will also change. Measuring these changes in the reflection properties can allow us to deduce the actual change in the thickness of the film. The most important application of ellipsometry is to study thin films. In the context of ellipsometry a thin film is one that ranges from essentially zero thickness to several thousand Angstroms. The sensitivity of an ellipsometer is such that a change of film thickness of a few Angstroms is usually easy to detect.

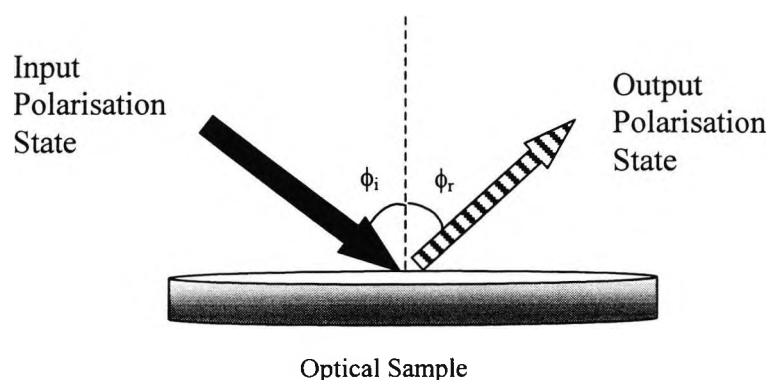


Fig. 2.2 The principle of reflection ellipsometry. The change in polarisation upon reflection carries information on the characteristics of the sample.

2.3 Mathematical description of polarised light

As mentioned before, polarised light is usually generated by passing unpolarised light through a polarising optical element. In the context of ellipsometry, this section will be confined to matrix representation [8] of polarised light and the respective linear polarising components are described.

Polarisers allow the transmission of only one polarisation state. A linear (or plane) polariser transmits light polarised in a single plane. The output polarisation axis orientation is independent of the input beam polarisation state. The plane of polarisation can be changed by rotating the linear polariser about the beam axis. A circular polariser transmits either left circular polarised light or right circular polarised light for an input beam of any polarisation state.

Ellipsometry, as defined before, is a measurement of the change of the state of polarisation of light. This change involves the amplitude of the two orthogonal polarisation components and/or a change in their relative phase difference. These parameters which are fundamental to the ellipsometric measurement cannot however be measured instantly. The reason for this is that the locus of the state of polarisation (SOP) goes through one period in a very short time of the order of 10^{12} cycles per second [8]. This instantaneous change is too fast for any conventional detection technique. Secondly the random statistical nature of the change of the SOP of unpolarised light is again too fast for any practical measurement. Time averaged observations overcome the above practical measurement problem. Such averaged measurement representation of polarised, partially polarised or unpolarised light involves the Stokes parameters, after G. G. Stokes, 1952 [8]. These parameters are

measurable quantities and are useful in analysing the evolution of the state of polarisation of light on passing through polarising optical components. The Stokes parameters are defined by letting I_0 to be the total intensity, I_x and I_y are the intensities of horizontal and vertical linear polarisation states respectively, I_{45} and I_{-45} represent the intensities of linear polarisation at a 45° and -45° angles, and I_r and I_l are the right and left-handed circularly polarised light beams respectively. The Stokes parameters (S_0, S_1, S_2, S_3) are then defined as:

$$\begin{aligned}
 S_0 &= I_0 = (I_x + I_y) = (I_{+45^\circ} + I_{-45^\circ}) = (I_d + I_s), \\
 S_1 &= I_x - I_y, \\
 S_2 &= I_{+45^\circ} - I_{-45^\circ}, \\
 S_3 &= I_r - I_l
 \end{aligned} \tag{2.4}$$

Where S_0 is the total intensity and S_1 and S_2 represent the intensity of the linearly polarised light at the angles indicated in equation 2.4 and S_3 is right or left circularly polarised light intensity. These measurable quantities are important in characterising the quality of partially polarised light in terms of its degree of polarisation (DOP), ellipticity angle, ε and the azimuth, θ of the ellipse of polarisation as shown in figure 2.3.

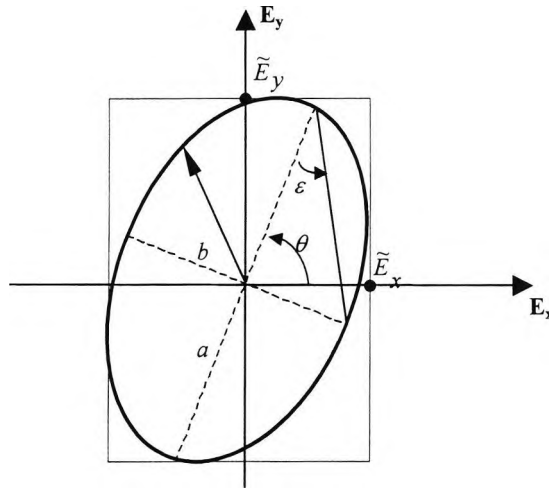


Fig. 2.3 Representation of the locus of elliptically polarised light and the parameters that define elliptically polarised light.

$$DOP = \frac{\sqrt{S_1^2 + S_2^2 + S_3^2}}{S_0} \quad (2.5)$$

$$\epsilon = \frac{b}{a} = \frac{1}{2} \arcsin \left[\frac{S_3}{(S_1^2 + S_2^2 + S_3^2)^{\frac{1}{2}}} \right] \quad (2.6)$$

$$\theta = \frac{1}{2} \arctan \left(\frac{S_2}{S_1} \right) \quad (2.7)$$

The Stokes parameters can describe the SOP of a light beam completely, further more they can be measured experimentally [8] as has been done in this work. The parameters are measured in order to analyse the quality of the polarisation of the light beam in the ellipsometer constructed. Thus a partially polarised light can be represented by a 4×1 column vector whose elements are the four Stokes parameters. If this beam of light is allowed to enter an optical device, the measured Stokes parameters at the output characterise the effect of the device on the SOP of the input beam, i.e. $S_{out} = MS_{in}$, where S_{in} and S_{out} are the Stokes vector of the input and output beam respectively, M is a 4×4 matrix which is characteristic to the optical device and

orientation of its optical axis. Such representation is called the Muller matrix, after its inventor [1][5][8].

Thus if a beam of light passes through a succession of optical devices, the SOP of the emerging light beam can be deduced from knowledge of the SOP of the input beam and the optical devices through which it passes. Refer to the appendix section for a list of Muller matrix of optical devices relevant to ellipsometry.

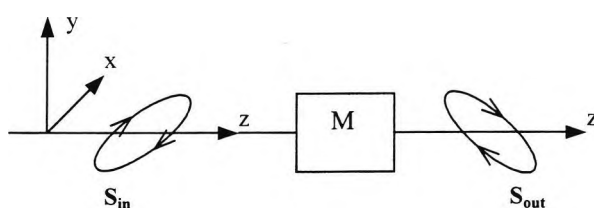


Fig. 2.4 Incident and transmitted polarisation states at the input and output of a polarising element, M.

Jones calculus, developed by R. Clark Jones [5][8] is another method of dealing with propagation of polarised light through polarising optical components. This involves a simpler 2×2 -matrix formulation for optical polarising component representation. Jones calculus is applicable to polarised light with 100% DOP only, otherwise Muller matrix formulation should be selected. Throughout most of this work, both Jones and Muller matrices will be applied to for mathematical analysis of propagation of polarised light through the optical components in the ellipsometric configurations under study.

2.4 Interaction of light with matter

Ellipsometric measurements involve the reflection of light from a surface or transmission through a transparent surface. The outcome of the process depends on

the initial polarisation of the incident light, angle of incidence and the optical characteristics of the sample. The ability to monitor the state of polarisation of light before and after the interaction with the substrate permits investigation of the process occurring at the substrate or characterising the optical properties of the sample.

2.4.1 Reflection by ambient-substrate boundary system

When a beam of light is incident at a boundary between two isotropic homogeneous media, with respective refractive indices, N_0 and N_1 as shown in figure 2.5, some of the light is reflected at the boundary and some of it is transmitted through the sample. The light can be resolved in to two orthogonal components, one with the direction of vibration parallel to and the other perpendicular to the plane of incidence. The plane of incidence is defined as the plane containing both the incident and reflected beams. The Fresnel reflection or transmission coefficients [5][9] are the ratio of the reflected electric vector to the incident wave. These are given by:

$$\frac{E_{rp}}{E_{ip}} = r_p = \frac{N_1 \cos \phi_0 - N_0 \cos \phi_1}{N_1 \cos \phi_0 + N_0 \cos \phi_1} \quad (2.8)$$

$$\frac{E_{rs}}{E_{is}} = r_s = \frac{N_0 \cos \phi_0 - N_1 \cos \phi_1}{N_0 \cos \phi_0 + N_1 \cos \phi_1} \quad (2.9)$$

Where the subscripts p and s refer to the waves parallel and perpendicular to the plane of incidence and E_{ip} and E_{is} refer to the complex amplitudes of the incident electric vector while E_{rp} and E_{rs} are the corresponding reflected components. N_0 and N_1 are refractive indices of the ambient and substrate system respectively and ϕ_1 and ϕ_2 are the angles of incidence and refraction respectively.

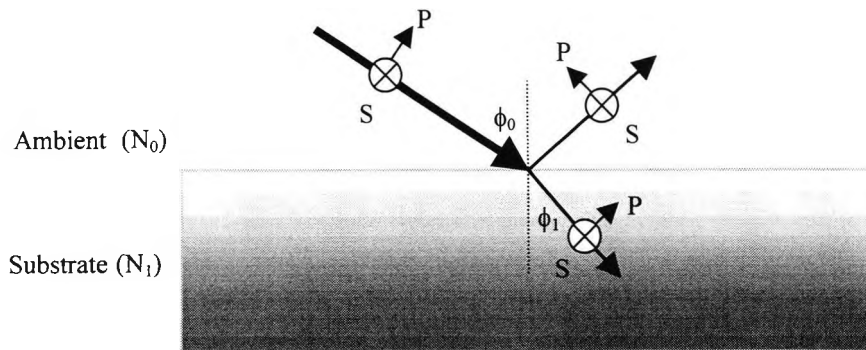


Fig. 2.5. Reflection and refraction of light at a boundary between two media.

Fresnel equations are the basis for examining the effect of reflection and refraction of polarised light on a boundary. It is convenient to express equations 2.8 and 2.9 in the form of exponential amplitude and phase representation.

$$r_p = |r_p| e^{j\delta_{rp}} \quad (2.10)$$

$$r_s = |r_s| e^{j\delta_{rs}} \quad (2.11)$$

Where $|r_p|$ and $|r_s|$ are the ratios of the amplitudes of the reflected sinusoidal waves to that of the incident wave with s and p polarisations. δ_p and δ_s give the respective phase changes after reflection.

For an isotropic optical sample represented by a Jones matrix, the effect of reflection on the incident polarisation can be represented mathematically as [3]

$$\begin{bmatrix} E_{rp} \\ E_{rs} \end{bmatrix} = \begin{bmatrix} r_p & 0 \\ 0 & r_s \end{bmatrix} \begin{bmatrix} E_{ip} \\ E_{is} \end{bmatrix} \quad (2.12)$$

Where E_{ip} and E_{is} represent the p and s polarisation states of the incident electric vector, E_{rp} and E_{rs} are the corresponding reflected electric vectors and r_p and r_s are the Fresnel reflection coefficients which are function of the optical properties of the sample as shown in equations 2.8 and 2.9. The changes in either the amplitude or phase or both of the p and s polarisations states after reflection leads to the determination of the ellipsometric parameters ψ and Δ as a ratio of the complex

Fresnel reflection coefficients r_p and r_s , and hence the fundamental equation of ellipsometry is defined as:

$$\rho = \frac{r_p}{r_s} \equiv \tan \psi \cdot e^{i\Delta} \quad (2.13)$$

$$\tan \psi = \frac{|r_p|}{|r_s|} \quad (2.14)$$

$$\Delta = \delta_{rp} - \delta_{rs} \quad (2.15)$$

Where Δ is the phase change between the p and s polarisations and $\tan(\psi)$ is the amplitude ratio. The value of Δ varies between 0° and 360° while ψ ranges 0° to 90° . Thus ψ and Δ quantify the differential changes in amplitude and phase respectively of the incident s and p polarisations upon reflection from an optical sample. Knowledge of ψ and Δ through measurement leads to the determination of the optical properties of a sample such as its refractive index, film thickness, composition of a substrate and over layers, surface roughness etc.

In an ambient-substrate system, the complex refractive index, N_1 , of the substrate is usually of measurement interest. With a single ellipsometric measurement of ψ and Δ , the complex refractive index can be computed. If we substitute for r_p and r_s in equation 2.13, their values from equations 2.8 and 2.9 and make use of Snell's law [3], we can get an equation for N_1 [3] such that:

$$N_1 = N_0 \tan(\phi_0) \left[1 - \frac{4\rho}{(1 + \rho)^2} \sin^2(\phi_0) \right]^{\frac{1}{2}} \quad (2.16)$$

Where N_0 is ambient refractive index

ϕ_0 is the angle of incidence

ρ is the measured complex reflectance ratio given by $\tan(\psi)e^{i\Delta}$.

In practice since the measured quantity is intensity of the reflected light, the reflectance measurements correspond to the square of the Fresnel reflection coefficients r_p and r_s . Thus,

$$\rho = \sqrt{\frac{|r_p|^2}{|r_s|^2}} = \sqrt{\frac{R_p}{R_s}}. \quad (2.17)$$

2.4.2 Reflection by ambient-film-substrate system

The most common application of ellipsometry is in the analysis of thin films. This application is particularly useful, as the measurement technique is non-destructive and thus very thin films can be measured with no structural damage to the substrate and with high accuracy.

When a polarised light is reflected from a substrate covered with a thin film, as shown in figure 2.6, some of the light is reflected from the front of the film while some of it traverses the film and is reflected back at the film substrate boundary.

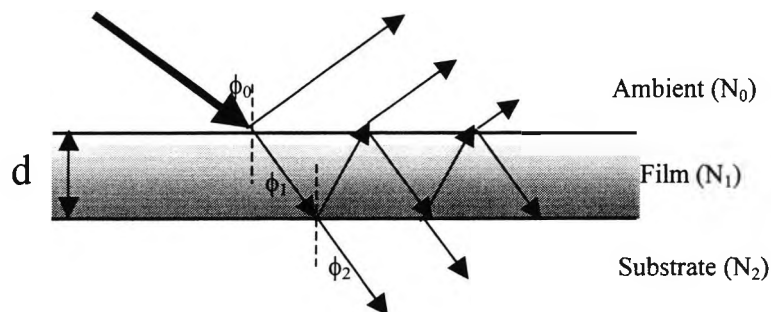


Fig. 2.6 Reflection and transmission of a plane wave by an ambient-film-substrate system. Where d , is the film thickness, ϕ_0 is the angle of incidence at the ambient-film boundary, ϕ_1 and ϕ_2 are angles of refraction at the film and substrate interface.

We assume that the film is optically isotropic and homogeneous with uniform refractive index N_1 , throughout its thickness, d . The ambient and substrate are also considered semi-infinite, homogeneous and optically isotropic with refractive indices

N_0 and N_2 respectively [10]. Unlike the two phase system, in which only the phase and amplitude changes of the reflected polarisation were measured, in the three phase system, an additional parameter is considered. This corresponds to the phase difference of the light rays traversing the film [4]. Consider light incident at the boundary between ambient and film, some of the light is reflected back to the ambient medium and some of it is transmitted through the film and is in turn internally reflected back to the film at the film-substrate interface and some of it is refracted back to the ambient. If the Fresnel reflection coefficients at the ambient-film and film-substrate interfaces are denoted by r_{01} and r_{12} , respectively for the s and p polarisation states and β is the phase change that the multiply reflected wave inside the film experiences as it traverses the film, we can formulate the overall complex amplitude reflection coefficients, R_p and R_s for the p and s polarisation states by adding the successive partial waves that make up the resultant reflected wave [3]. Thus R_p and R_s are given by:

$$R_p = \frac{r_{01p} + r_{12p}e^{-j2\beta}}{1 + r_{01p}r_{12p}e^{-j2\beta}} \quad (2.18)$$

$$R_s = \frac{r_{01s} + r_{12s}e^{-j2\beta}}{1 + r_{01s}r_{12s}e^{-j2\beta}} \quad (2.19)$$

Where the film phase thickness β is given by

$$\beta = 2\pi \left(\frac{d}{\lambda} \right) \left(N_1^2 - N_0^2 \sin^2(\phi_0) \right)^{\frac{1}{2}} \quad (2.20)$$

ϕ_0 angle of incidence

d is film thickness

$N_1 (= n-jk)$ is complex refractive index of the film

λ is the wavelength of the light

If we now express the measured quantity, ρ , in terms of R_p and R_s of equation 2.18 and 2.19 above, we have

$$\tan(\psi)e^{j\Delta} = \rho = \frac{r_{01p} + r_{12p}e^{-j2\beta}}{1 + r_{01p}r_{12p}e^{-j2\beta}} \times \frac{1 + r_{01s}r_{12s}e^{-j2\beta}}{r_{01s} + r_{12s}e^{-j2\beta}} \quad (2.21)$$

Equation 2.21 above relates the measured ellipsometric angles ψ and Δ to the optical properties of the three phase system. In most cases analytical inversion of equation 2.21 to determine N_1 and d is usually impossible except in some special cases. There are however various numerical techniques [10-20] for the determination of optical parameters of the sample.

For a given three phase system, measurement of ψ and Δ at one wavelength, λ and one angle of incidence, ϕ_0 , provides enough information to determine two real parameters of the system only, assuming all the remaining parameters are known. Thus, for example, the complex refractive index of a film $n -jk$ can be determined if the film thickness, d , and the refractive index of the ambient and substrate are known. When the number of unknown parameters of the three phase system exceeds two, as in most practical cases, for example in a case where the film complex refractive index, $n-jk$, and its thickness, d , are to be determined, additional data is required. There are a number of ways of increasing the number of independent ellipsometer readings [10] including:

- i. Assuming the refractive index of the film stays unchanged, multiple measurement can be taken with varying the thicknesses of the film.
- ii. Taking readings on a single film for a different media or substrate, provided the film properties remain unchanged.

- iii. Recording independent data readings for a single film at various angles of incidence.
- iv. Making multiple wavelength measurements on the same film at a fixed angle of incidence.

In practice, multiple angle of incidence (MAI) ellipsometry and multiple wavelength ellipsometry (MAE) are common due to the simplicity and non-destructive nature of the measurement technique [21].

2.5 Summary

The electromagnetic nature of light and its polarisation behaviour has been discussed; mathematical description of polarised light is also introduced to serve as an essential pre-requisite for discussions to ellipsometric measurements.

Finally the fundamental equation of ellipsometry is introduced based on Fresnel reflection theory. The objective of this chapter has been to present a theoretical background to ellipsometric measurement of optical properties of optical materials. In the next chapter, various ellipsometric configurations building on the theory provided in this chapter are discussed.

Reference

1. Shurcliff, W. A., (1969). "*Polarised light: Production and use*" (Harvard University press, Cambridge, Massachusetts).
2. Clark, D. and Grainger, J. F. (1971) "*Polarized light and optical measurement*" (Pergmon Press Ltd.).
3. Azzam, R.M.A. and Bashara, N.M. (1977) "*Ellipsometry and polarized light*" (Amsterdam: North Holland).
4. Vasicek, A. (1960) "*Optics of thin films*" (North-Holland Publishing Co. Amsterdam).
5. Hect, E., Zajac, A. (1979) "*Optics*" (Addisson-Wesley Publishing company, Inc.).
6. Harland, G. T. (1993) "*A User's Guide to Ellipsometry*" (Academic press, Inc.).
7. Bashara, N. M., Buckman, A. B., Hall, A. C. (1969) "*Recent developments in ellipsometry*" (North Holland Publishing Compant- Amsterdam).
8. Gerrard, A. and Burch, J.M. (1975) "*Introduction to matrix methods in optics*" (John Wiley and Sons).
9. Grant R. Fowles (1968) "*Introduction to Modern optics*" (Holt, Rinehart and Winston, Inc.).
10. McCrackin, F. L. and J. P. Colson (1964) "*Computational techniques for the use of the Exact drude equatins in Reflection Problems*" Symp. Proc. On the measurement of surfaces and thin films. Misc. Publication 256, p 61-81.
11. McCrackin, F. L., Elio Passaglia, Robert R. Stromberg and Harold L. Steinberg (1961). "*Measurement of the Thickness and Refractive Index of Very thin Films and Optical Properties of Surfaces*" A. Physiscs and Chemistry, vol 67A(4) p.362-377.

12. Mojun Chang and Ursula J. Gibson (1985) "*Optical constant determination of thin films by random search method*" Applied Optics, Vol. 24 (4), p. 504-507.
13. Manificier, J. C. Gasiot, J. and Fillard, J. P. (1976) "*A simple method for the determination of the optical constants n , k and the thickness of a weakly absorbing thin film*" Journal of physics E: Scientific Instruments. Vol. 9, p. 1002-1004.
14. William E. Case (1983) "*Algebraic method for extracting thin film optical parameters from spectrophotometer measurements*" Applied optics. Vol. 22(12) p.1832-1836.
15. Jean-pierre Drolet, Stoyan C. russev, Maxim I. Boyanov and Rogr M. leblanc (1994) "*polynomial inversion of the single transparent layer problem in ellipsometry*" Journal of Optical society of America (a) Vol 11(12) p. 32843291.
16. John Lekner (1994) "*inversion of reflection elleipsometric data*" Applied Optics. Vol 33(22). P.5159-5165.
17. Michael C. Dorf and John Lekner (1987) "*Reflection and transmission ellipsometry of a uniform layer*" Journal of Optical society of America (a) Vol. 4(11) p. 2096-2100.
18. Holtslag, A. H. M. and Scholte, P. M. L. O. (1989) "*Optical measurement of the refractive index, layer thickness and volum changes of thin films*" Applied Optics. Vol 28 (23). P. 5095-5104.
19. Loescher, D. H.m Detry, R. J. and Clauser, M. J. (1971) "*Least-Square Analysis of the Film-Substrate Problem in Ellpsometry*" Journal of the Optical Society of Amarica. Vol 61 (9). P. 1230-1236.
20. Kihara, T., and Yokomori, K. (1990) "*Simultaneous measurement of refractive index and thickness of thin film by polarized reflectances*" Applied Optics, Vol. 29. No. 34. p. 5069-5073.
21. Aspens, D. E. and Studna, A. A. (1975) "*High precition scanning ellipsometer*" Appl. Opt. (14). p. 220-228.

Chapter 3

History of Ellipsometry and polarisation control

Abstract

Ellipsometry can be generally defined as the measurement of the state of polarisation of a polarised light. The changes of polarisation come about with the interaction of polarised light and an optical sample, the optical properties of which are under measurement. Ellipsometry has been applied across a wide spectrum of fields such as Physics, Chemistry, Material science, Biomedical, optical and electronic engineering, etc. The steady growth of interest and wider application areas has led to the evolution of ellipsometry through a number of development stages. As a result, various laboratory as well as commercial ellipsometric configurations exist.

In this chapter, basic ellipsometric instrumentation is described. Various ellipsometric configurations and modulation techniques [7- 14] from several researchers on the field is presented and compared. The chapter concludes with the discussion of polarisation control and its importance in ellipsometry.

3.0 Introduction

The concept of ellipsometry dates as far back as 1800 [1] with the detection of polarisation by reflection by E. L. Malus. With the development of the classical theory of light and in the time that followed, ellipsometry became an established measuring tool. As such, ellipsometry has evolved through several stages of instrumentation and development and at the same time acquired a wider range of application from refractive index measurement to thin film thickness measurement and process monitoring.

3.1 Instrumentation and Optical Elements

Common to most ellipsometers, the configuration consists of two arms, one for generating an appropriate polarisation state of light to interact with a sample under measurement and another arm for collecting the reflected optical signal for detection and analysis. Usually the optical instrumentation (figure 3.1) consists of polarisers, analysers and compensators along with a monochromatic light source and a detection system.

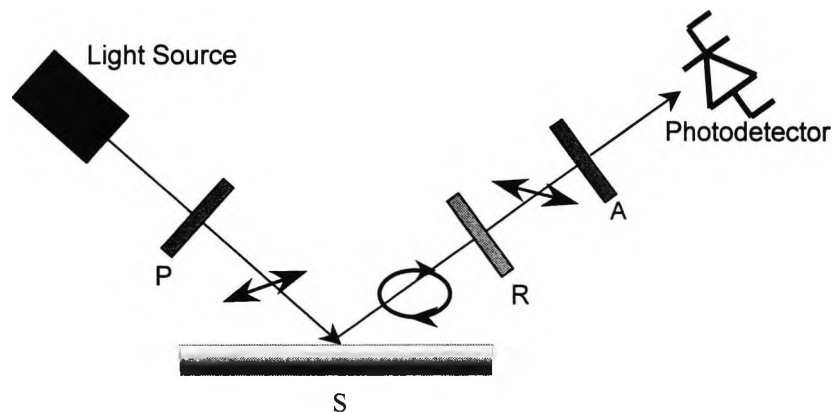


Fig. 3.1 Basic ellipsometric set up. P is linear polariser, R is a retarder, A is analyser and S is a sample.

Detailed discussion of the optical components comprising a typical ellipsometer is given in [2-4], Here; a brief discussion of these optical elements is given here for completeness.

3.1.1 Linear polariser

A linear polariser transforms unpolarised light into a linearly polarised light beam with angle of polarisation set by the polarisation axis of the polariser. The quality of polariser is specified in terms of their extinction ratio, which defines the percentage of transmitted polarisation state normal to the axis of polarisation. A Glan-Thompson polarising prism from Melles Griot such as one used here, has an extinction ratio of less than 1×10^{-5} .

3.1.2 Retarder

An optical retarder such as a quarter wave plate (QWP) is an anisotropic optical element. In general the wave plate has a fast and slow axes which are normal to each other and to the propagation direction of the light beam. When a light beam with normal polarisation components along the two axes of a QWP passes through a QWP, the component of light whose polarisation direction parallel to the slow axis is retarded by $\frac{\pi}{2}$ relative to the component parallel to the fast axis. Thus a linearly polarised light with a polarisation angle at 45° to the fast axis of a QWP is converted to a circularly polarised light. An ideal retarder has a retardance tolerance of zero, while in practice the retardance tolerance ranges from $\lambda/50$ to $\lambda/500$.

3.1.3 Optical sample

The sample being studied should be clean and free of contamination. It should also be smooth enough for specular reflection of the incident polarisation or transmission. Careful sample preparation is important in obtaining reproducible and meaningful ellipsometric data.

3.1.4 Analyser

An analyser is a linear polariser in a different role. When a polarised light is incident on an analyser, the transmitted light is resolved for polarisation detection. Light reflected of the sample is passed through the analyser before detection.

3.1.5 Light source

Visible spectrum has been commonly used for ellipsometric measurement applications. The choice of light source is usually dictated by the availability of polarising optical components at that particular wavelength. Laser sources offer monochromaticity and collimation, which are ideal for ellipsometric measurements. It is important that the stability of polarisation state of the laser source and its intensity maintained for an accurate and repeatable measurement.

3.1.6 Photo detector

The information carried on the polarisation state of the light beam reflected from an optical sample is converted into an electrical signal by a photodetector. The spectral response of the detector must cover the wavelength of the light source. Another important consideration is the noise characteristics of the photodiode. The photodiode

is usually followed by an amplifying stage to bring the detected signal to an appropriate level for further measurement and analysis. The combined noise level of the photodiode and amplifier stage must be minimised to increase the precision of the ellipsometric measurement.

3.2 The Null Ellipsometer

The null Ellipsometer [4][5] is one of the earliest ellipsometric configurations. The operation principle relies on manually or automatically turning a compensator and analyser axis so that the light reflected from the sample is null at the detection point. The angular orientations of the polarising components are then reduced to ψ and Δ by simple relationship [4].

There are a number of null ellipsometric configurations, the most common one in principle is the polariser-compensator-sample-analyser- (PCSA) arrangement [4][5] shown in figure 3.2 below.

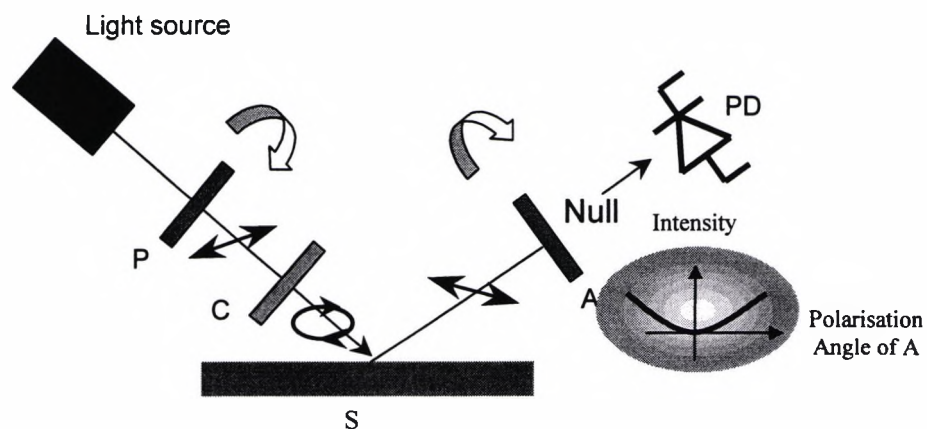


Fig. 3.2 Schematic diagram of a null ellipsometer. Where: P, polariser; C, compensator; S, sample; A, analyser; PD photo-detector.

The compensator or quarter wave plate (QWP) is fixed at 45° to the plane of incidence; the polariser and analyser are rotated until null is found. It should be noted that near the null point, the change in intensity as a function of azimuth angle is very small. In addition, near the null point, the detected light is very low to a level where the detector noise becomes a significant problem.

To overcome this problem a null may be obtained by taking two angular positions on either side of the minimum light detection and take the average value. The manual null ellipsometer described so far relies on careful calibration of the azimuth scales of the polarising components. Its operation, adjustment of optical components to reach null point and subsequent visual reading of the divided circles on the polarising components, introduces measurement dependent on the resolution of the azimuth scales. This requires several minutes per single measurement. For applications that require faster measurement speeds, i.e. to avoid surface contamination or rapid surface reaction to be followed during measurement or when measurements need to be repeated several times, the manual null ellipsometer is impractical and automated measurement becomes essential.

3.3 Automated Ellipsometers

Manually null ellipsometers provide acceptable performance when measurement time is of no concern, i.e. no changes occur at the surface under measurement or when measurements do not have to be repeated several times [4]. Frequently however rapid surface reaction is to be followed to control or monitor a chemical reaction, film deposition etc. Such applications call for an automated measurement system.

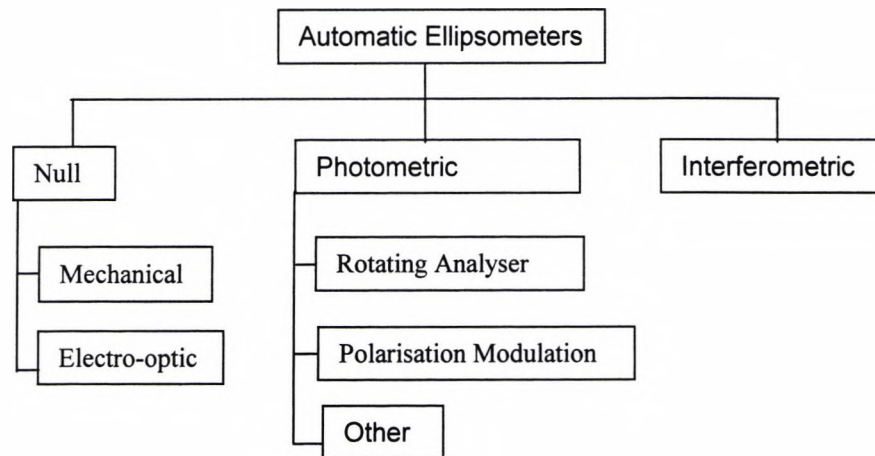


Fig. 3.3 Schematic Classification of Automatic ellipsometers (After Azzam et al. 1977).

The design of automatic ellipsometers [4] has progressed along two different lines as shown in figure 3.3 above. One of these types is a rotating null instrument; the second type is photometric or interferometric instrument.

3.3.1 Automatic Null Instruments

The principle operation of these instruments is the same as the manual null ellipsometer described earlier; in this case servo-system instead of manual adjustment is employed to achieve a null point.

There are two kinds of automatic null ellipsometers, those that employ motors to drive the polarising components and Electro-optic self-nulling ellipsometers with no moving parts. Early versions of motor driven null ellipsometers were those designed by Takasaki [4] and Ord Wills [4]. Here two ADP (Ammonium Dihydrogen Phosphate) modulators rotate the polariser and the analyser in the PCSA ellipsometer. The response speed was rather slow, 5 seconds was needed to reach a null point to 1° accuracy. The ac voltage applied for the ADP cells was $\sim 200\text{V}$ which is not attractive

for commercial instrument. Another limitation for Takasaki's servo null ellipsometer is the need for visual reading of the scales by the operator once null has been reached automatically. This was overcome by replacing the servomotors by stepper motors to drive the polariser and analyser [4]. Automatic read out of the polariser and analyser azimuthal settings is obtained by counting the pulses that drive the stepping motor to achieve null. Another advantage of having the stepping motor is the ease it could be interfaced with a digital data acquisition system for an online measurement. This system has 0.01° resolution and 1 second nulling time.

Winterbottom [4] suggested a stationary self-nulling Electro-optic ellipsometer. This one offers a high measurement speed and precision. The principle of this operation is to use Faraday cells to magneto-optically rotate the azimuth angles of the polariser and analyser instead of manual or motor driven adjustment. The Faraday cells are driven by variable dc current and an alternating modulation current. The component of the detector signal at the modulation frequency is feedback to control the dc current levels in the polariser and analyser Faraday cells [4] until null is reached. Ellipsometric parameters are derived directly from Faraday cell current supplies.

Yamaguchi and Hasunuma [4] developed a fast Electro-optic self-nulling ellipsometer. Two KDP (Potassium Dihydrogen Phosphate) crystals act as voltage controlled variable phase retardation plates. ($\lambda/2$ retardation induced by 75kV at 546nm) by controlling the voltages applied to the KDP, any polarisation state can be achieved. Automatic nulling is achieved by feedback control of the dc voltage levels applied to the KDP crystals. The voltage read out enables ψ and Δ to be obtained directly. The response time of this instrument was of the order of 1 second.

3.3.2 Automatic photometric ellipsometer

The second group of automatic ellipsometers is photometric instrument. These use the values of variation of light intensity for measuring ellipsometric parameters ψ and Δ . Intensity variation can be achieved as a function of one or more of the azimuth angle, retardation or angle of incidence. Two such systems are the rotating analyser ellipsometer (RAE) [4] and the polarisation modulated ellipsometer (PME).

3.3.2.1 The Rotating analyser ellipsometer

Aspen and Stude (1975) [6] introduced the rotating analyser ellipsometer (RAE). In this system the analyser is synchronously rotating at frequencies $\sim 100\text{Hz}$ with its rotation axis along the direction of the beam propagation while the polariser and compensator remain fixed with defined azimuthal orientations.

Plane polarised light reflected from a sample passes through a rotating analyser; the detected intensity signal is a sinusoidal function from which ψ and Δ are detected [4]. The operation of RAE is well established and in fact different versions of RAE are commercially available.

3.3.2.2 Polarisation Modulated Ellipsometry

In 1969, Jaspersen et al. [7] introduced polarisation-modulated ellipsometry as an improved system to replace the null ellipsometric techniques that existed prior to that time. The nulling techniques require several minutes for measurement. Such longer response time is undesirable in certain applications where rapid surface contamination is intolerable or when a fast process such as a chemical reaction or film deposition needs to be monitored. The principle of operation is that the state of polarisation of

the light beam is modulated by introducing a controlled phase retardation so that the information carried on the reflected light from the optical sample under measurement is retrievable by analysing the resulting time varying detected photo-electric current [4].

Several possible configurations exist depending on the application of modulation. An arrangement proposed by Jaspersen et al. is the Polariser Modulator sample Analyser (PMSA) arrangement. In this arrangement a fused quartz block is driven by an ac signal through piezoelectric crystal cemented to one end of the block. The oscillating strain induces modulated birefringence (dual refractive index axis). Thus the quartz block acts as a linear retarder with time varying retardation. The amplitude of the retardation is proportional to the applied varying voltage. In PME, all optical components remain stationary. This freedom of mechanical movement is a distinct advantage and allows high-speed measurement.

The primary observation at this stage is that the importance of automating the ellipsometer has been recognised since the advent of manual null ellipsometer and considerable attention has been given to the development of an automated fast and more accurate measuring. A clear advantage of an automated system is faster measurement time. The development of a faster measuring tool has increased the application of ellipsometry in the study of dynamic film growth or surface studies where fast changes occur during measurement.

Several techniques that have been used to design automatic ellipsometer have been described in this chapter. Automatic null ellipsometers have a disadvantage of slower response time due to the mechanical movements involved. In general the instruments

described thus far involving mechanically moving parts do not hold the promise to reduce measurement time significantly.

The conclusion of this chapter so far is that for real time high-speed measurements, polarisation modulated ellipsometry holds the key.

The RAE has a disadvantage in that it involves a mechanically rotating polarising element.

Since Jaspersen et al., several researchers have worked on PME and more attention has been given to this technique due to the obvious advantages it offers for time resolved measurement applications.

Shamir et al. in 1986 [8] proposed a polarisation-modulated ellipsometer, which was free from mechanically moving parts. An acoustic modulator and a waveplate are used to generate RPP beam.

Singher et al. (1990) [9] introduced an ellipsometric set up using a commercially available stabilised Zeeman laser, (SZL). An SZL emits a beam composed of two circularly polarised components that differ in frequency. This generates an RPP beam at the difference frequency, which is ideal for ellipsometric measurements but is expensive.

With the advent of polarisation maintaining fibre, Yashino and Kurosawa (1984) [10] introduced the first ellipsometer based on a high birefringence (HiBi) fibre as polarisation modulator. The authors demonstrated that their all fibre ellipsometer could be used to measure the optical constants of the materials and as a surface sensor.

3.4 The future of ellipsometry

So far the progress and direction of research carried out in the area of ellipsometry has been reviewed. The trend has been to realise an accurate, flexible and compact-measuring tool, which is capable of doing fast time resolved measurements. Polarisation modulated ellipsometry promises such features and has been worked on by several researchers [7-11]. With the development of telecom industry and fibre technology, HiBi fibre has been applied in developing an all fibre ellipsometer [10]. Thus the combination of polarisation modulation and fibre based ellipsometry looks set to dominate any future work developing better and affordable ellipsometers.

3.5 The need for an all fibre ellipsometer

The conventional ellipsometer consists of bulk polarising optical components, compensators and polarisation modulators that require precise alignment. Such a system is physically large and bulky and thus is limited for use within laboratory environment. Automation is usually achieved by mechanically moving one of the optical components for modulation, which limits operation speed. This is undesirable nature for many applications where dynamic processes are to be monitored. A compact system would broaden the applications areas of ellipsometry as a sensing device or as a field instrument for environmental applications at a fraction of the cost of the present commercial ellipsometers.

An all fibre ellipsometer offers a more compact and flexible system, immune to electromagnetic noise and enables remote sensing in hazardous environments. Such system is free of mechanically moving parts offering a potential for high-speed

measurements and does not rely on careful azimuthal alignment and component imperfections considerations discussed in chapter 6.

3.6 Polarisation state control and polarisation modulation

There are a number of sensor schemes in which polarisation azimuth control and measurement forms a basis for optical instrumentation. These include ellipsometry and polarimetry in which well-defined polarisation modulated beam is generated such that upon interaction of the beam with the sample, the changes in polarisation can be measured. These changes in polarisation characterise the sample.

To date, several techniques have been proposed for producing a linearly polarised beam of controllable azimuth [12]. Early work on the area mainly concentrated on free space instrumentation using bulky optical components such as beam splitters, polarisers, birefringent crystals, etc.

In 1961, Takasaki et al. [13] used electrooptic effect or pokels effect for modulating a linearly polarised light. A linearly polarised light is propagated through an ADP crystal. An ac signal current was applied to the ADP causing variations in the refractive indices of the two orthogonal components along the crystal axis normal to the beam propagation direction. The ADP thus acts as a retardation plate with modulated retardation.

Few years later Jaspersen et al. [7] introduced a strain induced polarisation modulation using a fused quartz crystal driven by an ac signal and were applied for ellipsometric measurements.

In 1986 shamir and Klein [8] introduced high frequency polarisation modulation using a Bragg cell as a frequency shifter. This approach was latter applied to

ellipsometric measurements by the same authors. Although the measuring process did not involve any mechanical movements and was reported to be applicable for fast time varying measurements, the Bragg cell modulator was bulky and expensive. Magneto-optically induced birefringence for polarisation control [14] has been achieved, however these components are large and expensive, and a large magnetic strength and OPD are required to generate a sufficient azimuth modulation.

Generally free space polarisation modulation involves bulky optical components, which are relatively large and expensive. With the development of fibre optic technology, a range of techniques has evolved for the generation of modulated polarisation state [12].

Optical fibres provide significant advantages over the free space medium, notably increased system tolerance to external influences such as vibration; higher speed of modulation and cheaper systems which are more compact. The nature of the fibre itself provides flexibility and confinement in light transmission, which is important for remote sensor systems.

3.7 Polarisation maintaining behaviour in single mode fibres

Conventional single mode optical fibres do not normally preserve the polarisation state of the light propagating along the fibre. In many applications in which polarisation state of the light is irrelevant, this is of little significance. However, in polarimetric or interferometric sensor applications, ellipsometry and in coherent communication systems, the polarisation state of the light injected in to the fibre should propagate unchanged. This requires a single mode fibre, which can support

single polarisation state along the entire length. Such a fibre would have a perfect circular symmetric core along its entire length.

In practice, imperfections such as asymmetrical stress and core ellipticity affect the polarisation of the propagating light, i.e. the light along the two normal eigenmodes of the fibre experience different refractive indices or birefringence and thus propagate with differing phase velocities.

The polarisation state is also dependent on external forces such as bends, twists, transverse pressure or temperature etc.

Thus for a conventional monomode fibre or low birefringence fibre, the SOP of the propagating light is not preserved. Polarisation applications with such fibres require attaching polarisation controller at the output end of the fibre and be restricted to high stability (e.g. Submarine) environments. [15]. Early work on polarisation control was directed towards exploiting the birefringence of the fibre by subjecting the fibre to some kind of external perturbations through various elasto-optic [16-20], magneto-optic [14][19] or Electro-optic [13] index changes. By using one of these methods the circular symmetry of the ideal fibre is broken as a result a phase shift is introduced between the two light polarisation components along the eigenmodes of the fibre. With proper value of the phase shift, a controlled polarisation state can be achieved [21].

Thus, in the absence of single polarisation fibres, the phenomenon of birefringence has been exploited to develop a high birefringent (HiBi) fibre that can preserve the SOP. In a HiBi fibre the intrinsic birefringence is increased deliberately by imposing some form of asymmetry in the cross-sectional fibre structure. The level of intrinsic birefringence achieved is far greater than that can be produced by external

perturbations, and thus the fibre is immune to unstable environment [22]. A single mode HiBi fibre is able to transmit two orthogonal polarisation modes or eigenmodes with slightly different velocities. It will preserve the linear polarisations of the propagating light when launched in one of the eigenmodes. There are various types of PM fibres each with different stress applying geometry fibre core structure.

Figure 3.4 shows a variety of polarisation preserving core/cladding structures presently used in the industry. The dashed lines in the drawings show the slow axis within each structure. More recently there has been the development of polarising fibres. These fibres only transmit light that is polarised along the transmission axis of the fibre.

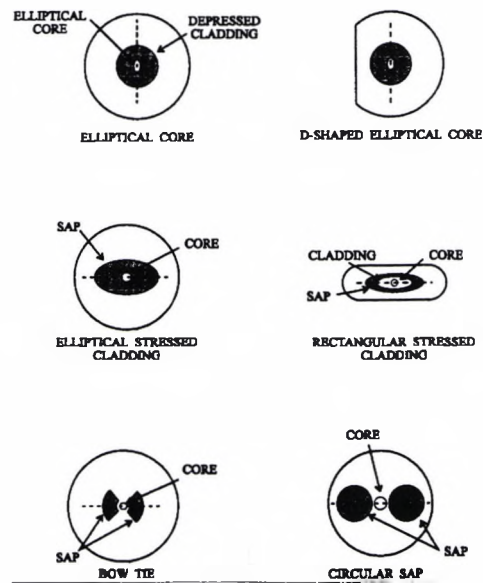


Fig. 3.4 Examples of polarisation preserving fibre core structures.

With the introduction of HiBi fibres in to the fibre-optic technology, optical sensor design and polarisation control techniques soon benefited from these fibres. Precision bulky mechanical systems were soon replaced by fibre-optic equivalents providing more compact and cheaper systems. Higher speed of modulation was also achieved.

Tatam et al. (1986) [12] describes a range of techniques in which polarisation control may be achieved based on fibre-optic or acousto-optic modulators. Perhaps the most attractive scheme for polarisation control proposed by the above authors is single birefringent fibre system with piezoelectric transducer (PZT) modulator. A schematic diagram is shown in figure 3.5 below.

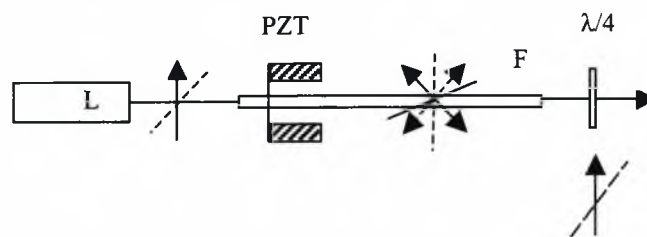


Fig. 3.5 Polarisation state azimuth control using a single highly birefringent monomode fibre. L, Ar laser; PZT piezo electric transducer; F, HiBi fibre; $\lambda/4$, QWP. (After Tatam et al. 1986)

In this scheme, a linearly polarised argon-ion laser was launched into a HiBi fibre with its polarisation angle at 45° to the fibre eigen axes to excite both the fibre orthogonal modes equally. At the output of the fibre, a QWP oriented at 45° to the fibre eigen axis was used to return the beam into a linearly polarised state. Polarisation modulation was achieved by applying longitudinal strain modulating the modal phase retardance of the HiBi fibre with a saw-tooth waveform driving a PZT. This technique provides better polarisation control and is free of bulky mechanical components since the modulation is achieved without bending twisting or subjecting the fibre to any transverse pressure, electric or magnetic fields.

If the eigen axes of a HiBi fibre are equally populated with a linearly polarised light, ideally there should be a constant phase relationship between the two orthogonal plane polarisations introduced by the fibre, however extrinsically induced birefringence effects, due to environmental effects such as temperature variations etc.

introduce random phase variation. In 1992, Johnson et al. [23] proposed feedback controlled HiBi fibre polarisation controller, their work highlighted environmental effects on HiBi fibre based systems and proposed phase variation compensation techniques. A number of schemes have been proposed for phase stabilisation in fibre optic systems [24-26].

3.8 Summary

In this chapter, the evolution of ellipsometry as a measuring tool has been presented. Various ellipsometric techniques have been discussed chronologically and compared on the merit of design, performance, modulation techniques and future viability. Polarisation modulation is found to hold a definite promise in ellipsometric applications. This point has been greatly helped with the advent of fibre-optic technology. The introduction of HiBi fibres into the polarisation control means that bulky and expensive precision mechanical components be replaced with more compact and rigid design based on fibre optic technology.

Single HiBi fibre polarisation control proposed by Tatam et Al. has been applied for ellipsometric measurement applications [11]. This approach is the subject of this thesis. In the next chapter, fibre based polarisation modulation is discussed and applied to for ellipsometric measurement applications.

Reference

1. Bashara, N. M., Buckman, A. B., Hall, A. C. (1969) "*Recent developments in ellipsometry*" (North Holland Publishing Company- Amsterdam).
2. Shurcliff, W. A., (1969). "*Polarised light: Production and use*" (Harvard University press, Cambridge, Massachusetts).
3. Longhurst, R. S. (1973) "*Geometrical and Physical Optics*" (London, Longman.).
4. Azzam, R.M.A. and Bashara, N.M. (1977) "*Ellipsometry and polarized light*" (Amsterdam: North Holland).
5. Harland, G. T. (1993) "*A User's Guide to Ellipsometry*" (Academic press, Inc.).
6. Aspens, D. E. and Studa, A. A. (1975) "*High Precision Scanning Ellipsometer*" Applied Optics, Vol. 14, p. 220-228.
7. Jaspersen, S.N. and Schnaterley, S. E. (1969) "*An improved method for high reflectivity ellipsometry based on a new polarization modulation technique*" Review of scientific instruments, Vol. 40(6), p 761-767.
8. Shamir, J. and Klein, A. (1986) "*Ellipsometry with rotating plane polarised light*" Applied Optics, Vol. 25, p 1476-1480.
9. Singher, L., Brunfeld, A. and shamir, J (1990) "*Ellipsometry with a Stabilised Zeeman Laser*" Applied optics, Vol.29, p. 2405-2408.
10. Yoshini, T. and Kurosawa, K. (1984) "*All Fibre Ellipsometry*" Applied optics Vol.23, p 1100-1102.
11. Chitaree, R., Weir, K., Palmer, A.W. and Grattan, K.T.V. (1994) "*A Highly Birefringent Polarisation modulation scheme for ellipsometry: System Analysis and performance*" Measurement science and Technology, Vol. 5, p. 1226-1232.
12. Tatam, R. P., Jones, J. D. C., Jackson, D.A. (1986) "*Optical polarisation state control schemes using fibre optics or Bragg cells*" J. Physics E. Sci. Instrumentation, Vol. 19, p. 711-717.
13. Tkasaki, H. (1961) "*Photoelectric Measurement of Polarised light by means of an ADP Polarisation modulator, II Photoelectric Elliptic polarimeter*" Journal of optical Society f America, Vol. 51, p. 463.
14. Jackson, D. A., Kersey, A. D, Akhavan, L. P., and Jones, J. D. C. (1985). "*High frequency non-mechanical optical linear polarisation state rotator*" J. Phys. E:Sci. instrum. 19, 146.

15. Noda, J., Okamoto, K. and Sasaki, Y. (1986) "*Polarisation maintaining fibres and their applications*" Journal of Light wave Technology, (LT-4), p. 1071-1089.
16. Ulrich, R. (1979) "*Polarisation stabilisation on single mode fibre*" Applied Physics Letters, Vol. 35, p. 840-842.
17. Kubota, M., Ohara, T., Furuya, K. and Suematsu, Y. (1980) "*Control on single mode optical fibres*" Electronics Letters, Vol. 16, p. 573.
18. Lefevre, H. C. (1980) "*Single Mode Fibre fractional wave devices and polarisation controllers*" Electronics Letters, Vol. 16, p 778-780.
19. Okoshi, T., Fukay, N. and Kikuchi, K. (1985b) "*New Polarisation State control device: rotatable fibre Cranks*" Electronics Letters, vol. 21, p. 895-896.
20. Matsumoto, T. and Kano, H. (1986) "*Endless Rotatable Fractional wave device for Single mode Fibre Optics*" Electronics Letters, Vol. 22, p. 78-79.
21. Ralsleigh, S.C., Burns, W. K. Moeller, R. P. and Ulrich, R. (1982a) "*Polarisation-holding in Birefringence single-mode fibres*" Optical letters, Vol. 7, p 40-42.
22. Malcolm, P. Varnham, David N. Payne, Arthur J. Barlow and Robin D. Birch (1983) "*Analytic solution for the birefringence produced by thermal stress in polarisation maintaining optical fibres*" Journal of Lightwave Technology, Vol. LT-1, No.2, p. 332-339.
23. Johnson, M. and Pannell, C. N. (1992) "*Remote State of polarisation control on Polarisation maintaining fibre.*" Optics Communications, Vol. 90, p 32-32.
24. Corke, M. Jones, J. D. C., Kersey, A. D. and Jackson, D. A. (1985) "*All single-mode fibre optic holographic system with active fringe stabilisation*" J. Phys. E: Sci. Instrum, Vol. 18, p. 185-186.
25. Jackson, D.A, Priest, R. Dandridge, A. and Tveten, A. B., (1980) "*Elimination of drift in a single mode optical fibre interferometer using piezoelectrically stretched coiled fibre*" Applied Optics, Vol. 19, No. 17, p. 2926-2929.
26. Shadaram, M., Medrano, J., Papert, S.A. and Berry, M.H. (1995) "*Techniques for satbilizing the phase of the reference signals in analog fiber-optic links*" Applied optics, Vol. 34, No. 36, p. 8283-8288.

Chapter 4

HiBi Fibre Polarisation Modulated Ellipsometry

Abstract

Polarisation modulated ellipsometry (PME) in which modulation is achieved by stretching a high birefringent (HiBi) fibre longitudinally in a periodic manner is described. The performance of such a device is analysed and the limitations examined. Finally the system is applied to the determination of optical properties of absorbing and non-absorbing bulk optical substrates.

4.0 Introduction

As discussed in the previous chapter, polarisation modulation has been found a preferred scheme for polarisation based measurements such as ellipsometry. Generation of a linearly polarised beam with a modulated azimuth is an attractive feature for ellipsometric and other polarimetric measurement applications [1-4]. It allows fast time resolved measurements with important applications for on line process monitoring, dynamic film growth etc.

Most ellipsometers, including commercial ones, involve bulky optical components requiring precise mechanical engineering and precise component alignment for measurement. Modulation usually involves mechanical movement of an optical component in the system, e.g. commercial rotating analyser ellipsometer (RAE). Mechanical movement and bulky components are undesirable features for rapid real time ellipsometric measurement [5]. Chitaree et al. in 1994 used a HiBi fibre polarisation modulation technique for ellipsometric application [1]. In their work, a rotating plane polarised beam (RPP) is generated by stretching a HiBi fibre longitudinally. The scheme has been applied to measurement of the refractive index of optical samples.

In this chapter, the theoretical aspects and practical performance as well as limitations of HiBi polarisation modulated ellipsometry is thoroughly investigated. Some experimental measurement results are presented and discussed.

4.1 Experimental Configuration

The basic configuration comprises a 10mw helium-neon (HeNe) laser at 632.8nm wavelength which is circularly polarised using a linear polariser and a quarter wave plate combination (from Melles Griot, 1995). The polarised light is then launched in to a HiBi fibre (YORK 600HB) via a 10× objective lens. Modulation is achieved by stretching the fibre longitudinally with a dynamic shaker (from LING Dynamic systems) driven at ~50Hz. The output beam from the fibre is then collimated by another 10× lens and in to a QWP with its optical axis at 45° to the fibre eigen axes. The QWP transforms the linear states from each eigenmode in to left and right circularly polarised beams which then recombine to give a rotating azimuth linear state.

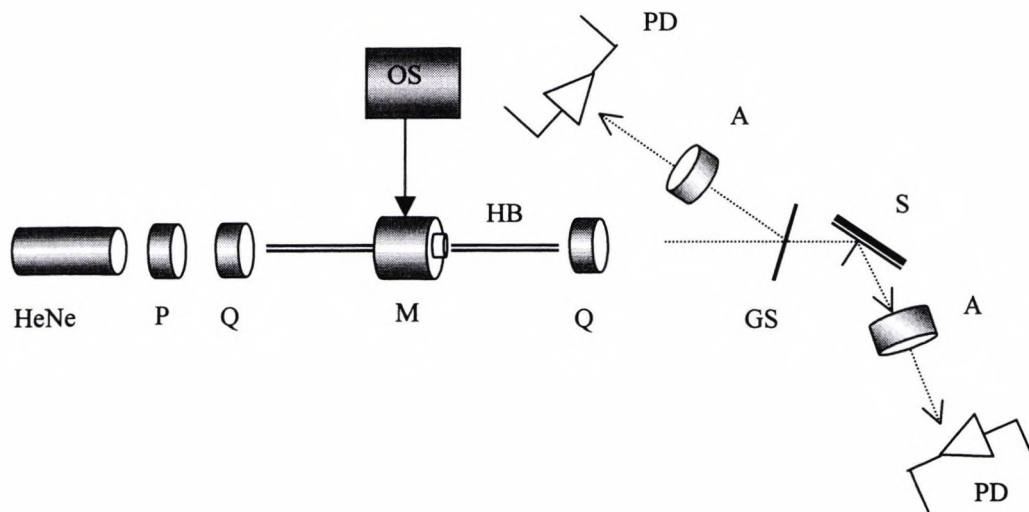


Fig. 4.1 Experimental configuration of the ellipsometer. A helium neon laser, HeNe, a linear polariser, P, QWP, Q, HiBi fibre, HB, fibre stretcher, M, signal generator, OS, glass reflector, GS, sample, S, linear analyser, A and a photodetector, PD.

4.2 Mathematical Analysis and measurement technique

For a complete mathematical description of the SOP of a light beam as it propagates through a train of optical components comprising the ellipsometer arrangement described above either Muller matrix or Jones calculus [6][7] can be utilised. As described in section 2.3, the Jones calculus has the advantage over the Muller calculus of employing a smaller 2×2 matrix instead of 4×4 of Muller calculus. The Jones vector representation of light is associated with the amplitude and transmittance, while the Muller matrix is based on phenomenological foundation, its matrix representation employs stokes vector whose elements are directly related to intensity and type of polarisation [7], two parameters of paramount interest in ellipsometry. For our analysis purposes, Muller matrix is preferred here as the Muller description is more closely linked to our experimental observations, although Jones calculus is also used where the simplicity of the 2×2 matrix is advantageous.

A list of Muller and Jones matrix representations of linear optical elements relevant to ellipsometric configurations described in this thesis is given in appendix A.

4.3 The PCMCSA Arrangement

An unpolarised HeNe source may be represented by a normalised stokes vector [7] of the form:

$$E_0 = I_0 \begin{bmatrix} 1 \\ 0 \\ 0 \\ 0 \end{bmatrix} \quad (4.1)$$

The PCMCA (Polariser-Compensator-Modulator-Compensator-Sample-Analyser) arrangement can be simplified into a combined single matrix. Each optical component is represented by a 4×4 Mueller matrix defined by its type and optical axis orientation relative to a predefined reference plane.

Consider the PCMC train, the polariser, P and the QWP, C are oriented so that the light at the output of the first QWP is circularly polarised, i.e. their optical axes are at 45° to each other. The QWP at the output of the modulator (HiBi fibre) is oriented with its axis at 45° to the fibre eigen axes. With the polariser adjusted so that the light source is polarised in the P (horizontal) direction, the matrix of the train is computed as:

$$E_0' = [C][M][C][P][L] \quad (4.2)$$

Where L is the Stokes vector of the unpolarised light source, M is the modulator matrix and C and P represent the Muller matrix of the compensator and polariser described above. E_0' is the Stokes vector of the resulting polarisation state.

$$E_0' = \begin{bmatrix} 1 & 0 & 0 & 0 \\ 0 & 0 & 0 & -1 \\ 0 & 0 & 1 & 0 \\ 0 & 1 & 0 & 0 \end{bmatrix} \begin{bmatrix} 1 & 0 & 0 & 0 \\ 0 & 1 & 0 & 0 \\ 0 & \cos(\phi_d) & \sin(\phi_d) & 0 \\ 0 & 0 & -\sin(\phi_d) & \cos(\phi_d) \end{bmatrix} \begin{bmatrix} 1 & 0 & 0 & 0 \\ 0 & 0 & 0 & -1 \\ 0 & 0 & 1 & 0 \\ 0 & 1 & 0 & 0 \end{bmatrix} \begin{bmatrix} \frac{1}{2} & \frac{1}{2} & 0 & 0 \\ \frac{1}{2} & \frac{1}{2} & 0 & 0 \\ 0 & 0 & 0 & 0 \\ 0 & 0 & 0 & 0 \end{bmatrix} \begin{bmatrix} 1 \\ 0 \\ 0 \\ 0 \end{bmatrix} \quad (4.3)$$

Where M, the modulator Matrix, in this case is a HiBi fibre, ϕ_d is the differential retardance between the fast and slow eigen polarisations introduced by periodic longitudinal stretching of the fibre under tension. Multiplying from right to left, the light launched into the fibre is a circularly polarised beam with a Stokes vector of the form:

$$\begin{bmatrix} S_0 \\ S_1 \\ S_2 \\ S_3 \end{bmatrix} = \begin{bmatrix} \frac{1}{2} \\ 0 \\ 0 \\ \frac{1}{2} \end{bmatrix} \quad (4.4)$$

As this light travels through the modulator, the resulting Stokes vector at the output of the fibre is given by:

$$\begin{bmatrix} S_0 \\ S_1 \\ S_2 \\ S_3 \end{bmatrix} = \frac{1}{2} \begin{bmatrix} 1 \\ 0 \\ \sin(\phi_d) \\ \cos(\phi_d) \end{bmatrix} \quad (4.5)$$

As ϕ_d varies between 0 and $\pi/2$, the SOP of the light at the output of the fibre varies between circular, elliptic and linear polarisation states in a periodic manner as shown in figure 4.2 below.

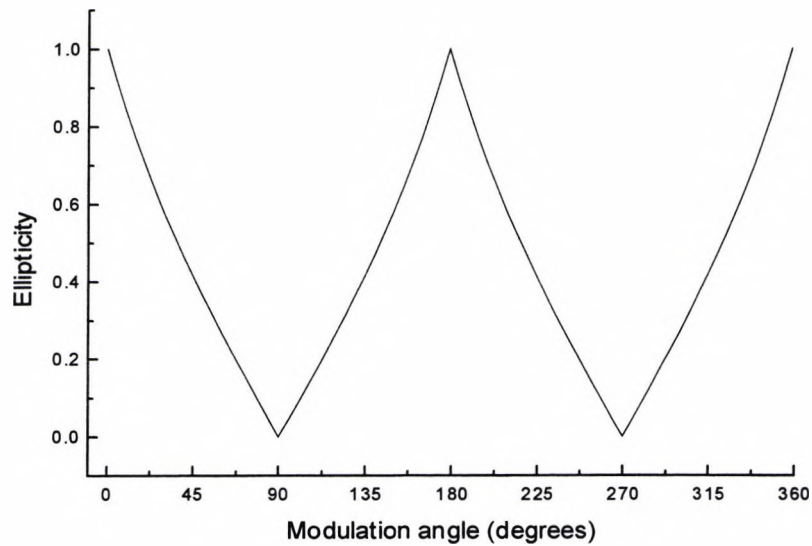


Fig. 4.2 Periodic polarisation evolution of the light beam at the output of the fibre.

The final compensator turns the light from the fibre in to a rotating plane polarised beam with a corresponding Stokes vector:

$$\begin{bmatrix} S_0 \\ S_1 \\ S_2 \\ S_3 \end{bmatrix} = \frac{1}{2} I_0 \begin{bmatrix} 1 \\ -\cos(\phi_d) \\ \sin(\phi_d) \\ 0 \end{bmatrix} \quad (4.6)$$

The RPP beam shown in equation 4.6 above has intensity of $0.5I_0$ and its azimuth $\phi_d/2$ varying according to the modulation angle ϕ_d . It has ellipticity angle of zero and DOP of 100%. The equivalent Jones matrix representation of equation 4.6 is given by:

$$E(\phi_d) = \begin{bmatrix} -\cos(\phi_d/2) \\ \sin(\phi_d/2) \end{bmatrix} \quad (4.7)$$

The RPP generated is then reflected from a sample under investigation. The Muller matrix of an isotropic surface with ellipsometric parameters ψ and Δ is given by:

$$S = \begin{bmatrix} 1 & -\cos(2\psi) & 0 & 0 \\ -\cos(2\psi) & 1 & 0 & 0 \\ 0 & 0 & \sin(2\psi)\cos(\Delta) & \sin(2\psi)\sin(\Delta) \\ 0 & 0 & -\sin(2\psi)\sin(\Delta) & \sin(2\psi)\cos(\Delta) \end{bmatrix} \quad (4.8)$$

The Stokes vector representation of the light reflected from the sample can be obtained by right multiplying the 4×4 Muller matrix of equation 4.8 by the RPP vector of equation 4.6. The resulting elliptically polarised beam is given by:

$$\begin{bmatrix} S_0 \\ S_1 \\ S_2 \\ S_3 \end{bmatrix} = \frac{1}{2} I_0 \begin{bmatrix} 1 + \cos(2\psi)\cos(\phi_d) \\ -\cos(2\psi) - \cos(\phi_d) \\ \sin(2\psi)\cos(\Delta)\sin(\phi_d) \\ -\sin(2\psi)\sin(\Delta)\sin(\phi_d) \end{bmatrix} \quad (4.9)$$

The reflected light is then analysed by an analyser with its polarisation axis at 45° to the plane of incidence. At this stage we are only interested in the form of the detected intensity signal which is given by the first term of the resulting Stokes vector in equation 4.10.

$$\begin{bmatrix} S_0 \\ S_1 \\ S_2 \\ S_3 \end{bmatrix} = \frac{1}{4} I_0 \begin{bmatrix} 1 + \cos(2\psi) \cos(\phi_d) + \sin(2\psi) \cos(\Delta) \sin(\phi_d) \\ ? \\ ? \\ ? \end{bmatrix} \quad (4.10)$$

Therefore:

$$I(t) = \frac{1}{4} I_0 (1 + \cos(2\psi) \cos(\phi_d) + \sin(2\psi) \cos(\Delta) \sin(\phi_d)) \quad (4.11)$$

Extracting ψ and Δ from equation 4.11 is not a straightforward procedure. Equation 4.11 can however be simplified into simpler forms from which ψ and Δ can be extracted. This is done with the help of a reference polarisation beam.

In practice the RPP beam is partially reflected with an isotropic glass slide at near normal incidence ($\sim 2^\circ$). At such small angles of incidence, the complex Fresnel reflection coefficients, r_p and r_s remain unchanged and the transmitted and reflected light beam can be reasonably assumed to have the same SOP. With this in mind, the reflected signal provides a reference polarisation state such that the information on the light reflected from the sample under measurement can be measured relative to the orientations of the linear analyser at the reference arm. The light on the reference arm is an RPP one, the analyser at the reference arm defines the direction of the polarisation of light on the detection arm. The polarisation axis of the reference arm analyser is set at 0° relative to the plane of incidence at the sample. The signal detected at the reference arm is then given by the first element of the resulting Stokes vector:

$$\begin{bmatrix} S_0 \\ S_1 \\ S_2 \\ S_3 \end{bmatrix} = \frac{1}{4} I_0 \begin{bmatrix} 1 - \cos(\phi_d) \\ ? \\ ? \\ ? \end{bmatrix} \quad (4.12)$$

$$I_{ref}(t) = \frac{1}{4} I_0 (1 - \cos(\phi_d)) \quad (4.13)$$

$$I_{ref}(t) = \frac{1}{2} I_0 (\sin^2(\phi_d/2)) \quad (4.14)$$

Thus we can make a three-point measurement to simplify equation 4.11. The peaks of the reference signal correspond to the in plane or p polarisations and the trough correspond to the normal or s polarisations. A point half way between the p and s polarisations gives intensity at 45° orientation of the beam. Thus respective intensities, I_p , I_s and I_{45} are measured at the detection arm from which ψ and Δ can be extracted by simple substitution and algebraic manipulation. The actual measurement is done via a 12-bit ADC with 100K samples per second. Both the reference and the detected signals are read in to a computer for processing.

4.4 Experimental analysis of the PCMCSA system

Before any measurements on optical samples are undertaken, the performance of the system and accuracy needs to be characterised. In this section, several experiments carried out in that respect are presented.

4.4.1 Calibration

The polarising components in the system are calibrated relative to a common reference plane. All angles are measured from the direction of the linear eigen polarisations of the optical system under measurement and are taken positive in the counter clockwise sense when looking against the propagation direction of the beam.

Calibration of linear polariser is done based on what is known as Brewster law [8] which states that when a beam of partially polarised or unpolarised light hits a boundary between two isotropic surfaces of refractive indices n_0 and n_1 where $n_0 < n_1$, at an angle of incidence ϕ_i equal to $\tan^{-1}\left(\frac{n_0}{n_1}\right)$, the reflected light is completely polarised with its \mathbf{E} -field perpendicular to the plane of incidence (parallel to the boundary surface). The reflected light is then used to calibrate the transmission axis of the polarisers.

The QWP's were calibrated by aligning one of them between two crossed linear polarisers. Rotating the QWP results in 4 null or zero intensity points. These points occur at 45° away from the fast-slow axes of the QWP.

4.4.2 Azimuthal Alignment

At the input end of the HiBi fibre, the alignment of the fibre eigen axis relative to the input polariser and QWP is immaterial. This is because the polariser and QWP preceding the fibre are oriented at 45° relative to each other so that a circularly polarised beam is launched into the fibre which could be resolved equally into two normal eigenmodes of the fibre irrespective of their angular orientations.

At the output end of the fibre however, the azimuthal alignment of the fibre eigen axis and the fast-slow axis of the QWP which follows is important. For this application a 45° azimuthal relationship is required. The way this is achieved is by launching a linear polarised light in to one of the eigenmodes of the fibre at the input and arrange a glass reflector with the angle of incidence equal to Brewster angle, twisting the fibre at the output until no light is reflected from the glass. This ensures the eigen axes of

the fibre to be aligned with the plane of incidence. The QWP is then oriented at 45° relative to the same plane.

Another way of verifying the angular alignment of QWP with the fibre eigen axes is in fact at 45° is by rotating the analyser. Varying the azimuthal orientation of the analyser just after the QWP should not change the amplitude or depth of modulation of the detected signal while the phase varies. This has been experimentally verified.

4.4.3 Signal Analysis

The reference and detected signals are analysed with no sample in place. At the reference arm, the signal is a sinusoidal function of the modulated phase, see equation 4.14. If the detection signal is looked at through an analyser at 45° with no sample, the stokes vector is given by

$$\begin{bmatrix} S_0 \\ S_1 \\ S_2 \\ S_3 \end{bmatrix} = \frac{1}{2} I_0 \begin{bmatrix} 1 + \sin(\phi_d(t)) \\ ? \\ ? \\ ? \end{bmatrix} \quad (4.15)$$

$$I_d(t) = \frac{1}{4} I_0 (1 + \sin(\phi_d(t))) \quad (4.16)$$

The straight through and the reference signals detected resulting from the polarisation modulation are shown below in figure 4.3 below.

The nature of the Doppler signal reflects the directional manner in which the fibre is being stretched. The signal on either side of the turning point is mirror images resulting from the rising and falling directions of the oscillator signal driving the modulation unit.

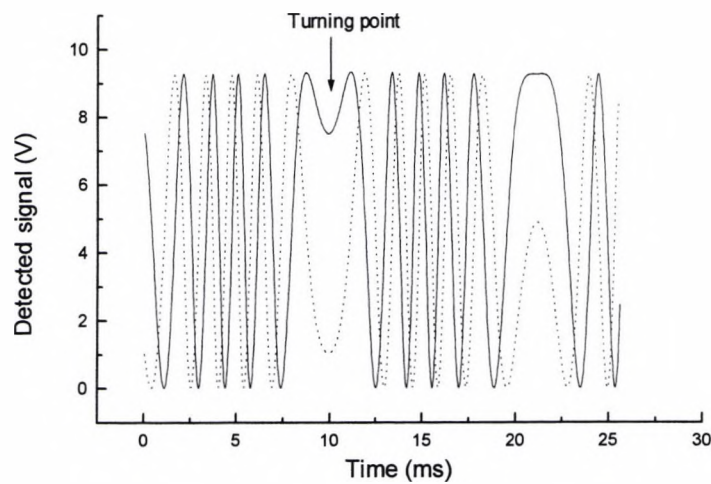


Fig. 4.3 Shows signal fringes, where '—' is the detection signal and '...', is the reference signal.

The signal processing described in section 4.3 is applied to the straight through signal for calibration. The results obtained from either side of the turning point differed slightly. This is due to the effect of the 4% back reflection from the fibre ends detected coherently with the main signal. Chitaree et al. [7] has given mathematical as well as experimental accounts for this phenomenon. A close study of the detected signals shows high frequency components superimposed on the main signal as well as a beat frequency fluctuating at the same frequency as the modulated signal. The low frequency content of the signal can be seen looking at the signal from the second compensator before the analyser.

Equation 4.6 shows that this signal should be a dc signal, while in practice it was found that the detected signal is composed of an envelope at the modulated frequency with high frequency components [1] see figure 4.4 below.

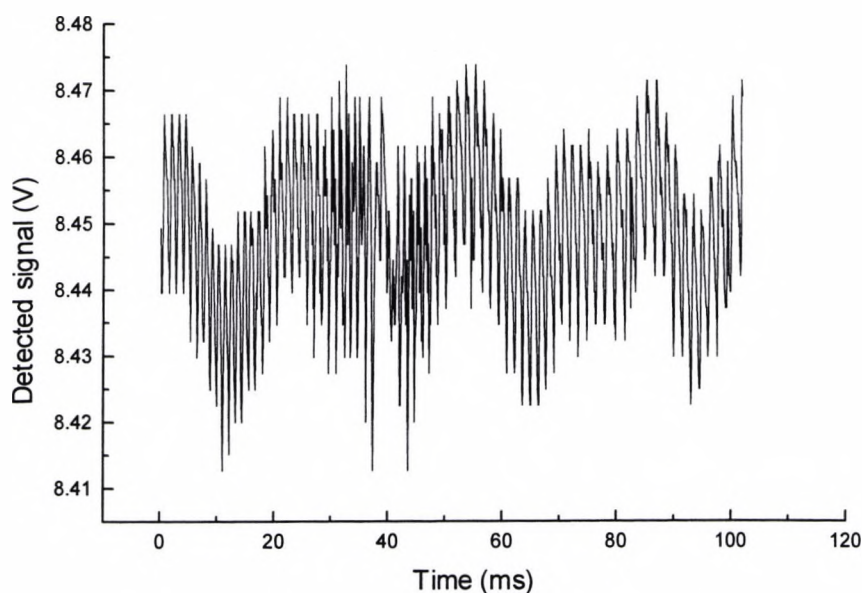


Fig. 4.4 Illustrating the beat pattern and high frequency fluctuation resulting from coherent interference of the main signal and back reflection signal.

The effect of back reflections gives rise to intensity fluctuations; it could also introduce variation in the SOP of the RPP beam. Cutting down the intensity of the reflected signal can reduce the beat effect. There are several techniques commonly applied to cancel the effect of back reflections. These include index matching gel, antireflection coating of the fibre ends or tilted end faces to deviate the reflected light [9]. In this application both the fibre ends were carefully cleaved at angles $< 10^\circ$. This technique was found to give better quality end face finish than hand polishing the fibre ends at an angle with films of differing grades of roughness.

Figure 4.5 shows the high frequency components superimposed with the main signal. It is also to be noted that the unequal amplitude levels of the fringes are due to the beat pattern resulting from back reflection interference. It shows that the back reflections have introduced $\sim 5\text{-}6\%$ amplitude uncertainty. The data on figure 4.6 are

taken with tilted end faces and show a reduction of the high frequency components (<1%) and thus the detected signal is more stable.

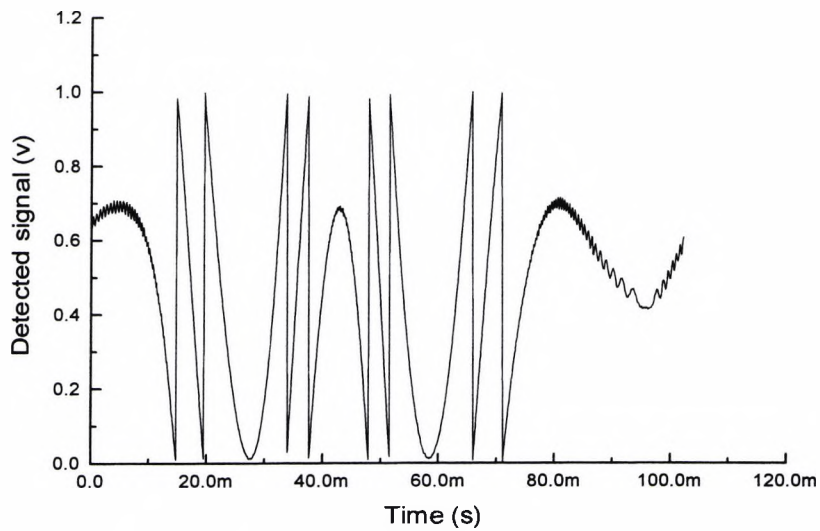


Fig. 4.5 detected signal with high frequency components from a fibre cut at 90° end face.

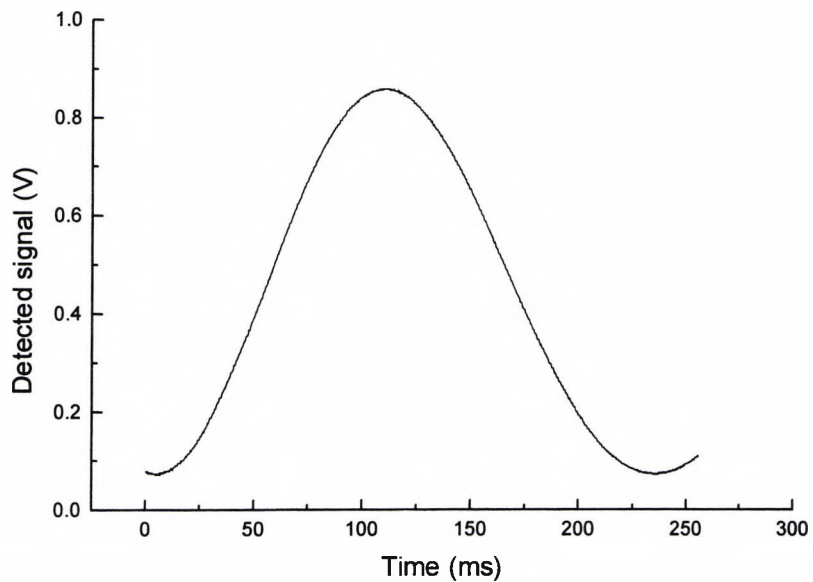


Fig. 4.6 Illustrating the reduction of high frequency components after the fibre end is cut at an angle.

The measurement uncertainty introduced due to the coherent detection of back reflections is perhaps highlighted by looking at the amplitude of the detected fringes on either side of the turning point. Figure 4.7 shows a model of the effect of beat pattern on the amplitudes of the fringes with the envelope signal at the modulation frequency. It can be seen that the signal not only consists of the fringes resulting from the interference of the main flux along the two eigenmodes, but also a signal resulting from the interface of back reflection at the modulation frequency is added to the main signal. This results in undesirable variation of measurements taken on either side of the turning point which suggests a differing performance of the overall measuring system depending on the direction of modulation. The reduction of the effect of back reflection is thus an important requirement for improved measurement accuracy. The overall result is that the measurements on either side of the turning point show a smaller spread around the average expected value. However, it should be noted that the inconsistency of the results on either side of the turning point is not the sole result of back reflections. Factors such as polarising components azimuthal misalignment, component imperfection or any fibre bending birefringence also contribute to such measurement inaccuracy, see chapter 5 for fuller analysis.

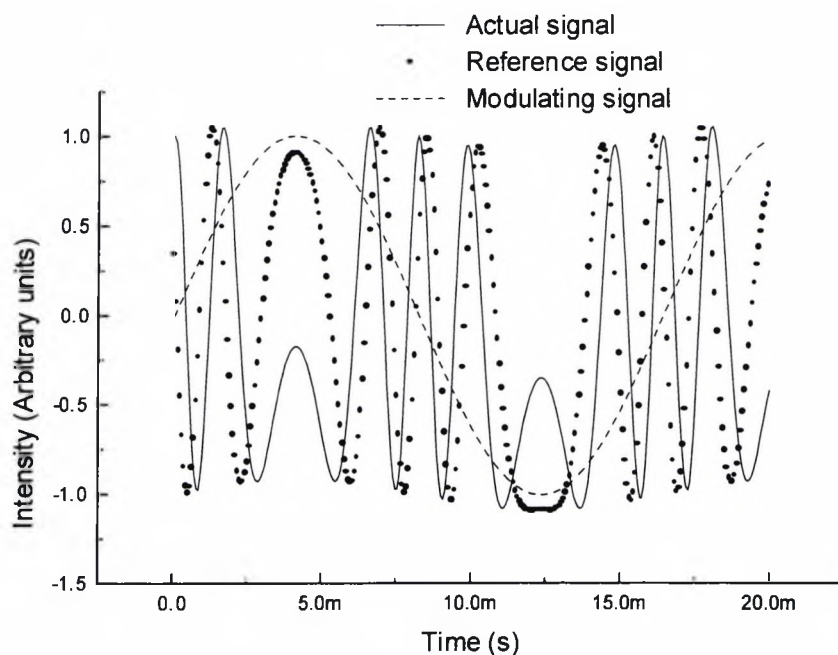


Fig. 4.7 Illustrating the effect of beat pattern resulting from back reflection. The simulated data shows that the amplitudes of the fringes on either side of the turning point are unequal.

The quality of the RPP beam was also analysed in terms of its DOP and ellipticity. To such end the Stokes parameters were measured. A DOP of 99.7% and ellipticity of 0.0118 have been measured. This indicated a good quality RPP beam has been generated which can be applied for ellipsometric measurements.

4.5 Ellipsometric parameters and system calibration

A number of experiments have been carried out to investigate the performance of the system and to evaluate average system errors associated with the ellipsometric parameters, Δ and ψ , as a basis for improvement in further measurements. The “straight through” optical signal is analysed to measure ψ and Δ , with no sample placed on the signal arm, and the results of this experiment are shown in figure 4.8

below, where $\cos(\Delta)$ and $\tan(\psi)$, are scattered around a theoretical value of unity with respective standard deviations of 3.46×10^{-3} and 1.82×10^{-3} . The system is found to have an acceptable average error of 1.31° in Δ and $6.2^\circ \times 10^{-2}$ in ψ , using known calibrated optical components.

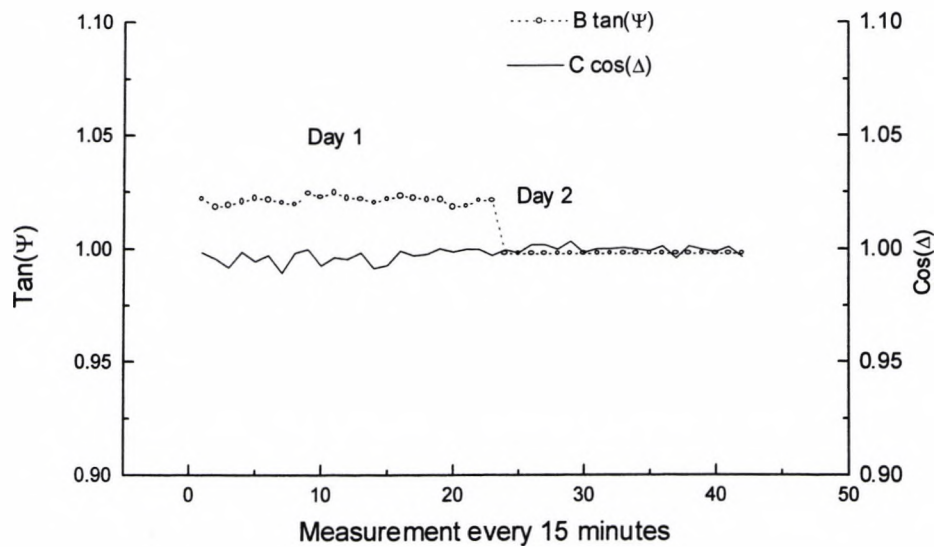


Fig. 4.8 Repeatability in the measurement of ψ and Δ over time.

In figure 4.8 above, the first 20 readings were taken on a same day at 15 minute intervals, and the further points were taken three days later on the same interval of 15 minutes every reading. The measurements show $\cos(\Delta)$ and $\tan(\psi)$ were repeatable with in $<1\%$, although $\tan(\psi)$ showed a slight change over the two days measurement. This could be due to systematic error introduced over time by alignment changes.

4.6 Determination of optical parameters of samples with a HiBi PME

So far the technique of PME for measurement applications has been analysed thoroughly and the performance of the system has been optimised.

As described before, the ellipsometer measures the quantities ψ and Δ . We use these quantities along with some model to calculate the optical properties of the given material, i.e. complex refractive index, film thickness, surface roughness etc. Although ψ and Δ are measured accurately to within the measurement resolution of the ellipsometer employed, the reliability of the calculated properties is only as good as the assumed model. Thus if an improper model is assumed, although the values of ψ and Δ are correct, the calculated refractive index or film thickness may well be meaningless [10].

Most of the time, ellipsometric measurements deal with characterisation of optical properties of substrates and films. The distinction here is that a material is considered as substrate if it is thick enough such that the light reflected at the lower boundary does not return to the ellipsometer measuring system or if it absorbs the reflected light beam before it reaches the lower boundary. A film on the other hand is a thin transparent material in which the light reflected from the upper and lower boundary of the sample is available for ellipsometric detection.

The transformation of the SOP of the light by reflection is the basis of ellipsometry for the determination of important optical properties of materials. One such property is the complex refractive index of a material. This parameter is important in

classifying optical medium in to absorbing or non-absorbing at certain wavelength, knowledge of which has obvious application in manufacturing optical devices.

In general the refractive index, N is defined as a complex quantity such that $N = n-jk$, where n is the real refractive index and k is the absorption coefficient [11]. For non-absorbing samples, k is zero.

4.6.1 Two phase system

In this case light is reflected at a boundary between the substrate and ambient phase of known optical properties. The ambient must be light transmitting and should not contaminate or disturb the optical properties of the substrate [80].

It is shown in chapter 2, equation 2.13, that the measured quantities Δ and ψ are related to the ratio, ρ , of the complex Fresnel reflection coefficients for p and s polarisation states. Thus a one point measurement of Δ and ψ provides enough data to calculate the complex refractive index of a sample.

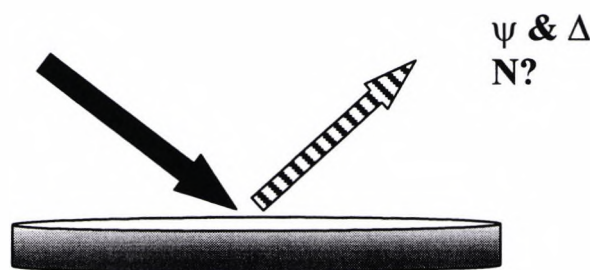


Fig. 4.9 Two-phase system.

4.6.2 Experimental results

The experimental set up described in section 4.1 and depicted in figure 4.1 is used in this experiment. Both non-absorbing and absorbing samples are studied with the ellipsometric set up to measure Δ and ψ and determine the complex refractive index of the sample.

4.6.2.1 Non absorbing sample: Air - glass interface

An industry standard BK7 glass (Commar Inst.) with known refractive index of 1.51 is used in this experiment. The glass is wedge shaped at 10° to separate the reflections from the upper and lower boundaries and thus avoid unwanted interference that could result in measurement inaccuracy. The glass was mounted on a calibrated micrometer with rotation of 360° along a central axis. Δ and ψ measurements were recorded at various angles of incidence ranging from 10° to 70° with steps of 5° . The results of this experiment are shown in figure 4.10 below.

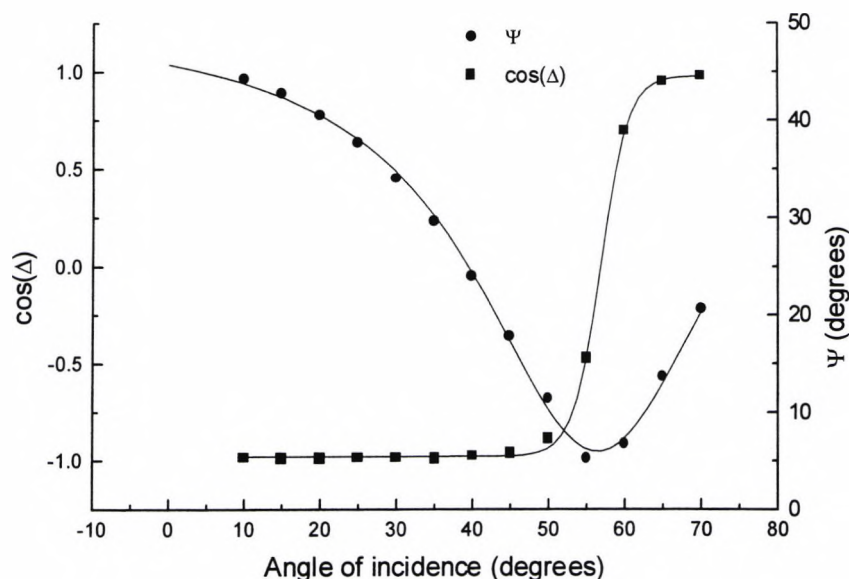


Fig. 4.10 ψ and $\cos(\Delta)$ measurements for a Bk7 glass sample. Dotted line represents measured data, smooth line is calculated data.

The shapes of the curves agree with theoretically simulated ones as shown by the smooth line curve. For a glass of refractive index 1.5, the Brewster angle, ϕ_b is at 56.3° . For angles below ϕ_b , $\Delta=180$, while for angles less than ϕ_b , Δ becomes zero. This is verified in the results obtained in figure 4.10.

Notice also ψ reaches minimum at ϕ_b as expected, since the p component of the reflected light at ϕ_b is theoretically zero. The slight deviation of ψ from zero is explained by the fact that r_p being minimum near ϕ_b introduces a large error as I_p becomes small and comparable to the degree of background noise, this is not considered as a major weakness of this instrument as measurements near Brewster angle could be avoided. It should also be remembered that there is some error ($<\pm 0.5^\circ$) in the accuracy of the angle of incidence setting.

As shown in figure 4.10, at 70° , on average Δ and ψ deviate from ideal values for BK7 glass by $<2^\circ$ and $<0.5^\circ$ respectively. This gives a refractive index of 1.505-

$j0.071$ in comparison to the manufacturer quoted value of 1.51. The small imaginary component of calculated refractive index is partly the result of systematic errors on Δ measurement partly due to sample surface contamination. Similar refractive index values were calculated at other angles of incidence. The error figure mentioned above is not a big concern for non absorbing or strongly absorbing samples. In the case of weakly absorbing samples however, in which case 'k' is very small and may lie within the measurement uncertainty, the accuracy of measuring $\cos(\Delta)$ is important. One suggestion [1] is to add a further 90 phase shift to the light reflected from the sample with an additional QWP so that the measurement is carried out at the more sensitive region of the cosine curve. This however comes with added cost and complication to the system as the QWP should have a very low retardance error or at least well quantified, otherwise it would introduce further systematic error.

4.6.2.2 Absorbing sample: Air-silver interface

Similarly an air silver interface was investigated for the determination of the complex refractive index of the silver substrate. Silver substrate was prepared on a glass surface by sputtering in a vacuum chamber. The silver layer was developed so that it is thick enough to be considered as a bulk substrate. Soon after the substrate was prepared, measurements were carried out to avoid contamination of the silver surface by atmospheric gases. Again Δ and ψ measurements were taken at angles of incidence 10° to 80° . The results are shown in figure 4.11 and figure 4.12.

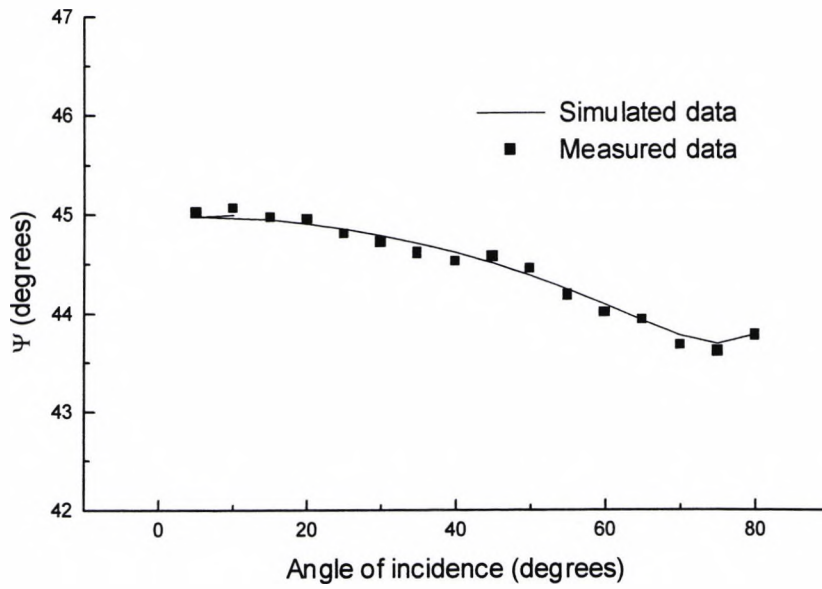


Fig. 4.11 Measurement of ψ for an air/silver interface at various angles of incidence.

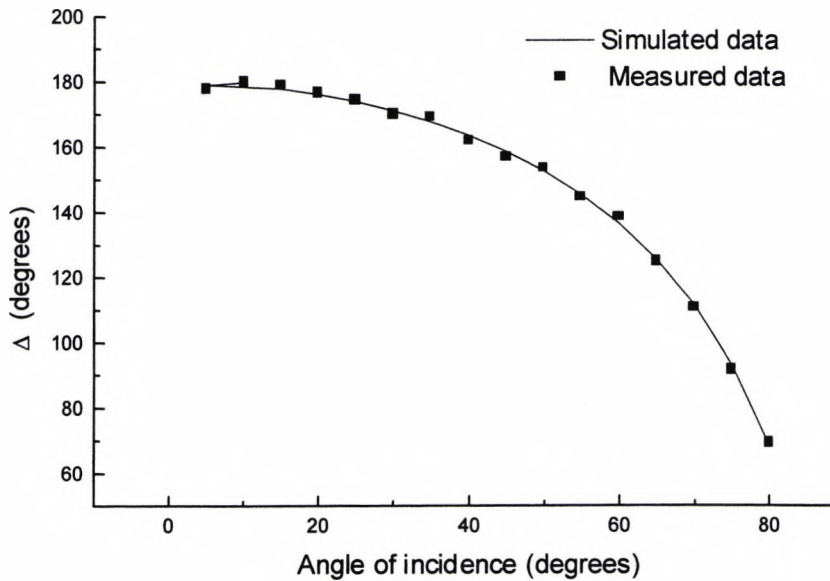


Fig. 4.12 Measurement of Δ for an air/silver interfaces at various angles of incidence.

Notice that the value of ψ does not equal to zero at any angle of incidence, but rather it exhibits a minimum whose value depends on the extinction coefficient, k . The angle

of incidence at which this happens is called pseudo-Brewster angle, ϕ_b [6]. Thus for absorbing samples there is no restriction on the useful angle of incidence. Δ and ψ show deviations of $\sim 1^\circ$ and 0.1° respectively around their mean values. The complex index of refraction was measured at various angles of incidence, and the average result obtained was $0.143-j3.032$ in comparison to text book figure of $0.18-j3.67$, showing a strong absorption represented by the higher extinction coefficient, k .

4.7 Summary

The performance of FPME has been investigated thoroughly. In particular a simulated as well as an experimental account of the effect of coherent detection of back reflection light from the fibre ends on the measurement system has been given. Steps have been taken to minimise the overall effect of the back reflections on the measurement system. This resulted in a closer performance of the measurements taken from both sides of the Doppler signal. Further measurement accuracy improvement is achieved by averaging the measurement from either side of the turning point. Averaged measurement values of both absorbing and non-absorbing samples were presented with respectable accuracy. In the next chapter, measurements carried out on the three-phase system are presented.

Reference

1. Chitaree, R., Weir, K., Palmer, A. W. and Grattan, K. T. V. (1994) "*A Highly Birefringent Polarisation modulation scheme for ellipsometry: System Analysis and performance*" Measurement science and Technology. Vol. 5, p. 1226-1232.
2. Shamir, J. and Klein, A. (1986) "*Ellipsometry with rotating plane polarised light*" Applied Optics, Vol. 25, p 1476-1480.
3. Singher, L., Brunfeld, A. and shamir, J (1990) "*Ellipsometry with a Stabilised Zeeman Laser*" Applied optics, Vol.29, p. 2405-2408.
4. Tatam, R. P., Jones, J. D. C., Jackson, D. A. (1986) "*Optical polarisation state control schemes using fibre optics or Bragg cells*" J. Physics E. Sci. Instrumentation, Vol. 19, p. 711-717.
5. Yoshini, T. and Kurosawa, K. (1984) "*All Fibre Ellipsometry*" Applied optics Vol.23, p 1100-1102.
6. Azzam, R.M.A. and Bashara, N.M. (1977) "*Ellipsometry and polarized light*" (Amsterdam: North Holland).
7. Gerrard, A. and Burch, J. M. (1975) "*Introduction to matrix methods in optics*" (John Wiley and Sons)
8. Hect, E., Zajac, A. (1979) "*Optics*" (Addison-Wesley Publishing company, Inc.)
9. Ulrich, R., Rashleigh, S. C. (1980) "*Beam to fibre coupling with low standing wave ratio*" Applied Optics vol. 19, p. 2453-2456.
10. Harland, G. T. (1993) "*A Users Guide to Ellipsometry*" (Academic Press Inc.)
11. Grant R. Fowles (1968) "*Introduction to Modern optics*" (Holt, Rinehart and Winston, Inc.)
12. Bashara, N. M., Buckman, A. B., Hall, A. C. (1969) "*Recent developments in ellipsometry*" (North Holland Publishing Company- Amsterdam)

Chapter 5

Ellipsometer for following dynamic film growth and sensor applications

Abstract

Optical sensor technologies for chemical and biological sensing applications have a number of advantages as mentioned briefly in chapter one. In this chapter an attempt is made to demonstrate the ability of the ellipsometer for film thickness measurements and also monitoring surface interactions of a film with external perturbations. A study of formation of oil films on water surface and variation of thickness is followed with the HiBi ellipsometer. The purpose of this chapter is to present dynamic measurements of a surface with the fibre ellipsometer for potential sensing applications.

5.0 Introduction

Ellipsometry is a useful non-destructive technique for characterisation and observation of time resolved events at an interface between two media [1]. The most important application of ellipsometry is in the study of thin films. The determination of optical parameters of thin films such as its complex refractive index and film thickness accurately is important in the design and fabrication of optical and semiconductor devices [2][3]. Other important industrial applications include monitoring oxidation and corrosion of metals, adsorption, electrochemistry etc. in which time resolved measurements provide important information on the dynamic process and the materials involved.

Ellipsometry has been applied for thin film measurements extensively, as such a number of different configurations have been introduced by several authors [4-8]. The theoretical background behind thin film measurement is briefly described in chapter 2. In this chapter, the PCMCSA ellipsometer is configured to monitor dynamic film growth of oil films on water surface and also the response of sol-gel films developed on silicon substrate to environmental perturbations such as humidity and temperature variations is studied. The potential application here is in sol-gel based chemical sensor applications. The aim of such experiments is to serve as a demonstration that the HiBi fibre polarisation modulated ellipsometer can be used as a thin film or surface sensor. In the first section of this chapter, thin sol-gel films developed on silicon substrates (obtained from Dublin City University) with different thickness were measured for their thickness as verification that the HiBi ellipsometer could measure differing

thickness levels. The sol-gel films are then subjected to environmental perturbations in which the variation in time of the properties of the films is followed by the FPME.

In the latter part of the chapter, results obtained from the spread of oil films on water surface are presented.

5.1 Sol-gel based thin film measurement

It has been described in chapter 1 that optical sensor technology for chemical sensing applications has several advantages over conventional methods. In particular, the advantages of real time *in situ* detection has drawn a considerable interest in a new class of chemical transducers which utilises specifically sensitised films on substrates [9]. The use of sol-gel to produce such films has been found attractive [11-14] in that the chemical or biological reagents can be entrapped in sol-gel derived materials relatively easily, furthermore, sol-gel based sensors can be mass produced easily.

Although the sol-gel films provided were not specifically tailored for ellipsometrically film thickness or refractive index changes sensing, such tailoring of sol-gel films for film thickness or refractive index sensing are possible [9][10].

5.1.1 Experimental condition

The PCMCSA set-up described in chapter 4 is used here in the measurement. The sample is a set of sol-gel films developed on a silicon substrate.

5.1.1.1 Film preparation

A mixture of SiO_2 and TiO_2 is used in the preparation of sol-gel processes. Production of thin films involves dip coating by lowering the substrate into the solution and

withdrawing it a defined speed [15]. The thickness of the films increases with increasing speed and viscosity of the solution.

In this case, silicon substrates were dipped and withdrawn from the solution at different speeds to obtain a range of film thickness. The refractive index of the films depends on the SiO₂: TiO₂ mixture ratio, which was kept uniform throughout the preparation of the films, provided for this experiment.

5.1.1.2 ψ and Δ measurements

Unlike the bulk optic two phase system measurements of chapter 4, in the case of thin film measurements, the parameters ψ and Δ are not only a function of the refractive index of the film and substrate, but also are affected by the thickness of the film which subjects the incident light in to multiple reflections between the ambient-film and film-substrate interfaces.

Three sets of sol-gel films of different values of thickness on silica substrate were measured using a HiBi ellipsometer. The films and substrate were calibrated at the Dublin City University. The refractive index of the sol-gel film was recorded as 1.58 and the complex refractive index of silicon is measured at $3.85 - j0.018$ at 632.8nm wavelength light. These figures are used to validate ψ and Δ measurements of the HiBi ellipsometer.

The samples were placed for measurement and the results are depicted on figures 5.1 and 5.2. Measurements were taken at angles of incidence from 5 ° through to 80° in steps of 5°.

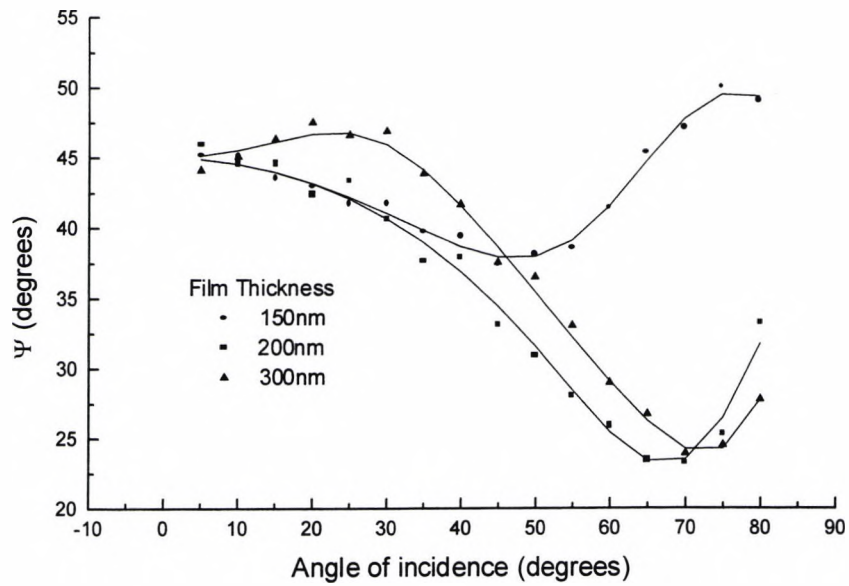


Fig. 5.1 Ψ Measurements of three sol-gel films of different thickness on silica substrate at various angles of incidence. Dotted curves are measured values. Smooth lines represent calculated values.

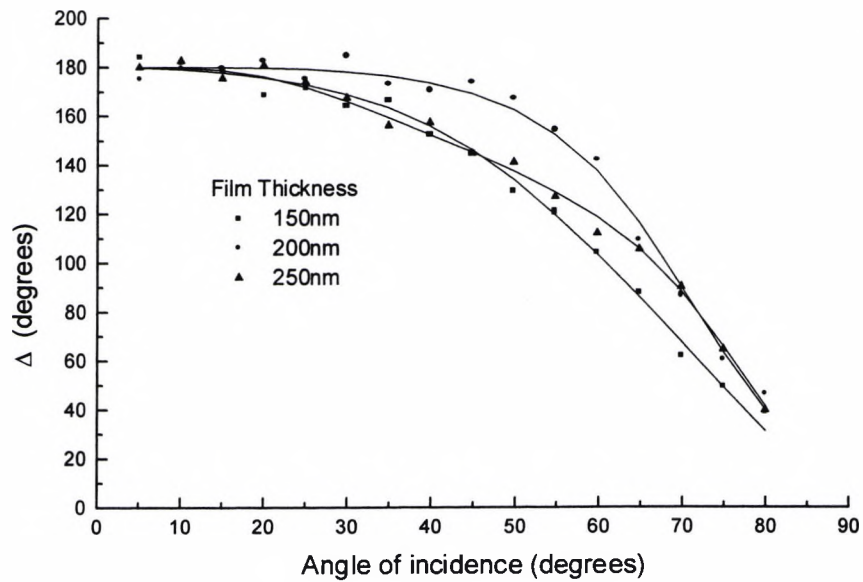


Fig. 5.2 Δ Measurements of three sol-gel films of different thickness on silica substrate at various angles of incidence. Dotted curves are measured values. Smooth lines represent calculated values.

In Figures 5.1 and 5.2, the scatter curves show measurement results and the smooth curves show calculated ψ and Δ values. These values were calculated assuming the ambient refractive index of air is 1 and silicon substrate index of $3.858-j0.018$. The sol-gel samples were prepared with controlled Silica: Titania (SiO_2 : TiO_2) ratio so as to give similar refractive index of 1.58, while the values of the thickness were made different with varying coating speeds.

The results shown on Figures 5.1 and 5.2 show a relatively small spread of measured results from calculated values. On average, ψ showed a smaller spread of $<2^\circ$ while Δ differed by slightly higher value of $<10^\circ$ partly in agreement with the fact discussed in chapter 4 that Δ values are less accurate in this particular measurement system. Although the measurements were carried out in few days of receiving the samples from Dublin City University, it is understood that the film characteristics may vary due to environmental effects and ageing [16]. Thus temperature and humidity variation as well as systematic errors such as optical component imperfection are presumed to have contributed the small discrepancy between measured and calculated ψ and Δ values.

5.2 Thin film based sensor system

So far the ellipsometric measurements carried out have been on the determination of optical constants of samples. If however the properties of a particular sample are known to vary by external effects such as the presence of a certain gas or a biochemical reagent, humidity, heat etc. it is possible that the present system can be utilised as a sensing device. As the measurements in section 5.1.2.2 show, various thicknesses among the three different films resulted in different sets of measured ψ

and Δ values. This opened up a potential for the fibre ellipsometer in sensing applications where the polarisation of light is affected by variations of the properties of the sample, namely thickness or refractive index change.

In the last few years, there has been a growing interest in a new class of chemical transducers which utilise a specifically sensitised films formed via sol-gel processing techniques [9]. Sol-gel films enable suitable reagents to be entrapped within the sol-gel matrix [17]. In addition it is possible to control the film properties. Such sensors operate by monitoring the changes in refractive index; fluorescence or absorption spectrums [9][10] of the films as it interacts with the chemical species.

In this work, the potential use of a fibre ellipsometer in a sol-gel based sensor system is demonstrated. In the experiment carried out a sol-gel films on silicon substrates were measured as the samples were subjected to varying temperature and humidity. It should be noted that the set of sol-gel films tested here were not specifically made for humidity or temperature measurements, the objective of the test is to demonstrate the potential use of the fibre ellipsometer as a sensing device.

5.2.1 Temperature effects

In optical sensing, sol-gel films are useful as representing a typical porous matrix into which various sensing agents may be doped. The ellipsometer provides an excellent means to interrogate such films, as is investigated here for such a purpose. One such sensor application was tested to quantify the effects of temperature on sol-gel films, as it varies from 22°C to 90°C; the results in figures 5.3 and 5.4 below show the time response of the film in terms of the two ellipsometric parameters.

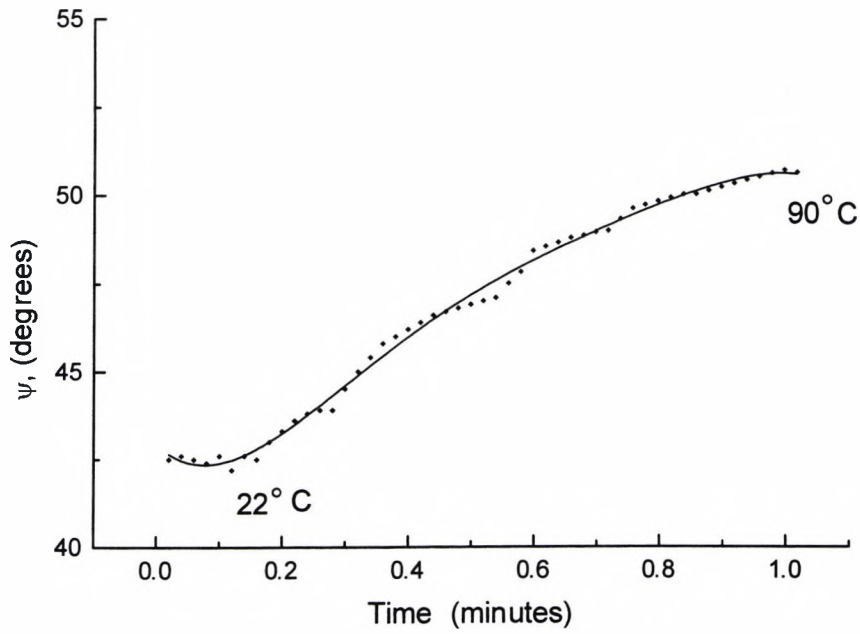


Fig. 5.3 Variation of, ψ of the thin film on exposure to temperatures up to 90° over a period of 1 minute.

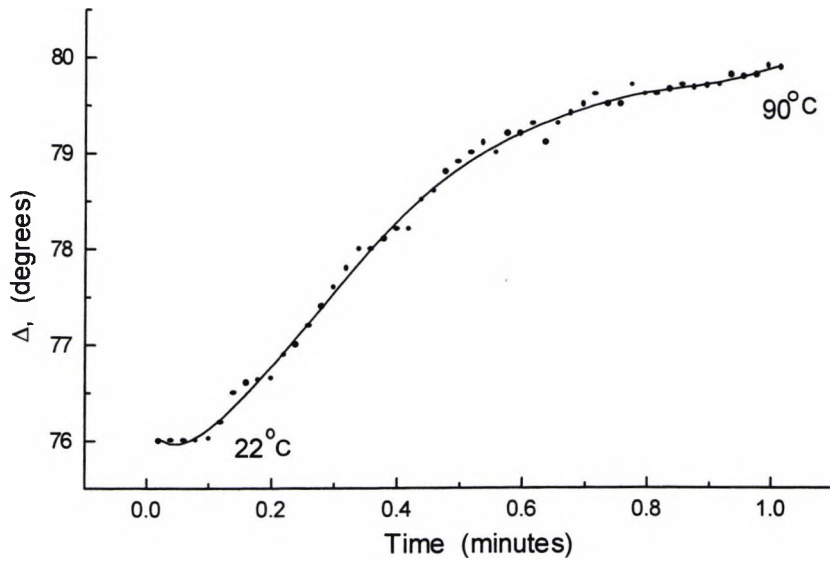


Fig. 5.4 Variation of, Δ of the thin film on exposure to temperatures up to 90° over a period of 1 minute.

In the first few seconds, temperature is kept constant at laboratory temperature. It is then followed by a rise in temperature up to about 90°, a ceramic resistor with an adjustable current placed in contact with the silicon side of the sample is used a source of heat. The data produced shows the sensitivity of the film to temperature, the results also show that the change in the ellipsometric parameters, ψ and Δ were found to be irreversible, thus the technique with these particular sol-gel films could not be used as a temperature sensor. The results do however highlight need for careful temperature compensation in other sensor applications using such films.

5.2.2 Humidity effects

Another application considered is the effect of humidity on the sol-gel sensing application: this being done by evaporating small amount of water on the film for several minutes as a measurement is taken. The results of this are shown in figures 5.5 and 5.6. The measurements show that, with the application of humidity, the porous structure of the sol-gel matrix structure entraps this humidity which changes the film properties that are reflected in changes to ψ and Δ . The results with this particular sol-gel sample also show that once the film is exposed to humidity, the interaction is not reversible. The general observation is that the effect of humidity on the films tested was not uniform for various films of different thickness. In fact some of the films were found to respond slower than others and not all the films respond to the same level of sensitivity. Such results would help in the design of sol-gel based sensor films with desired levels of sensitivity to humidity.

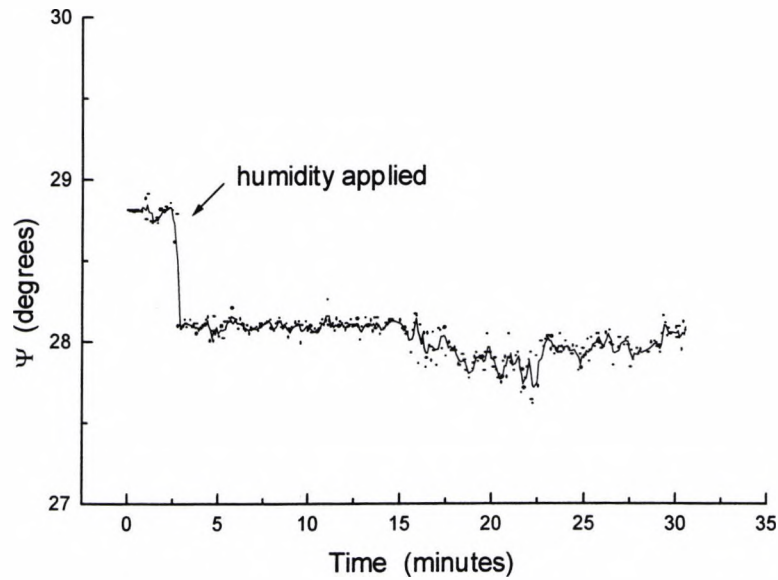


Fig. 5.5 Variation of ψ , as the sol-gel film is exposed to humidity.

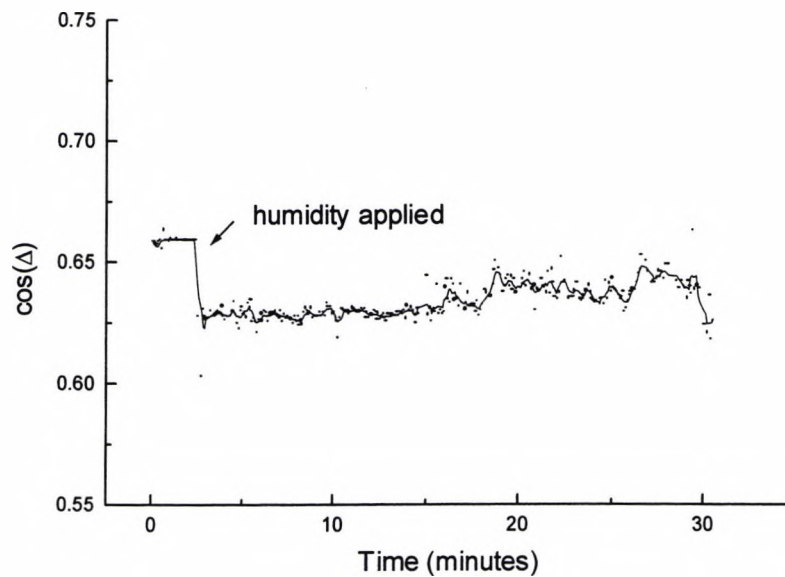


Fig. 5.6 Variation of $\cos(\Delta)$, as the sol-gel film is exposed to humidity.

Although this batch of sol-gel based films did not show any real prospect of temperature or humidity measurement using ellipsometry, with the development of sol-gel manufacturing techniques and availability of certain dopants sensitised to

specific parameters, the potential for such a system cannot be ruled out. The experiment does however highlight the need for careful consideration of temperature and humidity variations in sol-gel based sensing systems. It should also be mentioned that although fluorescence and adsorption have been major techniques on sol-gel based chemical sensor [9][11] monitoring changes in refractive index of the film as it interacts with chemical species is a real prospect [10]. In that respect, inexpensive FPME such as that discussed here offers the advantages of real time measurements in chemical sensing applications.

5.3 Dynamic oil film thickness measurements

Dynamic measurement of films of rapidly varying thickness or film deposition is very useful in a number of industrial applications. In this study it is shown that a simple ellipsometer of this type can be easily configured for such measurements.

The motive behind this study has been to demonstrate the potential application of the HiBi PME in rapid time resolved measurements. This will have applications in surface monitoring, chemical reaction and film deposition on liquid or solid surfaces etc. As mentioned before, based on the ratio of two reflectance coefficients, ellipsometry is insensitive to ambient conditions and thus is ideally suited for real time process monitoring in various environments. One interesting application is in the formation of Lagmiur-Blodgett (LB) films. These are made by forming monolayers on liquid substrates and transferring them to a solid support for deposition [18]. LB films offer high potential for bio-chemical sensing applications [19] and ellipsometry has been applied in the study of such films [20][21].

In this study, ellipsometry is applied to monitor dynamic oil film formation on water surface.

5.3.1 Experimental configuration

The PCMCSA arrangement described chapter 4 is reconfigured for an angle of incidence of 75° . This angle being chosen for experimental convenience. Figure 5.7 below shows the experimental set up. The sample under measurement is oil film spreading over water surface. Continuous ellipsometric readings are taken in to a computer for analysis via a 12-bit ADC as the process of film formation progresses.

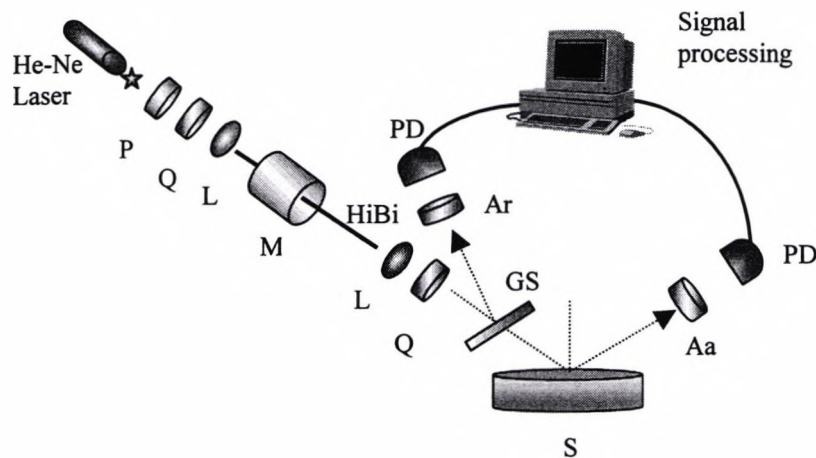


Fig. 5.7 Experimental set up of the Hi-Bi ellipsometer. P, polarising prism, Q, quarter wave plate, L, Lens, M, fibre stretcher, HiBi, birefringent fibre, GS, glass, A_r and A_a , analysers, S, sample, PD, photodetector.

5.3.2 Results and discussion

A series of oil films ranging from light cooking oil, engine transmission oil, synthetic engine oil, multipurpose MOBIL oil and 'three in one' lubricant oil etc were applied to water surface. On application of the oil to the water surface, the oil sample spreads and forms a thin film. As the oil spreads, the thickness of the film formed varies which can be calculated from knowledge of the ellipsometric parameters ψ and Δ . Measurements of ψ and Δ were taken continuously as the process of film formation progresses. Figures 5.8 and 5.9 show the results of ψ and Δ . readings for the spread of MOBIL lubricant oil on water surface. In the first 20 seconds, measurements were taken on water surface to produce a reference. A small drop of oil was then applied at one end of the tray while continuous measurements were taken. Figure 5.8 depicts results of ψ versus time. On application of the oil sample ψ increases abruptly and follows the wave of oil film formation. Measurements continued until the film thickness variation was seen to stabilise. This is noted by the measurements taken at the latter stage of the process after about 1 minute. At this point ψ varies slowly until it was seen to stabilise at a uniform level. The parameter Δ was found to be less sensitive to the thickness changes for this particular oil sample at 75° of incidence.

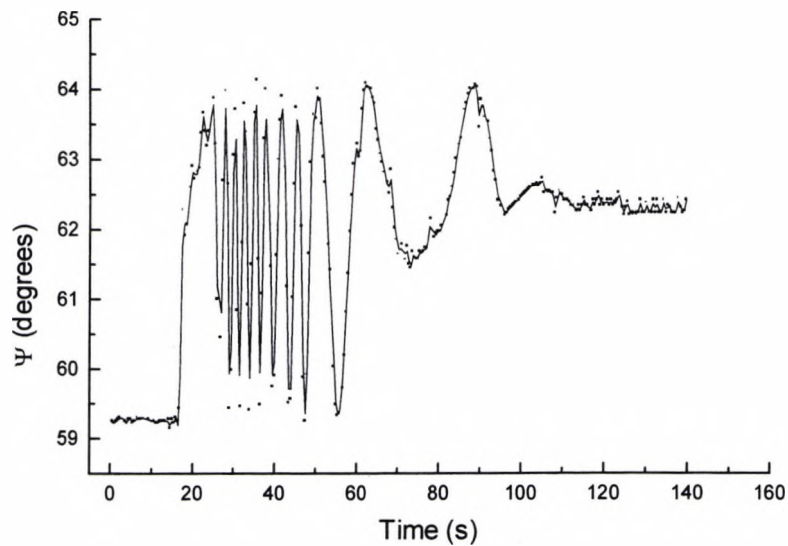


Fig. 5.8 variation of ψ with time as the oil spreads on water surface. The oil sample here is MOBIL lubricant oil.

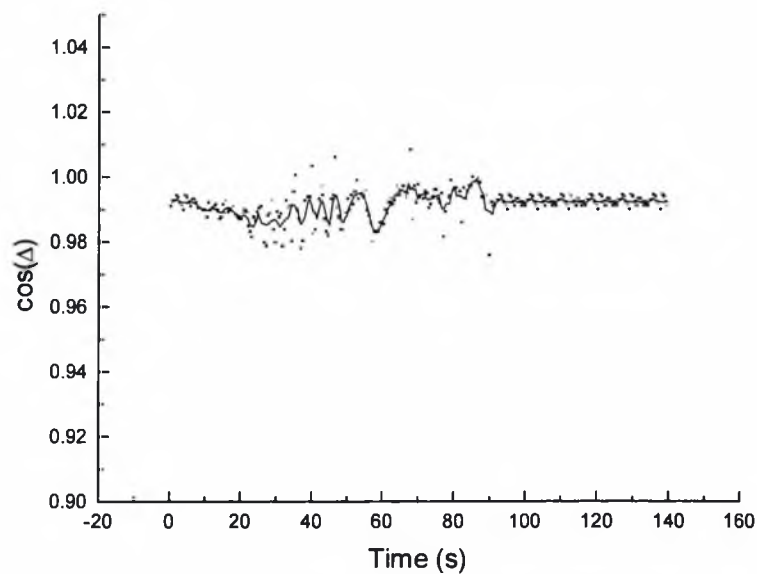


Fig. 5.9 variation of $\cos(\Delta)$ with time as the oil spreads on water surface. The oil sample here is MOBIL lubricant oil.

Similar measurements showing a different set of terminal parameters are seen for the other oil films. As a second example, the results obtained for transmission oil spread on water surface to form a film are also presented here.

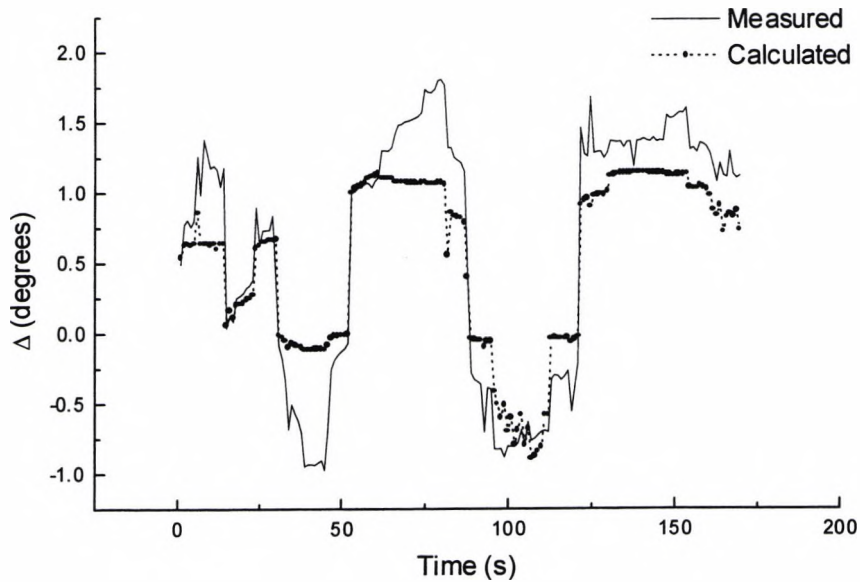


Fig. 5.10 Variation of Δ with the spread of transmission oil film, as the oil film thickness varies with time. Smooth curve is measured data Δ_m . Dotted curve is calculated, Δ_c data.

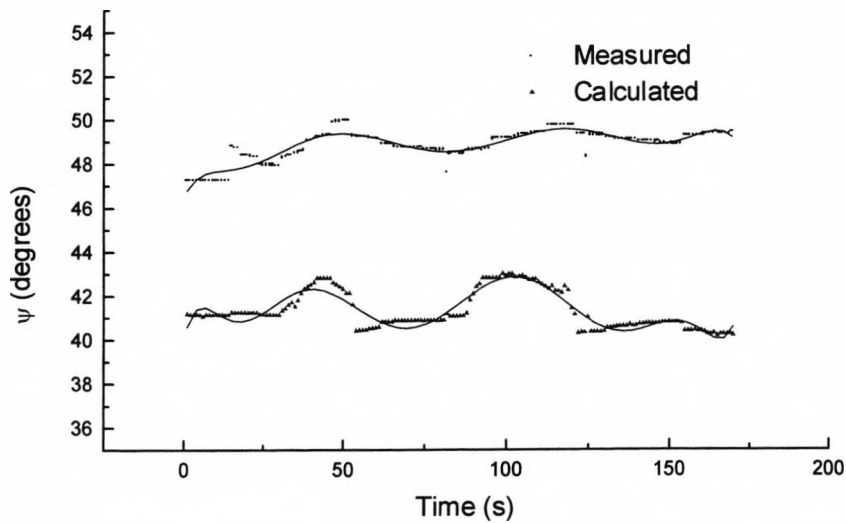


Fig. 5.11 Variation of ψ with the spread of transmission oil film, as the oil film thickness varies with time. Smooth curve is measured data ψ_m . Dotted curve is calculated, ψ_c data.

Figures 5.10 and 5.11 show the results obtained from the film formation process during the spread of transmission oil on water surface. Again a small drop of oil was

applied carefully without disturbing excessively the water surface. The thickness is seen to vary with time as the oil spreads.

The discontinuities in the graph show abrupt film thickness changes. This is due to the oil film breaking up on the surface. As a means of check on our measurements, a forward computation is carried out to calculate ellipsometric values, Δ_c and, ψ_c from the thickness measurements, the results are shown in figures 5.10 and 5.11. As it is shown in the above figures, there is a slight difference between the measured, Δ_m , and ψ_m and calculated Δ_c and ψ_c ellipsometric parameters. This is caused by film inhomogeneity, i.e. variation of refractive index through the thickness of the film and non-continuous film formation. Further more as the oil spreads it reacts with water consequently changing the refractive index of the oil film and also the substrate, in this case water. This is shown by forward computation [5] of film refractive index from measured thickness, Δ_m and ψ_m values. The computation assumes that the film-substrate model maintains stability and that the initial refractive index of the film and substrate remain unchanged. In practice of course this was not the case due to the cases listed above in the process of film formation. In an ideal situation it should be ensured that the film and the substrate do not react so that the refractive index of both the film and the substrate do not change as the oil spreads and that the film formation assumes homogeneity.

Although the experiments carried out with various oil films were not repeatable; the results however do show clearly the capacity of the ellipsometer to follow the film thickness changes. Different sensitivity levels for the ellipsometric parameters, ψ and Δ could also be noticed from the results among the range of oil films tested. A careful selection of the angle of incidence could improve the sensitivity to either ψ or Δ or

both, although due to practical limitations this was not an option in this particular laboratory set up. Another point worth mentioning of course might be the fact that the ellipsometer measurement was limited in time resolution which partly explains the abrupt changes of the measured parameters during the oil formation. With the present system a bandwidth of about 5-10Hz could be achieved. This however could be improved with faster data acquisition and processing techniques.

5.4 Summary

A birefringent fibre based PME has been employed for measurement of solid and liquid surfaces. The aim has been to demonstrate the ability of the system to follow dynamic process changes with a sensor application in mind. Although numerical inversion was not carried out on all the measurements, sol-gel films of different thickness ranging from 100nm to 300nm have been measured in terms of Δ and ψ . Tests carried out on the environmental as well as temperature and humidity effects on sol-gel films clearly showed a potential sensor application for the FPME. It must be stressed however, that the results obtained do not suggest the use of the ellipsometer in temperature and humidity sensing. The reason here is that the films did not show reversible or repeatable characteristics, which is necessary in sensing systems. For a successful use of the FPME in a sol-gel based sensor system, careful tailoring of the sol-gel film characteristics is required. This might entail reversible change of refractive index or film thickness in response to measurands of interest. These could be bio-chemical substances, gases etc. Oil film measurements also showed a promise for use of the fibre PME in dynamic process monitoring. The FPME is particularly suited for such application because polarisation modulation allows rapid time resolved

measurements. The problem with the measurements carried out on a liquid surface has been non-uniform film formation and film substrate mixing. Although this effect did not allow accurate comparison of the measured results and those obtained by numerical inversion, such results would be useful in characterising oil lubricants in terms of film formation, film strength and film continuity, water rejection etc for lubricant applications.

With careful film formation procedures such as those used in the manufacture of LB films on liquid surfaces, the potential for such simple FPME is good.

Reference

1. Azzam, R. M. A. and Bashara, N. M., (1997) "*ellipsometry and polarized light*" (Amsterdam: North Holland)
2. Lukosz, W. and Tiefenthaler, K. (1983) "*Embossing technique for fabricating integrated optical components in hard inorganic waveguiding material*" Optics Letters (8): p. 537-537.
3. Liddell, H. M., (1981) "*Computer-Aided techniques for the design of multilayer filters*" (Adam Hilger, Bristol)
4. Jaspersen, S. N. and Schnaterley, S. E. (1969) "*An improved method for high reflectivity ellipsometry based on a new polarization modulation technique*" Review of scientific instruments, Vol. 40(6). p 761-767.
5. Shamir, J. and Klein, A. (1986) "*Ellipsometry with rotating plane polarised light*" Applied Optics, Vol. 25, p 1476-1480.
6. Singher, L., Brunfeld, A. and shamir, J (1990) "*Ellipsometry with a Stabilised Zeeman Laser*" Applied optics, Vol.29, p. 2405-2408.
7. Yoshini, T. and Kurosawa, K. (1984) "*All Fibre Ellipsometry*" Applied optics Vol.23. p 1100-1102.
8. Chitaree, R., Weir, K., Palmer, A.W. and Grattan, K. T. V. (1994) "*A Highly Birefringent Polarisation modulation scheme for ellipsometry: System Analysis and performance*" Measurement science and Technology, Vol. 5. p. 1226-1232.
9. McCulloch, S., Stewart, G., Guppy, R. M. and Norris, J. O. W. (1994) "*Characterisation of TiO₂ – SiO₂ sol-gel films for optical chemical sensor applications*" International journal of Optoelectronics, Vol. 9, No. 3, p. 235-241.
10. Piraud, C., Mwarania, E. K., Yao, J., O'Dwyer, K., Schiffrin, D. J. and Wilkinson, J. S. (1992) "*Optoelectrochemical transduction on planar optical waveguides*" J. Light wave Technology. (10) p. 693-699.
11. MacCraith, B. D., McDonagh, C., McEvoy, A. K., Butler, T., O'Keeffe, G. and Murphy, V. (1997) "*Optical Chemical Sensors Based on Sol-Gel Materials: Recent Advances and Critical Issues*" Journal of Sol-Gel Science and Technology 8, p. 1053-1061.
12. Ding, J. Y., Shahriari, M. R. and Sigel, J. G. H. (1991) "*Fibre Optic pH Sensors Prepared by Sol-Gel; Immobilisation technique*" Electronics Letters, Vol. 27 (17) p. 1560-1562.

13. Yunfeng L., Ling, H., Jeffrey, C. B., Niemczzk, T. M., and Lopez, G. P. (1996) "*Chemical sensors based on hydrophobic porous sol-gel films and ATR-FTIR spectroscopy*" Sensors and Actuators B (35-36), p. 517-521.
14. Hidehito, N., Tsubakino, S., Habara, M., Kondo, K., Morita, T., Douguchi, Y., Nakazumi, H. and Waite, R. I. (1996) "*A novel chemical sensor using $CH_3Si(OCH_3)_3$ sol-gel thin film coated quartz resonator microbalance*" Sensors and Actuators B (34), p. 312-316.
15. Sumio Sakka (1994) "*Preparation and properties of Sol-gel Coating Films*" Journal of Sol-Gel Science and Technology 2, p. 451-455.
16. Badini, G. E. and Grattan, K. T. V. (1995) "*Sol-gels with fibre-optic chemical sensor potential: Effects of preparation, ageing and long-term storage*" Rev. Sci. Instrum. 66 (8) p.4034 - 4040.
17. McEvoy, A. K., McDonagh, C. and McCraith, B. D. (1997) "*Optimisation of Sol-Gel derived Silica Films for Optical Oxygen Sensing*" Journal of Sol-Gel Science and Technology 8, p. 1121-1125.
18. Roberts, G. G. (1985) "*An Applied science perspective of Langmuir-Blodgett films*" Advances in Physics, Vol. 34, No. 4, p. 475-512.
19. Toyosaka Moriizumi, (1988) "*Langmuir-Blodgett films as chemical sensors*" Thin Solid films, (160) p. 413-429.
20. Gabrielli, G., Puggelli, M. Ferroni, E. Carubia, G. and Pedocchi, L. (1989) "*Mono and Multilayers of Bivalent Ion Stearates*" Colloids and Surfaces, 41, p. 1-13.
21. Bornong, B. J. (1969) "*Ellipsometric study of films of polar organic molecules on chromium*" Surface Science (16), p.321-446.
22. McCrackin, F. L. and Colson, J. P. (1969) "*Computational Techniques for the Use of the Exact Drude Equations In Reflection Problems*" Symp. Proc. On Ellipsometry in the Measurement of Surfaces and Thin Films

Chapter 6

Sources of errors in PME

Abstract

Measurement errors in the PCMCA arrangement result from the non-ideal behaviour of the optical components as well as the accuracy of azimuthal alignment among other factors including detector noise and data acquisition errors. In this chapter component imperfection and azimuthal errors are considered. The aim is to identify major factors contributing to the overall measurement error. The result is useful for further improving and simplifying the system.

6.0 Introduction

Ellipsometry is a useful and accurate optical technique in the study of reflecting or transmitting surfaces. Optical constants of surfaces and thin film parameters can be measured accurately. However it makes use of bulky optical and mechanical components that are always prone to systematic errors. An ellipsometer, whether it involves angular measurements (Null ellipsometer) or irradiance measurements (RAE or PME) rely on accurate azimuthal alignment of polarising components, angle of incidence setting etc. relative to a predefined plane [1-3].

In the case of null ellipsometer, analysis of systematic errors has been thoroughly dealt by several researchers [1]. The nature of null ellipsometry is such that the final irradiance is set to be zero or minimum. This requirement leads to simple analytical expressions that can be used to account for systematic errors.

Error analysis in the case of PME is more complex, and there has not been a generalised analysis on the subject. The effect of systematic errors on the operation of a PME has been made by O' Handley [4]. However no detailed study of the precision of such instrument has been conducted. In this chapter an attempt is made to point out the sources of systematic and other errors and the effect of such errors on the final measurement will be analysed in reference to the PCMCSA ellipsometer described. The quantities measured in ellipsometry, ψ and Δ are functions of the azimuth angles of the polarising components, quality of the polarising components, errors arising from electronic noise of the detection circuitry, angle of incidence and also properties of the surface under measurement. For accurate, reliable and repeatable measurements, the above parameters must assume as near to ideal settings and

characteristics as possible. In practice, all the components are susceptible to errors. An investigative study in to the sources and magnitude of errors helps in system calibration, define measurement resolution limits and point out possible improvements.

The purpose of doing error analysis in this work is thus, to investigate possible windows of improvement to the PME described so far. The study will therefore concentrate mainly on errors introduced due to the presence of polarising optical components.

Errors, which will be considered here, come under two classifications.

1. Errors arising from misalignment of azimuth angles of all polarising optical components.
2. Errors due to components Imperfection, i.e. elliptic polarisers instead of perfect linear polarisers or retardance tolerance in the case of QWP's. Other sources of errors, such as incorrect angle of incidence setting, electronic noise on the detectors are not discussed here in great detail.

Although it is understood that a parametric treatment of the Jones matrix [5][6] of all the optical components would give a more practical view in to the propagation of the combined errors introduced by each component to the final measurement result, the volume of the mathematics involved soon gets cumbersome. Because of such difficulty, the error analysis looks at the effect of one source of error per component at a time, although a combination of more than one source of errors is also considered. Owing to the complexity of the analysis, a computer program (MATLAB/ HPVEE) is employed in modelling the optical components and the SOP of the light with Jones matrix formulation [8][9].

For simplification purposes, a straight through arrangement is used for calibration. All ideal alignments and component specification in the PCMCSA configuration shown in figure 6.1 will refer to the table below.

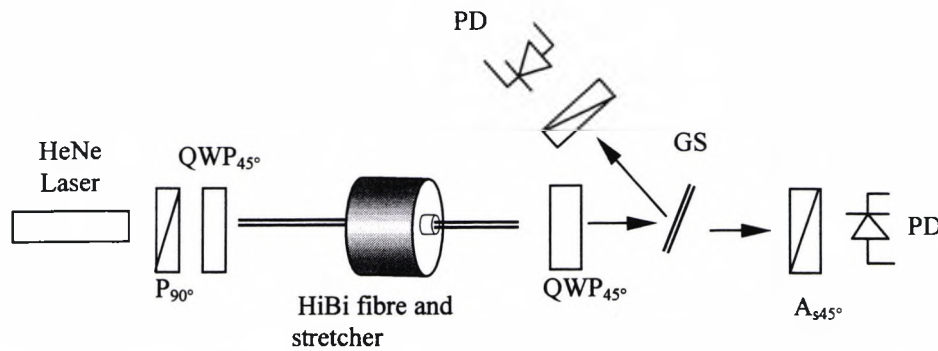


Fig. 6.1 The PCMCSA arrangement. Where all the components are labelled as described before.

Component	Azimuth	Retardance	Extinction ratio
P	0°	-	0
QWP1 & QWP2	45°	90°	-
M	-	$\phi_d(t)$	-
A_a	45°	-	0
A_r	0°	-	0
S	Isotropic		

Table 6.1. Ideal component specification and alignment. Where P is the polariser, QWP1 and QWP2 are quarter wave plates, M is the modulator. A_a and A_r are analysers and S is a sample. All angles are measured relative to the pane of incidence.

6.1 Azimuth angle errors

As described before in the PCMCSA arrangement, all the polarising components are fixed at a predefined angle and need not be changed between measurements. The accuracy of the angular setting of the polarising optical components affects the

measurement resolution. Thus it is important to characterise the level of errors that can be introduced by any of the components making up the complete system. The effect of such orientational misalignment are best calculated by assuming the components are set at a certain fixed angle relative to a common reference plane. A rotation matrix [5][7] is used to introduce angular misalignments for theoretical analysis purposes.

6.1.1 Polariser Misalignment

Consider the polariser in the PCMCSA arrangement is set at 0° relative to the x-y reference frame, the Jones matrix is given by:

$$P_0 = \begin{bmatrix} 1 & 0 \\ 0 & 0 \end{bmatrix} \quad (6.1)$$

The process of misalignment can be accomplished by multiplying the polariser Jones matrix of equation 6.1 by a rotation matrix, $R_{\pm\sigma}$ given by :

$$R_{\pm\sigma} = \begin{bmatrix} \cos(\sigma) & \pm \sin(\sigma) \\ \mp \sin(\sigma) & \cos(\sigma) \end{bmatrix} \quad (6.2)$$

Where σ is the rotation angle.

Thus a polariser misaligned by an angle, σ , relative to a fixed reference frame is given by P_σ , such that the matrix product is given by:

$$P_\sigma = [R_{-\sigma} P_0 R_{+\sigma}] \quad (6.3)$$

At this stage, the effect of the angular misalignment on the polariser as indeed is the case with the rest of the polarising components is to use a computer program modelling the transfer function of the complete PCMCSA arrangement. The model is based on Jones matrix for simplicity, although Muller matrix formulation could also

be used. Figure 6.2 shows simulation data of the resulting ψ and Δ errors when a small azimuth error is present in the polarisation axis setting. For calculation purposes an error angle in the range of -3° to 3° is assumed. In practice the angular setting on the polarising components mount could be set accurate to about 0.5° . A maximum error of 0.8° is predicted on ψ , while Δ measurements are unaffected.

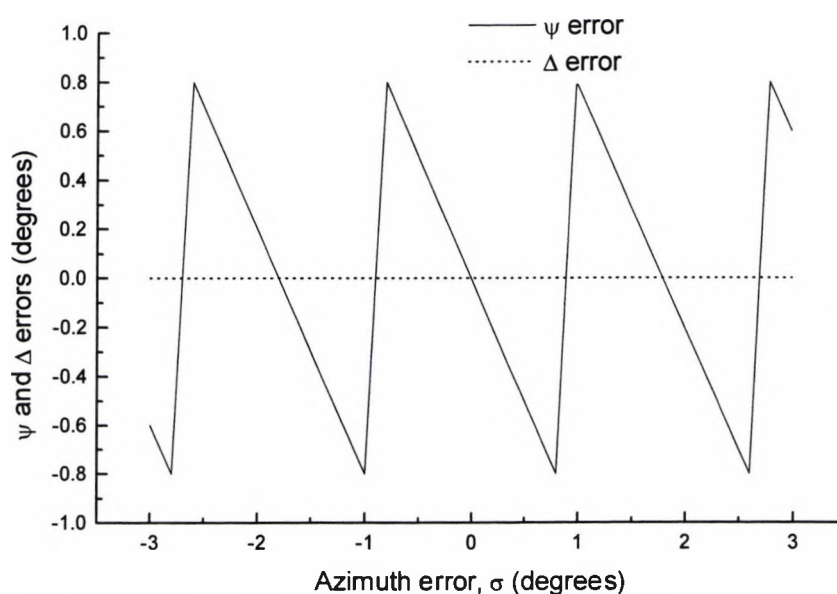


Fig. 6.2 Calculated ψ and Δ errors resulting from a small azimuthal error on the polariser, P, at the input of the fibre.

6.1.2 Analyser Misalignment

Figures 6.3 and 6.4 show errors of ψ and Δ resulting from a small misalignment on the analyser at the reference arm and detection arms. On both cases Δ is not affected by azimuth errors. ψ varied linearly and in the opposite sense with the azimuth error on the detection arm analyser, while on the reference arm it showed a stair case variation. Interestingly the errors within $\pm 1^\circ$ azimuthal error on the analyser on the

detection arm can be tolerated as it did not affect ψ values showing that with the system having 0.5° azimuthal error on all polarising components, the angular setting on the reference arm analyser is not too critical.

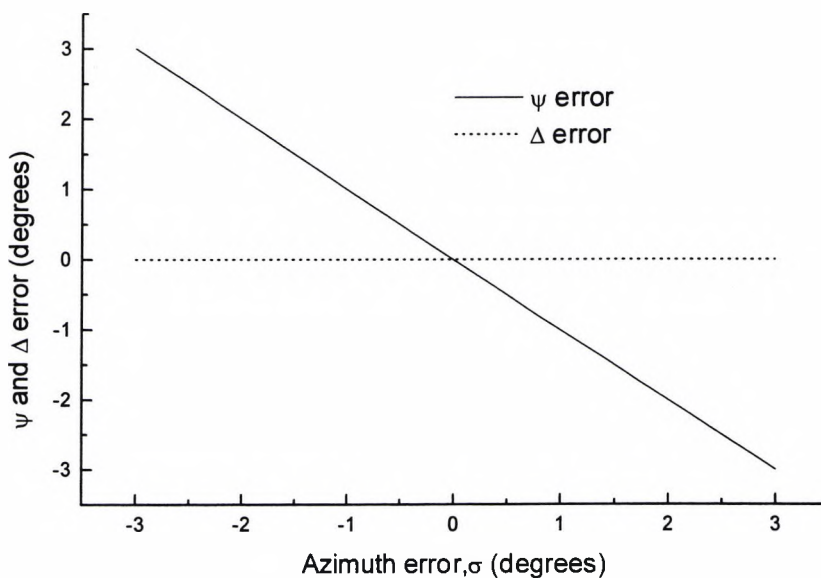


Fig. 6.3 Calculated ψ and Δ errors resulting from a small azimuthal error on the analyser, A_d , at the detection arm.

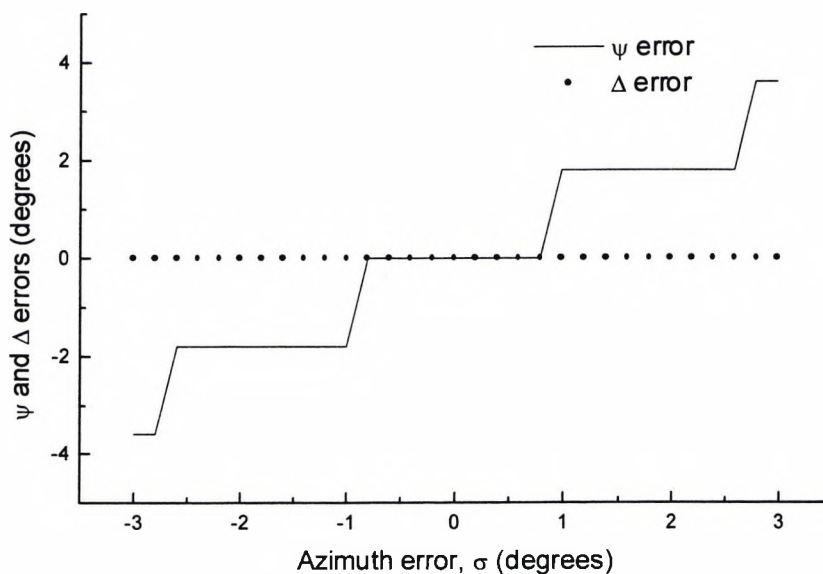


Fig. 6.4 Calculated ψ and Δ errors resulting from a small azimuthal error on the analyser, A_r , at the reference arm.

6.2 Quarter wave plates: component Imperfection and azimuthal misalignment

There are two QWP's in the PCMCSA system. In addition to errors arising from angular misalignment, QWP's suffer what is called retardance tolerance. This parameter is a measure of how well the phase delay introduced by a QWP matches to a theoretical value of $\pi/2$.

6.2.1 Azimuthal errors

Orientalional errors on the quarter wave plates introduce ellipticity angle on the RPP beam, which results in to errors on, ψ and Δ measurements. Figure 6.5 shows ellipticity angle introduced by angular misalignment of the quarter wave plate at the input of the fibre. An angular error of 0.5° results in to ellipticity of about 0.00025. This value is 100 times smaller than the experimental measurement data in section 4.4.3.

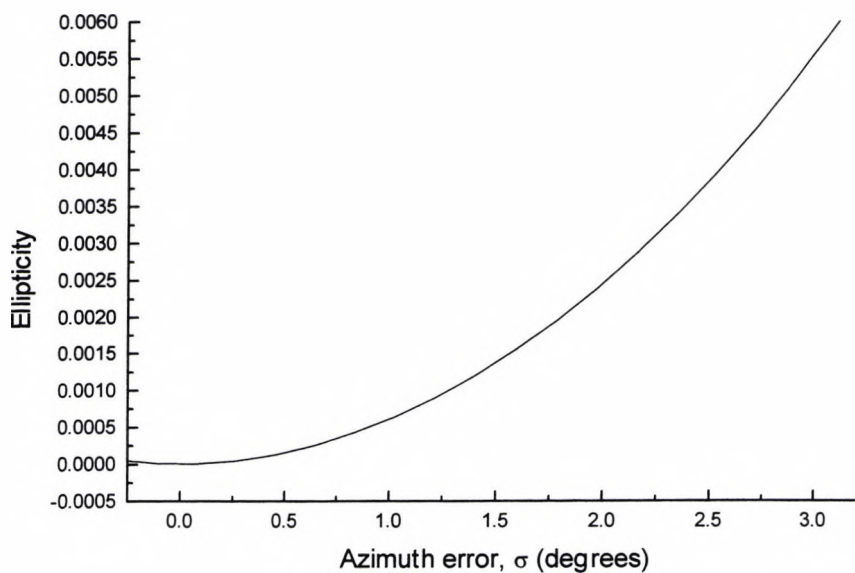


Fig. 6.5 Calculated ellipticity resulting from a small azimuthal error on the QWP at the input of the fibre.

The resulting errors on ψ and Δ for small azimuth errors shown in figure 6.6 indicate that while ψ suffers a maximum error of $\pm 0.6^\circ$, Δ errors are found to be smaller. This is verified to be so experimentally.

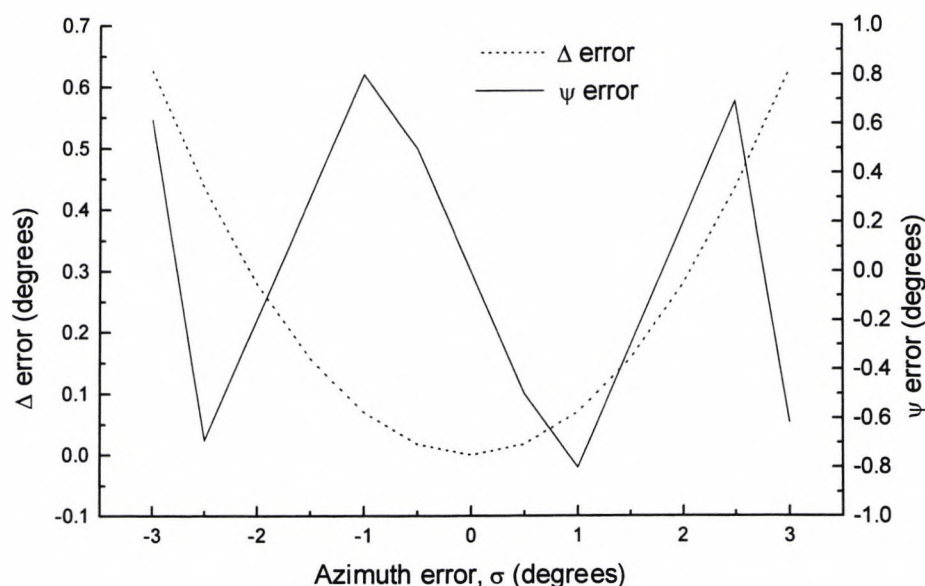


Fig. 6.6 Calculated ψ and Δ errors resulting from a small azimuthal error on the QWP at the input of the fibre.

At the output of the fibre, another QWP turns the beam in to a RPP beam. In this case with the presence of small angular misalignment, the output beam is no longer the same as RPP beam predicted theoretically. In fact as shown in figure 6.7, it has ellipticity varying with modulation angle. Ellipticity is maximum when the modulation angle is $\pi/2$, i.e. when the SOP of the light at the output of the fibre is linear and minimum for a circular state. It is interesting to note that the maximum ellipticity introduced with 0.5° azimuth error is comparable to the ellipticity measured experimentally. (See section 4.4.3). Measurement error introduced on ψ and Δ due to such ellipticity is shown in figure 6.8. It is found that for azimuth errors, σ in the range $\pm 0.5^\circ$, the error on ψ and Δ is approximately $\pm 2\sigma$ and $-\sigma$ respectively. The

above simulation results show that there is more strict azimuth setting tolerance on the QWP at the output of the fibre than the QWP at the input.

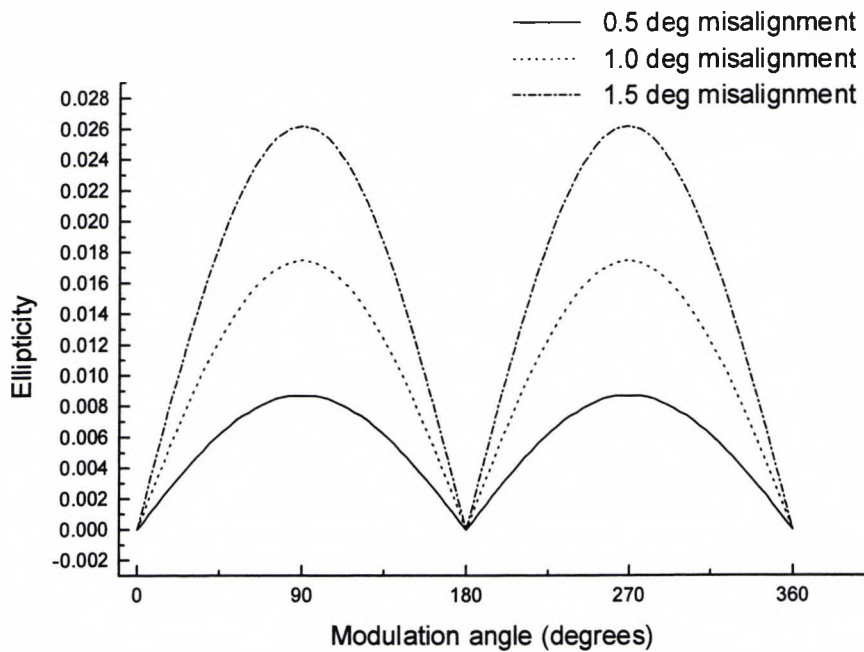


Fig. 6.7 Calculated ellipticity resulting from a small azimuthal error on the QWP at the output of the fibre.

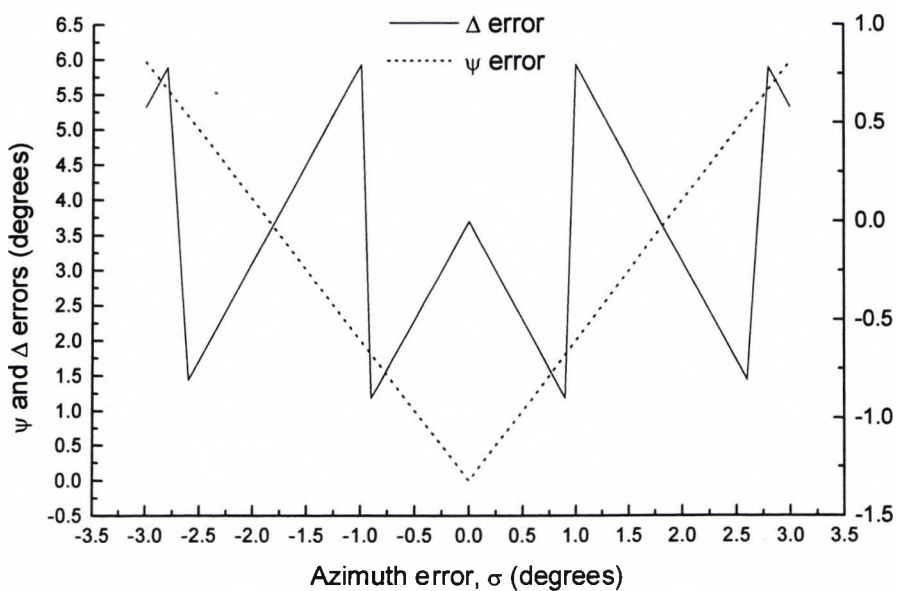


Fig. 6.8 Calculated ψ and Δ errors resulting from a small azimuthal error on the QWP at the output of the fibre.

6.2.2 Component imperfection

In practice the phase retardance of a QWP is not exactly equal to $\pi/2$. There is a small error, δ which is referred to as retardance tolerance. The Jones matrix of an imperfect QWP with its optical axis at 0° to the horizontal in the x-y reference frame may be written as

$$Q_0 = \begin{bmatrix} e^{j\delta} & 0 \\ 0 & 1 \end{bmatrix} \quad (6.4)$$

Where δ is the retardance tolerance.

A good QWP will have a retardance tolerance of $\pi/500$. Usually δ has values of $\pi/25$ or $\pi/50$ for a standard mica retardation plates and $\pi/250$ or $\pi/500$ for a quartz retardation plates. In this work a quartz QWP of δ of $\pi/250$ and a mica retardation plate with δ of $\pi/50$ were used.

The existence of a small retardance error on the QWP at the input of the fibre produces ellipticity angle on the RPP beam. This is shown in figure 6.9. A similar treatment of the QWP at the output of the fibre reveals that a modulation varying ellipticity is generated. Figure 6.10 shows ellipticity levels for QWP's of various retardance tolerances. It should be noted that with a quality QWP with retardance $\pi/500$, the amplitude of the ellipticity is reduced significantly. It also interesting to note that from the results shown in figure 6.9 and figure 6.10, for the same level of retardance error, the maximum ellipticity introduced by QWP2 is equal to that introduced by QWP1 and is also comparable to ellipticity of 0.018 measured experimentally in section 4.4.3. The retardance error on QWP2 is found not to affect ψ and Δ measurements, while the same error on QWP1 as shown in figure 6.11

introduces a bigger error in the measurement accuracy of ψ and Δ . This means that the quality of the QWP at the input of the fibre is an important consideration in the system design.

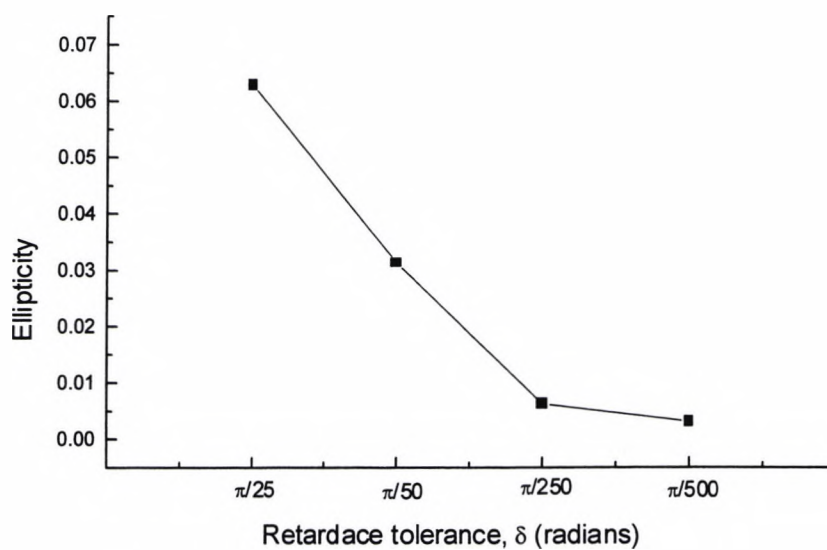


Fig. 6.9 Calculated ellipticity resulting from retardance error of an imperfect QWP at the input of the fibre.

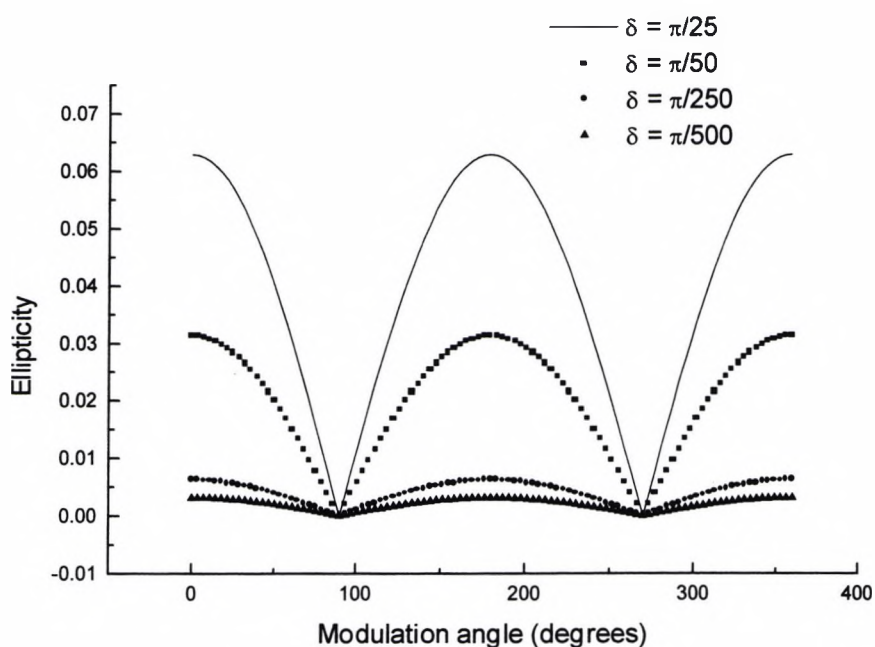


Fig. 6.10 Calculated ellipticity resulting from retardance error of an imperfect QWP at the output of the fibre.

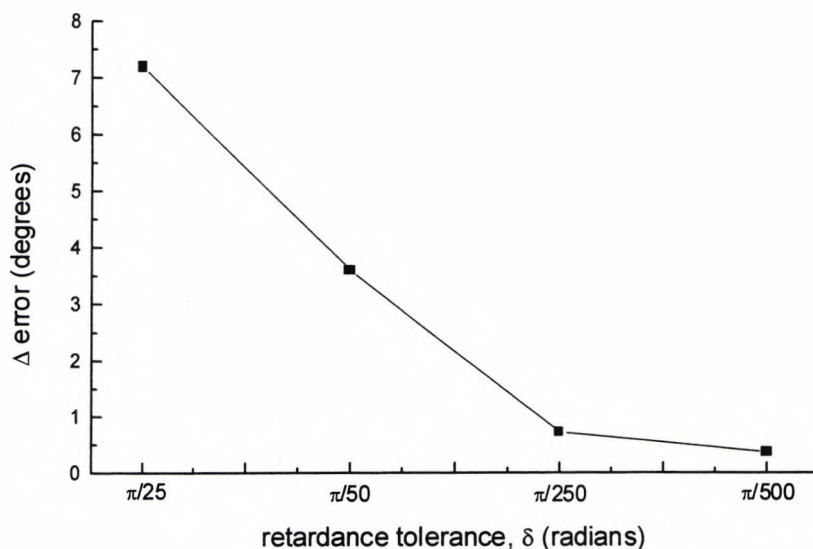


Fig. 6.11 Calculated Δ errors introduced by an imperfect QWP at the input of the fibre with various retardance tolerance levels.

Figure 6.12 shows ellipticity variation of the RPP beam with modulation. In this case an imperfect QWP with a small azimuth error is considered. Again the maximum ellipticity introduced by combined azimuth and imperfection errors is comparable to the value obtained experimentally. Note that in figure 6.12, the ellipticity curves are out of phase with each other due to the different azimuth errors.

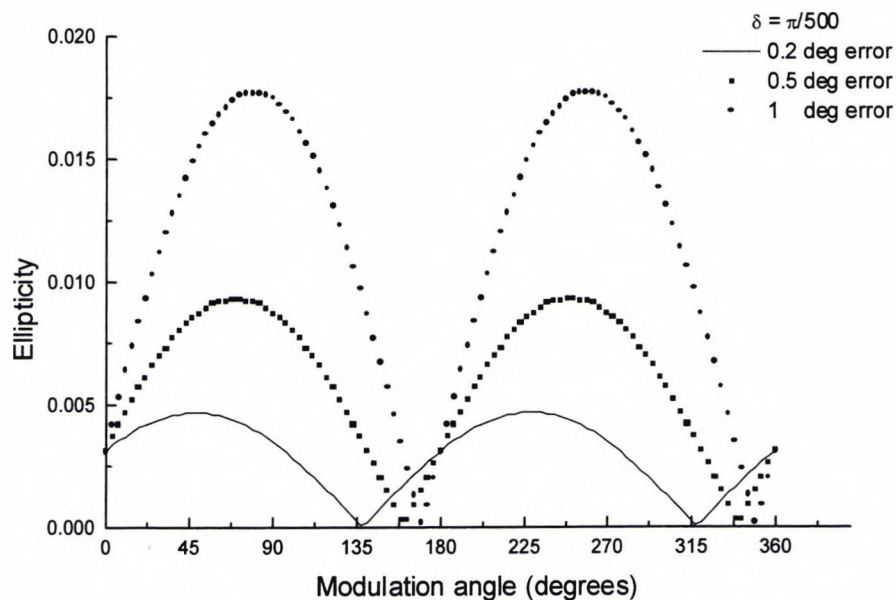


Fig. 6.12 Calculated ellipticity due to an imperfect QWP with small azimuth errors at the output of the fibre.

6.3 Other sources of errors

Signal detection involves conversion of light into electrical signal. This process uses a photodiode with intrinsic noise level. The photodiode is usually followed by an amplifier stage to bring the signal to a level suitable for further analysis. In the system, an amplifier with a bandwidth of 20KHz and a signal to noise ratio of $\sim 500:1$ was designed and built. The detector noise, however small, compared to other sources, also contributes to measurement errors. Signal processing technique involves data acquisition via ADC and filtering techniques through curve fitting [10-12] of the measurement data. This also introduces noise in the overall measurement system. These error sources are not quantified in this work, as they are deemed to be of a

secondary importance compared to the higher error levels introduced by component imperfection and azimuthal errors.

6.4 Summary

This chapter has given an important insight into sources of errors from optical component imperfection and azimuthal alignment errors. Such results are useful in system specification design and further improvements. The simulation results found that, errors introduced from misalignment of the linear polarisers and analysers were relatively small compared to the errors measured experimentally, further more careful alignment and precision mounting techniques could improve the measurement accuracy. The simulation results showed that the effect of misalignment and component imperfection on the quarter wave plates introduced errors comparable to those obtained experimentally. The results of such analysis provide important conclusion in that while the azimuthal alignment on the quarter waveplate at the input of the fibre is not too critical, its retardance tolerance should be as small as possible for better accuracy. In this work the QWP at the input of the fibre has a retardance tolerance, δ of $\pi/250$.

On the other hand the QWP at the output of the fibre introduced higher errors, comparable to those measured experimentally due to small azimuth errors than component imperfection. This shows that while a higher quality QWP should be used at the input of the fibre, azimuthal alignment is more critical for the QWP at the output of the fibre.

Important conclusions have been drawn from this chapter in identifying major sources of errors. At this stage it would seem appropriate to devise an alternative approach for

the ellipsometric configuration. An obvious candidate for improvement is to eliminate the major sources of error, i.e. the two QWP's and thus make the system more accurate and also cheaper with fewer number of optical components. This is dealt in the next chapter where a new set up is introduced.

Reference

1. Azzam, R. M. A. and Bashara, N.M. (1977) "*Ellipsometry and polarized light*" (Amsterdam: North Holland).
2. Harland, G. T. (1993) "*A Users Guide to Ellipsometry*" (Academic Press Inc.)
3. Bashara, N. M., Buckman, A. B., Hall, A. C. (1969) "*Recent developments in ellipsometry*" (North Holland Publishing Company- Amsterdam)
4. O'Handley, R. C. (1973) "*Modified Jones calculus for the analysis of errors in polarisation-modulation ellipsometry*" J. Opt. Soc. Am. Vol. 63, No. 5, p.523-528.
5. Gerrard, A. and Burch, J. M. (1975) "*Introduction to matrix methods in optics*" (John Wiley and Sons)
6. Hect, E., Zajac, A. (1979) "*Optics*" (Addison-Wesley Publishing company, Inc.)
7. Nussbaum, A. and Philips, R. (1976) "*Contemporary Optics for Scientists and Engineers*" New Jersey, Prentice-hall
8. Hanselman, D. C. and Littlefield (1996) "*Mastering MATLAB: a comprehensive tutorial and reference*" (Prentice-Hall, London)
9. Helsel, R. (1998) "*Visual Programming with HPVEE*" (Prentice-Hall PTR)
10. Anthony Ralston (1965) "*A first course in numerical analysis*" (McGraw-Hill Kogakusha Ltd.)
11. Nakamura, S. (1993) "*Applied numerical methods in C*" (Prentice-Hall International inc.)
12. Rojiani, K. B.(1996) "*programming in C with numerical methods for engineers*" (Prentice-Hall international inc.)

Chapter 7

A high birefringence fibre polarisation modulation scheme:

A new configuration for Ellipsometric measurement

Abstract

A birefringence modulated ellipsometry technique is described in which polarisation modulation is achieved by stretching a 20cm section of a HiBi fibre held under longitudinal tension. The system has two optical channels in which one is used as a measuring probe and the other channel is used in stabilising temperature and other external effects on modulation via a simple lock-in amplifier feedback system. Both ellipsometric parameters, ψ and Δ can be determined from one optical channel by harmonic analysis of the detected signal with two lock-in amplifiers and a low pass filter (LPF).

7.0 Introduction

In the previous chapter, investigation of sources and analysis of systematic errors have been described. In this chapter, an alternative and more compact ellipsometric configuration with improved signal processing technique is described.

The ability to achieve control of the state of polarisation of a beam of light launched in a HiBi fibre has been extensively studied. This control has been successfully employed to characterise different materials via an ellipsometric system based on the modulation of birefringence of the fibre. Several improvements have been made in order to optimise the performance of the actual configuration. The sources and degree of error in the measurement system have been estimated in the previous chapter. We can characterise the sources of this error as:

- Alignment and adjustment of every optical component
- Precision and quality of optical components employed
- Detection noise and D/A converter resolution during the signal processing stage
- Extra modulations introduced which affect the characteristic of the output polarisation.

It is worth noticing that the first two problems may be solved by simply reducing the number of bulky optical components used in the configurations. This would also make the system more attractive in terms of cost and miniaturisation possibility in the prospect of an all-fibre arrangement.

The third point is a direct consequence of electronic noise and the signal processing technique, which allows a time-domain analysis of the two signals coming from the

reference and detection arms. The comparison between the two signals permits extraction of the ellipsometric information.

The signal processing technique involves analogue-to-digital conversion and data filtering by means of curve fitting. Each of these steps introduces errors as an intrinsic consequence of the nature of the signal processing. It is shown previously that the technique of modulation permits a measurement whose speed is related to the speed of modulation, the quality of the measurement will be dependent on the speed and performance of the data acquisition and storing system. Furthermore, although the nature of measurement is real-time, the signal processing technique employed to calculate the ellipsometric parameters requires a fast analogue to digital conversion card for an on-line measurement where a fast process is to be monitored. This will add to the overall cost of the system.

As is discussed further on this Chapter, a point of concern in the new configuration is the presence of signal drift with temperature variation. In fact small, unwanted modulation acting on the fibre such as temperature change affects the phase of the modulated signal. This is due to the nature of the HiBi fibre where the modal phase retardance of its eigen axis is dependent on the environmental parameters. The key to solve this problem is achieving a control over these unknown parameters and compensate for their effect.

At this stage it is appropriate to look at polarization maintaining behavior of single mode HiBi fibres.

It has been discussed so far that polarization is an important phenomena in fibre optics. Many fibre optic applications today are affected by the polarisation of the light

traveling through the fibre. These include fibre interferometers and sensors, fibre lasers, and electro-optic modulators. The operation of such systems shows polarisation dependence, which can affect system performance. Thus, analysing, controlling, and manipulating the polarisation state of light in fibre has become increasingly vital.

Polarisation theory mainly deals with three different possible types of polarised light, namely linear, circular and elliptical polarisation states as discussed in section 2.1. In the simplest case, linearly polarised light, the electric field just vibrates up and down in a specific direction. In most applications, it is this form of polarisation we are interested in and wish to preserve.

While in theory one can produce perfectly linearly polarised light by passing light through a linear polariser, in practice this is not the case. As shown in chapter 6, quality of polarisers and angular alignment are among the determining factors. A measure of the quality of the polarised beam is its extinction ratio (E_r). This parameter is measured by passing light beam through a rotatable polariser and onto a detector. By rotating the polariser about its polarization axis, the output signal will vary in intensity. If the maximum and minimum intensities are measured, then the extinction ratio of the output beam is given by $10 \times \log(P_{\max}/P_{\min})$. Where P_{\min} and P_{\max} are the measured maximum and minimum signal intensities..

When a normal fibre is bent or twisted, stresses are induced in the fibre. These stresses in turn will change the polarisation state of light traveling through the fibre. If the fibre is subjected to any external perturbations, such as changes in the fibre's position, stress or temperature, then the final output polarisation will vary with time. This is true for even short lengths of fibre, and is undesirable in many applications

that require a constant output polarisation from the fibre. To solve this problem, several manufacturers have developed polarisation-maintaining fibres (PM fibres). These fibres work by inducing a difference in the speed of light for two perpendicular polarisations traveling through the fibre. This birefringence creates two principal transmission axes within the fibre, known respectively as the fast and slow axes of the fibre. Provided the input light into a PM fibre is linearly polarised and orientated along one of these two axis, then the output light from the fibre will remain linearly polarised and aligned with that axis, even when subjected to external stresses.

Naturally, how well a PM fibre maintains polarisation depends on the input launch conditions into the fibre. Perhaps the most important factor is the alignment between the polarisation axis of the light with the slow axis of the fibre. A perfectly polarised input beam into an ideal fibre, misaligned by an angle θ with respect to the slow axis of the fibre will suffer extinction ratio of not less than $10 \times \log(\tan(\theta^2))$.

Generally, the input source is not ideally polarised, but instead is polarised with a small extinction ratio, this also contributes to the final extinction ratio of the output beam. The polarisation extinction ratio can also be degraded by any stresses or microbends in the fibre or by external optical components that do not maintain polarisation properly. In this regard, it is important that the polarisation maintaining behavior of the fibre is controlled for accurate and drift free measurement system application. Simple precautions must be exercised when working with HiBi fibres, these may include among other things: special termination procedures, stress free glues, and top quality lenses and optics must be used to minimize these stresses and thus maintain the highest possible extinction ratios.

Given the importance of the alignment of the PM axis relative to the input polarization and other predefined planes, careful alignment procedure should be followed although this step is increasingly becoming simpler task with the introduction of PM connectors (NTT-FC style connector, OZ Optics) which have a positioning key, to preserve the angular orientation of the fibre.

It should be noted that in the case where a linear polarized light beam is launched into the fibre core at an angle to the fast-slow axis of the HiBi fibre so as to populate both modes equally, as in the present ellipsometric configuration discussed in this chapter, the polarisation of the light fluctuates in response to external perturbations the fibre may be subjected to. This calls for polarisation control techniques.

In the remaining section of this chapter, the proposed solutions to the problems outlined above will be discussed and the resulting new configuration will be analysed and supported with experimental tests and measurement results.

7.1 Theoretical analysis

The reduction of the optical components in the high birefringence fibre polarisation scheme described so far is seen as a first step to improving the system in terms of accuracy, simplicity and cost effectiveness. A thorough investigation on the optical configuration discussed in the previous chapter clearly showed that the performance of the system is critically dependent on the quality and alignment accuracy of quarter wave plates employed in the configuration.

The previous system employed two-quarter wave plates, one at the entrance of the fibre, QWP1, and one at the output, QWP2. At the input side of the fibre, QWP1 is

aligned with its axis at 45° to the axis of polarisation of a linear polariser at the HeNe laser output. Thus a circularly polarised beam is launched in to the fibre to populate the two normal eigenmodes of the fibre equally, the second retarder, QWP2, changes the polarisation state of the output in to a rotating plane polarised beam. The advantage of having these two-quarter wave plates is that the alignment of the optical axis of the fibre relative to the plane of incidence or to the optical components at the output of the fibre is not important. With present fibre technology, fibre axis alignment is not seen to be a major problem, as there are commercial FC/PC terminated HiBi fibres which their eigen axes direction can be aligned relatively easily and accurately. Thus it would seem a sensible step to remove QWP1 and QWP2 from the system with a possible advantage of system simplicity and accuracy. The proposed Polariser-Modulator-Sample-Analyser (PMSA) configuration is shown in figure 7.1 below.

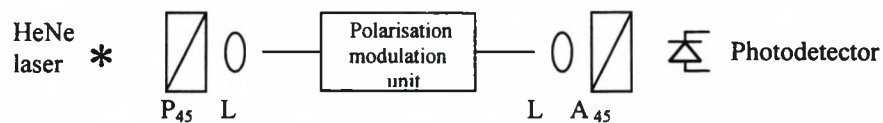


Fig. 7.1 The PMSA experimental configuration with no QWPs. P₄₅, A₄₅: polarisers at 45° respect to the fibre eigen axis; L, lens.

A mathematical analysis of the system shows that removing the two quarter wave plates from the system, as shown in the configuration of figure 7.1, we get an output intensity which is varying with modulation phase and also dependent on the mutual orientation of fibre optical axis and polarisers. If both the polarisers are orientated at

45° relative to the optical fibre eigenmodes we can express the output electric field E_{output} as:

$$E_{\text{output}} = P_{45} M A_{45} E_{\text{input}} \quad (7.1)$$

Where E_{input} is the electric vector of the input light from the HeNe laser, P_{45} and A_{45} respectively are the Jones matrices [1][2] for a polariser and analyser at 45° and M is the HiBi fibre modulator such that,

$$E_{\text{input}} = \frac{E_o}{\sqrt{2}} \begin{bmatrix} 1 \\ 1 \end{bmatrix} e^{i\omega_o t} \quad A_{45} = P_{45} = \frac{1}{2} \begin{bmatrix} 1 & 1 \\ 1 & 1 \end{bmatrix}; \quad M = \begin{bmatrix} e^{i\varphi_f(t)} & 0 \\ 0 & e^{i\varphi_s(t)} \end{bmatrix}; \quad (7.2)$$

Where E_o is the amplitude of the beam, ω_o is the angular frequency and t is the time;

The output vector is given by:

$$\begin{aligned} E_{\text{output}} &= \begin{bmatrix} 1 & 1 \\ 1 & 1 \end{bmatrix} \begin{bmatrix} e^{i\varphi_f} & 0 \\ 0 & e^{i\varphi_s} \end{bmatrix} \begin{bmatrix} 1 & 1 \\ 1 & 1 \end{bmatrix} \begin{bmatrix} 1 \\ 1 \end{bmatrix} \frac{E_o}{4\sqrt{2}} e^{i\omega_o t} \\ &= \begin{bmatrix} e^{i\varphi} + 1 \\ e^{i\varphi} + 1 \end{bmatrix} \frac{E_o}{2\sqrt{2}} e^{i(\omega_o t + \varphi_s)} \end{aligned} \quad (7.3)$$

Where $\varphi = \varphi_f - \varphi_s$,

$\varphi = \varphi_f - \varphi_s = \varphi(t)$ is the difference between the phase retardances corresponding to the fast (φ_f) and the slow (φ_s) eigenmodes. The intensity detected after the analyser A_{45} may be given by:

$$\begin{aligned} I_{\text{output}} &= (E_{\text{output}}) \cdot (E_{\text{output}})^* \\ &= I_o [1 + \cos(\varphi(t))] \end{aligned} \quad (7.4)$$

Where $I_o = \frac{E_o^2}{8}$ and $\varphi(t)$ represents the phase shift introduced by the modulation,

which can be written as:

$$\varphi(t) = (k_y - k_x)(L + L(t)) \quad (7.5)$$

Where k_x and k_y are the propagation constants for each eigenmode defined as

$$k_x = n_x \frac{2\pi}{\lambda_0}, \quad k_y = n_y \frac{2\pi}{\lambda_0} \quad [3] \text{ and } L(t) \text{ is the fibre length extension due to the}$$

modulation unit.

7.2 Experimental alignment Procedure

The experimental arrangement is shown in Figure 7.2 below.

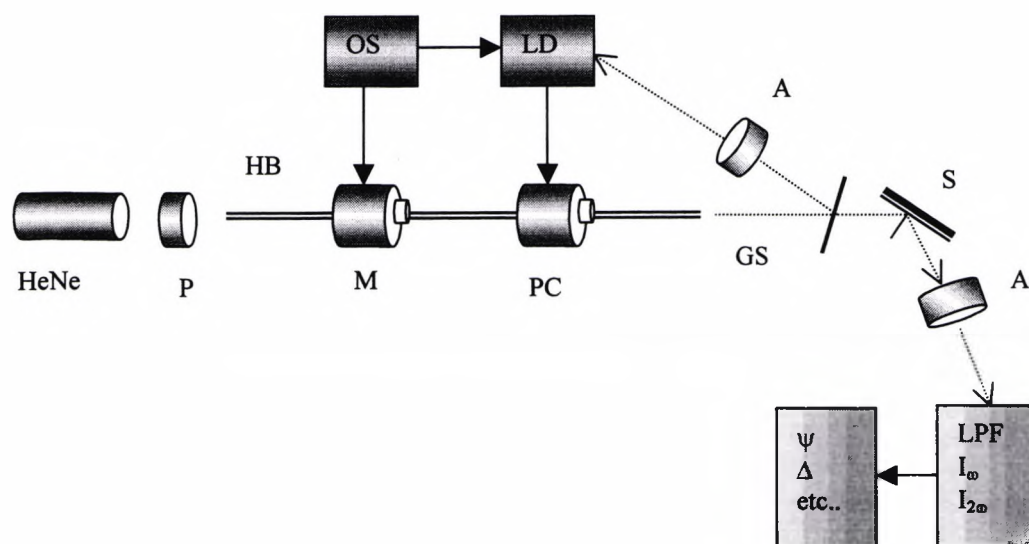


Fig. 7.2 Experimental configuration of the Ellipsometer. A helium neon laser, He-Ne, a linear polariser, P, HiBi fibre, HB, fibre stretcher, M, phase compensator, PC, signal generator, OS, lock-in detection, LD, glass reflector, GS, sample, S and linear analyser, A.

A HeNe laser is used as the light source here. In order to reach the optimum alignment, the axis of the first polariser P_{45} is rotated relative to the eigen axis of the fibre until a dc signal is detected at the output. At this point, despite changing the orientation of the analyser A_{45} , at the output, no modulation was present in the output signal. This clearly shows that the polarisation azimuth of the input beam was parallel

to one of the fibre eigenmodes. Rotating the polariser P_{45} by 45° allows the linear polarised light beam to be launched in to the fibre with its polarisation axis at 45° relative to the two normal eigenmodes of fibre. At the output, the fibre axis is aligned at 45° relative to the plane of incidence this is easily done by aligning a glass at Brewster angle ($\sim 56^\circ$) [4], the fibre is then rotated until the reflected light from the glass is null. Alternatively, if a polariser oriented at 90° to the plane of incidence is inserted between the fibre output and a photodetector. The fibre at the output end is then rotated until the modulated signal is reduced to dc as detected by the photodetector in which case the fibre axis is in the same plane as the plane of incidence. The resulting signal from this experimental set-up agrees with the theoretically expected signal represented by equation 7.4. This simple configuration does not use any quarter wave plates, unlike the PCMCSA configuration, although it does not produce the characteristic rotating plane polarised beam, the two fibre axes are equally populated with a linearly polarised light beam. The output beam is a phase modulated light which, is a linear polarised light with a fixed azimuth, (in the direction of the polariser A_{45}) and an amplitude changing with time periodically according with the modulating phase shift.

The polarisation modulation scheme employed was produced by stretching the fibre longitudinally, using a dynamic shaker which was driven sinusoidally to modulate the birefringence and length of the fibre.

In the next section, the system is characterised theoretically in order to analyse the phase-modulated beam.

7.3 Theoretical analysis and calibration

An Electro-dynamic shaker is used to stretch the fibre and modulate its birefringence thus introducing polarisation modulation [5]. The modulation unit is driven by a function generator to introduce a sinusoidal phase change, which can be represented as:

$$\phi(t) = \phi_A \sin(\omega t) \quad (7.6)$$

Where ϕ_A is the relative phase amplitude as a function of the peak to peak voltage of the driver signal, $\phi(t)$ is proportional to the birefringence change phase modulation and ω is the frequency of the driver signal. There is also a phase bias, ϕ_B associated with the static fibre length [6]. Thus the overall phase relation, $\phi(t)$ may be represented as:

$$\phi(t) = \phi_B + \phi_A \sin(\omega t) \quad (7.7)$$

A Jones matrix analysis of the PMSA arrangement shows that the detected signal is of the form:

$$I(t) = I_0 [1 + \cos(\phi_B + \phi_A \sin(\omega t))] \quad (7.8)$$

Where $I(t)$ is a time variant intensity.

The signal can be expanded in to a series of Bessel functions [6][7] such that,

$$\begin{aligned} I(t) = & I_0 [1 + \cos(\phi_B)J_0(\phi_A)] + \\ & 2I_0 \left[\sum_{m=1}^{\infty} \cos(\phi_B)J_{2m}(\phi_A) \cos(2\omega m t) \right] + \\ & 2I_0 \left[\sum_{m=0}^{\infty} \sin(\phi_B)J_{2m+1}(\phi_A) \sin(2m+1)\omega t \right] \end{aligned} \quad (7.9)$$

Where $J_m(\phi_A)$ is Bessel function of the first kind with order, m , and argument, ϕ_A .

The above expression shows that the output beam consists of three parts: a dc term, the summation of the even frequency terms, all of them multiplied by $\cos(\phi_A)$, and the summation of the odd frequency terms multiplied by $\sin(\phi_A)$; thus the information from the phase modulated beam can be extracted from the resultant intensity in several different frequency channels simultaneously.

As shown below, the above complex harmonic expression can be simplified by controlling the parameters ϕ_A and ϕ_B which are functions of the amplitude and the dc offset level of the modulating signal respectively.

The phase bias, ϕ_B , can be varied between zero and $\pi/2$ by applying a controlled strain to the fibre so that equation 7.9 would be simplified to contain either odd or even frequency components along with a dc level [6]. Further necessary simplification is also achieved by setting the amplitude of the modulating signal so that $J_0(\phi_A) = 0$.

At this point the amplitude of the modulating signal corresponds to a Bessel angle of 2.4048° and $J_1(\phi_A)$ and $J_2(\phi_A)$ are within 12% of their peak values [8][9]. Accuracy figure less than 0.1% is easily achievable in this calibration. The calibration procedure followed to set $J_0(\phi_A) = 0$ is such that when the odd or the even harmonic frequency components are selected through varying phase, ϕ_B , between zero and $\pi/2$, the amplitude of the shaker signal is set so that the dc level in either case must be the same. This means that the dc contribution by $J_0(\phi_A)$ in the signal is cancelled. An alternative procedure involves rotating the analyser at the output of the fibre until the modulation fringes disappear and the signal is reduced to dc, i.e. $I(t) = I_0$. If the

analyser is then set to 45° and adjust the amplitude of the shaker signal until the same dc level as above is achieved, $J_0(\phi_A)$ is then set to zero. At this point rotating the analyser should not change the dc level in the signal.

Once $J_0(\phi_A) = 0$ condition is satisfied and setting, ϕ_B , to either $\pi/2$ or zero, equation 5 can be simplified to:

$$I(t) = I_0 [1 + 2J_1(\phi_A) \sin(\omega t) + \dots] \quad (7.10)$$

Or

$$I(t) = I_0 [1 + 2J_2(\phi_A) \cos(2\omega t) + \dots] \quad (7.11)$$

From these simplified expressions, $J_1(\phi_A)$ and $J_1(\phi_B)$ can be calibrated from the appropriate frequency component by controlling the phase bias, ϕ_B , such that:

$$R_{\omega cal} = \frac{I_\omega}{I_{dc}} = 2J_1(\phi_A) \quad (7.12)$$

$$R_{2\omega cal} = \frac{I_{2\omega}}{I_{dc}} = 2J_2(\phi_A) \quad (7.13)$$

Where I_ω , $I_{2\omega}$ and I_{dc} are the intensities of the first two dominant frequencies and a dc intensity respectively.

7.4 Lock-In phase bias control and feedback compensation

If the calibrated signal is to be used for measurement, it is a requirement that the signal is stable at a certain frequency and amplitude [10-12]. The behaviour of the HiBi fibre is such that the phase bias, ϕ_B , responds to environmental perturbations [13], mainly temperature as is found in this work, which tend to vary the birefringence

randomly. This phenomenon is apparent in the case when the polarisation axes of the fibre are both populated with normal polarisation light components, as is the case in the HiBi polarisation modulation fibre ellipsometry described here. The result is that the phase variation becomes random and thus the amplitude of the odd and even frequency components as well as the dc level fluctuate randomly.

The basis of the ellipsometric scheme described so far is that the modulation unit permits some level of control of the state of polarisation of the output beam. In fact the fibre length extension, $L(t)$, due to the modulation unit is reflected in the phase shift introduced between the light travelling on the fast and the slow axes as shown in equation 7.9. This is due to the intrinsic properties of the highly birefringent fibre specially manufactured to have a high degree of linear birefringence. These two axes can be represented in terms of pseudo-Jones matrix as in equation 7.2.

The modal phase retardances of the two linear states are dependent on the environmental parameters such as temperature (T), pressure (P), and strain ($\Delta L/L$). We can express this relation as:

$$\varphi_i = 2\pi n_i L / \lambda, \quad i = f, s$$

$$\frac{d\varphi_i}{dj} = \frac{2\pi}{\lambda} \left(n_i \frac{dL}{dj} + L \frac{dn_i}{dj} \right) \quad j = P, T, \Delta L, \quad (7.14)$$

Where φ_f and φ_s are the phase retardances corresponding to the fast and slow eigenmodes respectively in the fibre length L with a source wavelength λ , and n_i is the effective refractive index of the appropriate eigenmodes. Thus the phase difference of the two guided beams may be modulated by the application of physical stimuli to the fibre:

$$\frac{d\varphi}{dj} = \frac{2\pi}{\lambda} \left(\Delta n \frac{dL}{dj} + L \frac{d(\Delta n)}{dj} \right) \quad (7.15)$$

Where $\Delta n = n_f - n_s$; $\varphi = \varphi_s - \varphi_s$.

In this configuration, it is realistically assumed that the phase modulating effect induced by the shaker is predominant with respect to the other uncontrolled environmental parameters that can be neglected. Nevertheless, as it is found experimentally, these unwanted factors influence the quality of the modulation of polarisation and as such the overall performance of the system. It is observed that that the major extra modulation introduced in the system is due to temperature variation and air movement around the fibre, and in fact this effect was found to decrease by shielding the fibre in small enclosed environment. Typically the temperature response is 100 rad/°C for a HiBi fibre such as used in this work (YORK 600HB) [5]. The effect of temperature and other environmental effects on the output signal spectrum can be explained mathematically as shown below.

With temperature and other external effects taken in to consideration, the effective phase modulation signal of equation 7.7 can be represented as:

$$\phi(t) = \phi^*(T, t) + \phi_B + \phi_A \sin(\omega t) \quad (7.16)$$

Where the total modulated phase shift $\phi(t)$, which affects the output intensity, is now a function of ϕ_A , ϕ_B and a third term ϕ^* which is temperature, T, dependent and changing with time, t. These variations affect the amplitude and shape of the harmonic content of the spectrum, but they are more evident in the first few harmonic frequencies of the spectrum, I_{dc} , I_ω , $I_{2\omega}$, due to the nature of the slow varying temperature and other environmental effects. If we consider the Fourier expansion of

the output intensity signal previously used to calibrate the system, taking the time varying phase, $\phi^*(T,t)$, in to account, expansion of equation 7.8 becomes:

$$\begin{aligned}
 I(t) = I_0 & \left[1 + \cos(\phi_B + \phi^*(T,t))J_0(\phi_A) \right] + \\
 & 2I_0 \left[\sum_{m=1}^{\infty} \cos(\phi_B + \phi^*(T,t))J_{2m}(\phi_A) \cos(2\omega mt) \right] + \\
 & 2I_0 \left[\sum_{m=0}^{\infty} \sin(\phi_B + \phi^*(T,t))J_{2m+1}(\phi_A) \sin(2m+1)\omega t \right]
 \end{aligned} \tag{7.17}$$

Clearly the above expression compared to equation 7.9 above shows that the calibration procedure followed thus far to simplify the spectrum equations of 7.10 and 7.11 is not reliable. In particular, the method followed to select either the odd or the even frequency components by simply adjusting the dc offset level so that $\cos(\phi_B)=0$ or $\sin(\phi_B)=0$, varies with time. It is proposed that the apparent problem of signal stability can be overcome by somehow adding an extra controlled strain to the fibre in order to compensate the unwanted effect of $\phi^*(T,t)$ by means of a feedback network. The extra phase shift introduced is such that the time varying phase shift is cancelled. This is achieved with a variable dc offset voltage to stretch the fibre appropriately; so that the general form of the modulating signal is now:

$$\phi(t) = \phi_B(T,t) + \phi_B + \phi_A \sin(\omega t) \tag{7.18}$$

Where $\phi_B(T,t)$ is a control signal proportional to the time dependent phase fluctuation, ϕ_B is the original phase bias due to the initial fibre tension and, ϕ_A is amplitude of the sinusoidal shaker signal. It is worth noticing that this feedback method assumes that the spectrum contents of the fluctuation $\Delta\phi^*(T,t)$ is at very low frequency compared to the frequency of modulation ω .

In other words we hope that the unwanted fluctuations act very slowly. This condition has been checked experimentally and found true for every modulation frequency ω greater than 10Hz.

So far it is analysed that the stability of detected signal is critically dependent on the intensity fluctuation due to phase bias variation; we can eliminate, or at least minimise fluctuations of phase shift, with a feedback compensation that permits to stabilise the measurement signal.

A feedback control is thus employed to set the phase bias, ϕ_B , at zero so that only even frequencies and dc components are selected. A correction signal is generated by locking [14][15] the free running interferometric signal to the driver signal. This phase sensitive signal is then feedback in to an Electro-dynamic shaker attached to the fibre section under tension to cancel the effect of the unwanted external modulation effects on the fibre. As a figure of merit, a reduction of more than 60dB is achieved in attenuating the odd frequency component which is found to be better than an acceptable level for the ellipsometric measurements carried out in this work.

Figure 7.3 and figure 7.4 show the detected signal before and after the lock-in feedback system is switched on. When the feedback is on, the error signal is reduced to zero level, as shown in figure 7.4 and the signal becomes stable at the required, 2ω , frequency component.

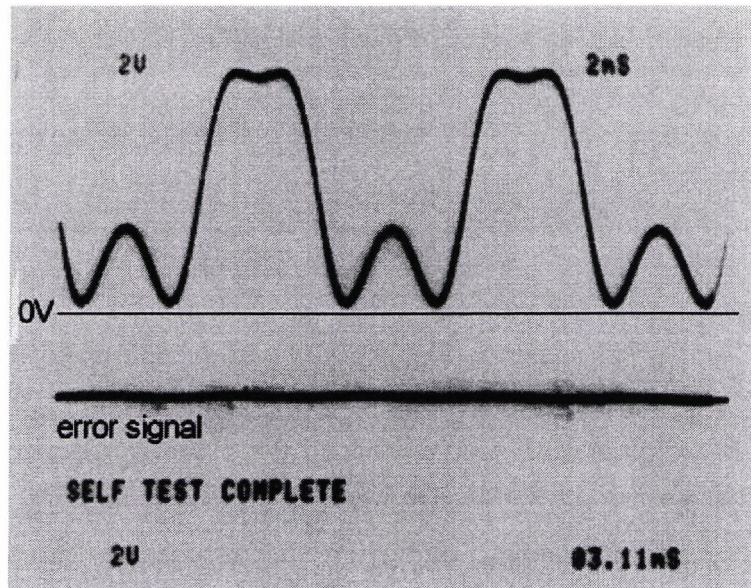


Fig.7.3 A free running interferometric signal and a dc error signal.

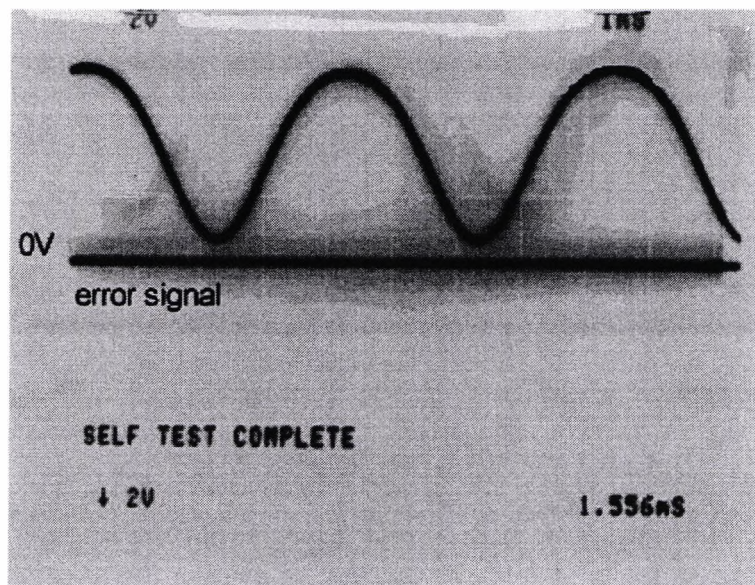


Fig.7.4 A stabilised interferometric signal with a 0V dc error signal.

7.5 Measurement technique

Now we can see how this new arrangement may be used for an ellipsometric measurement of the parameters, ψ and Δ .

A sample under measurement with its plane of incidence aligned to the fibre eigen axis is placed between the fibre and an analyser, which is oriented at 45° to the same plane. After the calibration procedure outlined above, the feedback control is switched on to produce a dc and even frequency harmonics. This signal is then reflected from a sample and analysed by a linear analyser.

In the configuration shown in figure 7.5 the polariser, P_{45° , and the analyser, A_{45° , are oriented with the respective axes at 45° to the eigen axis of the fibre. The main difference compared with the previous configuration is that in this case we must control the orientation of the fibre eigen axis at the output of the fibre with relative to the plane of incidence as explained before.

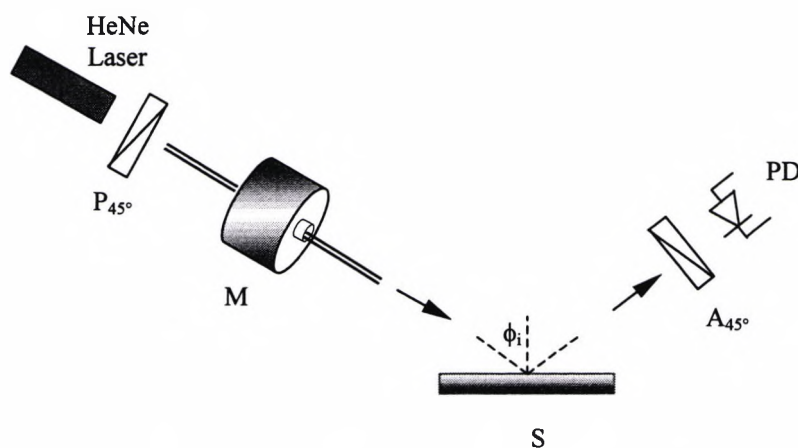


Fig. 7.5 Experimental configuration of a HiBi fibre based Ellipsometer with no quarter wave plate. P_{45° , A_{45° , are polarisers at 45° to the fibre eigen axes, M is a fibre modulator, S is a sample and PD is a photodiode.

In order to calculate the detected signal output we can use the same formulation used for the previous orientation. In this case we have:

$$E_{output} = P_{45} S M A_{45} E_{input} \quad (7.19)$$

Where S is the Jones matrix of the sample where the light is reflected from; it may be expressed as:

$$S = \begin{bmatrix} r_p & 0 \\ 0 & r_s \end{bmatrix} \quad \text{with} \quad r_p = |r_p| e^{i\delta_p} \quad \text{and} \quad r_s = |r_s| e^{i\delta_s} \quad (7.20)$$

$$\begin{aligned} E_{output} &= \begin{bmatrix} 1 & 1 \\ 1 & 1 \end{bmatrix} \begin{bmatrix} r_p & 0 \\ 0 & r_s \end{bmatrix} \begin{bmatrix} e^{i\varphi} & 0 \\ 0 & 1 \end{bmatrix} \begin{bmatrix} 1 & 1 \\ 1 & 1 \end{bmatrix} \frac{E_o}{4\sqrt{2}} e^{i(\omega_o t + \varphi_s)} \\ &= \begin{bmatrix} r_p e^{i\varphi} + r_s \\ r_p e^{i\varphi} + r_s \end{bmatrix} \frac{E_o}{4\sqrt{2}} e^{i(\omega_o t + \varphi_s)} \end{aligned} \quad (7.21)$$

The total intensity can be calculated as:

$$\begin{aligned} I_d &= (E_{output}) \cdot (E_{output})^* \\ &= I_o \{ r_p^2 + r_s^2 + 2 r_p r_s \cos[\varphi(t) + \Delta] \} \\ &= I_o r_s^2 \{ 1 + \tan^2 \psi + 2 \tan \psi \cos[\varphi(t) + \Delta] \} \end{aligned} \quad (7.22)$$

Where $I_o = \frac{E_o}{16}$ and Δ and ψ are the usual ellipsometric parameter defined as $\Delta =$

$\delta_p - \delta_s$ and $\tan \psi = r_p / r_s$.

In the next section, extracting Δ and ψ from equation. 7.22 is described.

7.6 Signal processing

We can extract the ellipsometric information from the two different channels at the frequencies, which are already used to calculate $J_1(\varphi_B)$ and $J_2(\varphi_B)$. In fact if we develop the spectrum of the detected signal, supposing φ_A and φ_B previously set to

make $J_0 = 0$ and $\cos(\phi_A) = 1$ as described before, it is evident that the intensity still possesses all harmonics of ω , including a dc term:

Expanding equation 7.22 and taking the first two dominant frequency components, it can be expressed as:

$$I(t) = I_0 r_s^2 \left[1 + \tan^2(\psi) - 4J_1(\phi_A) \tan(\psi) \cos(\omega t) \sin(\Delta) + 4J_2(\phi_A) \tan(\psi) \cos(\Delta) \sin(2\omega t) \right] \quad (7.23)$$

Variations in the source intensity and in the power loss in the optical system can be rendered inconsequential by normalising the component intensities with respect to the dc intensity.

The normalised intensity for the two lowest frequencies is thus

$$R_\omega = \frac{I_\omega}{I_{dc}} = 2J_1(\phi_A) \sin(2\psi) \sin(\Delta) \quad (7.24)$$

$$R_{2\omega} = \frac{I_{2\omega}}{I_{dc}} = 2J_2(\phi_A) \sin(2\psi) \cos(\Delta) \quad (7.25)$$

The Bessel functions, which characterise the modulation and the detected intensity, can be removed by normalising these ratios with respect to the calibration ratios $R_{\omega cal}$ and $R_{2\omega cal}$ of equations 7.12 and 7.13.

Thus the signals obtained in the two frequency channels are proportional to

$$\frac{R_\omega}{R_{\omega cal}} = \sin(2\psi) \sin(\Delta) \quad (7.26)$$

$$\frac{R_{2\omega}}{R_{2\omega cal}} = \sin(2\psi) \cos(\Delta) \quad (7.27)$$

The information in the two frequency channels provides two independent quantities, in terms of which ellipsometer parameters can be evaluated.

This new signal processing technique does not require the reference arm to make a comparison between the signal before the reflection and after, but by means of a simple initial calibration, Δ and ψ are extracted as a ratio of intensities detected at different frequencies in the same reflected beam.

If these levels of intensities are taken simultaneously, the value of their ratio will vary only in proportion to the sample optical changes independently on light source fluctuations.

The simplicity of this signal processing technique is an advantage in real time fast process monitoring applications where faster time resolved measurements are important. Furthermore, it does not require expensive signal processing hardware or software for its implementation. In the present system the number of bulky optical components used in the configuration is reduced which should be an advantage in terms of system cost, instrument size and in minimising component imperfection introduced systematic errors.

7.7 System performance and calibration

The performance of the two-arm PME is investigated thoroughly with the ellipsometer set in the straight through configuration and both the input polariser and output analyser are set at 45° relative to the fibre axis which is aligned to the plane of incidence at the output. In this case the ellipsometric parameters, ψ and Δ , have numerical values of 45° and 0° respectively. The technique described relies on few critical calibration procedures, these procedures however do not have to be performed often. The azimuthal angle of the input polariser and output analysers relative to the

fibre eigen axes, once aligned is found to be stable for longer than initially anticipated. This can be easily improved with better optical aligning systems. The relative azimuthal angles of the sample, the fibre axes and analyser with the plane of incidence is also kept fairly uniform from sample to sample to within 0.5° limited by the mechanical aligning system. The calibration of the drive voltage required for setting $J_0(\phi_A)$ to zero is done in an open loop system with a straight through arrangement and analyser set at 45° to the fibre axes. If the modulator is turned off, i.e. the modulating signal amplitude, $A=0$, consequently $J_0(\phi_A)=1$. At this point only a dc signal is detected. A , is then increased until the dc level of both the odd and even harmonic frequency components measured at each instant is set to the same value, here the value of $J_0(\phi_A)$ becomes zero. The accuracy with which $J_0(\phi_A)$ can be set to zero is repeatable to within 0.8% accuracy of the drive signal level and does not change significantly with time, in fact a weeks measurement showed a drift of only 1.7%.

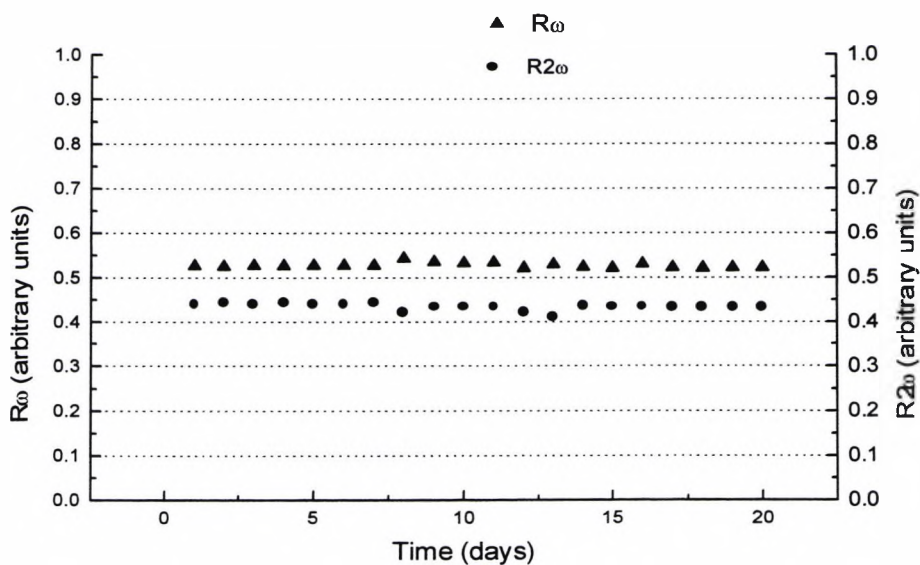


Fig. 7.6 Repeatability of Δ and ψ measurements taken over a period of 20 days.

The above graph in figure 7.6 shows the stability of modulation and repeatability of calibration. The readings of $R_{\omega\text{cal}}$ and $R_{2\omega\text{cal}}$ are taken over a period of twenty days.

From the results in figure 7.6, it is seen that the calibration parameters, $R_{\omega\text{cal}}$ and $R_{2\omega\text{cal}}$ spread around their respective mean values with a standard deviation, σ , of 0.006 and 0.008 respectively. This corresponds to an average error better than 0.5° on ψ and Δ measurements.

7.8 Measurement results

In this section the results obtained with PMSA system on two and three phase systems are presented and discussed.

7.8.1 ψ and Δ measurements on a two phase system

In this section Ellipsometric measurements were carried out on glass and silicon substrates as means of checking the accuracy of the system. The results from the glass of refractive index 1.51 show that more accurate readings are taken at higher angles of incidence, this is in agreement with the fact that the system accuracy is much better for higher reflective samples. In particular, ψ is more sensitive at higher incidence angles due to the higher sensitivity of $\sin(2\psi)$ curve away from higher ψ values. ψ and Δ measurements for silicon sample of refractive index $3.85-j0.018$ at a range of incidence angles is shown below. The smooth line curves are theoretical values and the scatter curves are experimental measurements.

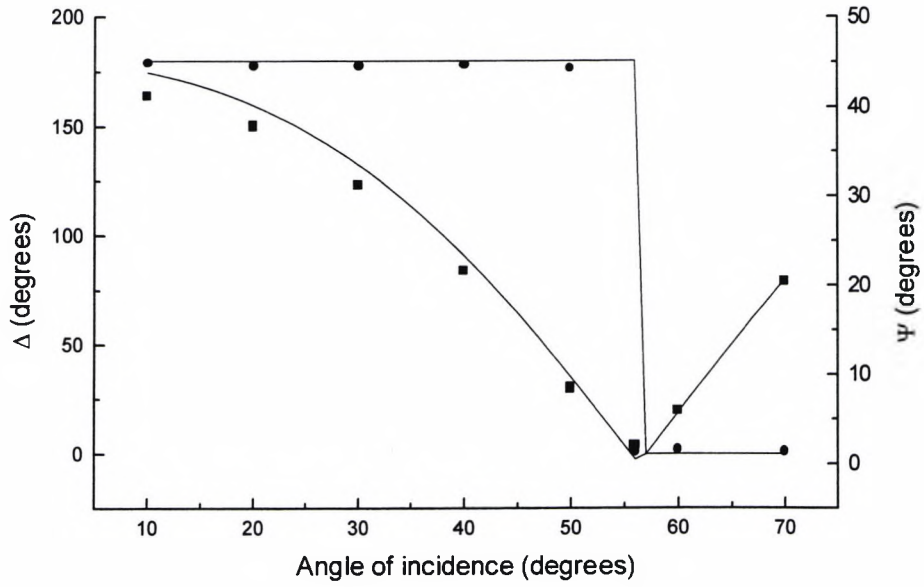


Fig. 7.7 Ellipsometric angles, ψ and Δ as functions of incidence angles for reflection at an air/glass interface. Dotted curves represent measured data. Smooth lines are calculated data.

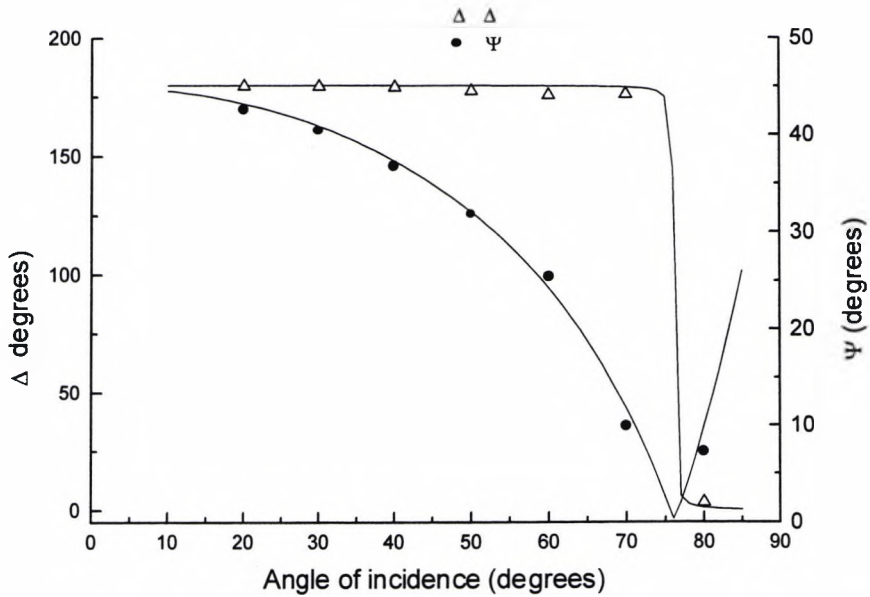


Fig.7.8 Ellipsometric angles, ψ and Δ as functions of incidence angles for reflection at an air/silicon interface. Dotted curves represent measured data. Smooth lines are calculated data.

7.8.2 ψ and Δ measurements on a three phase system

In this section thin film measurements on sol-gel films which were carried out in section 5.1.2.2 in chapter 5 are repeated with the new ellipsometric configuration. Three thin sol-gel films of thickness of around 100nm, 200nm and 400nm provided by Dublin City University with the batch tested earlier on chapter 5 are used in this experiment. Similarly ψ and Δ were measured for each sample and these measured values were compared to values obtained by computation of the inversion process [16]. Numerical inversion is carried out based on the assumption that the ambient refractive index of air is 1 and silicon substrate index of $3.858-j0.018$ and the sol-gel samples has a refractive index of 1.58. The scatter curves in figure 7.9 and 7.10 show measurement results and the smooth curve show calculated ψ and Δ values. The results show that ψ could be measured with an error of 1° to 2° while Δ has an error margin of 5° for the films of thickness 100nm and 400nm. It is interesting to note that the sample of thickness 200nm showed higher error margin as shown in figure 7.9 and 7.10. This is due to the fact that, the particular sample had been exposed to laboratory environment for weeks while the other two were kept in a closed environment. It is to be recalled that the same sample of 200nm thickness has been used for measurement with the PCMCSA ellipsometer earlier, the results of which are given in chapter 5. It is therefore note worthy that the error margins given in this measurement are not the true instrument errors as environmental effects could change the quoted optical characteristics of the sol-gel films on which the measurement comparison is based in this case.

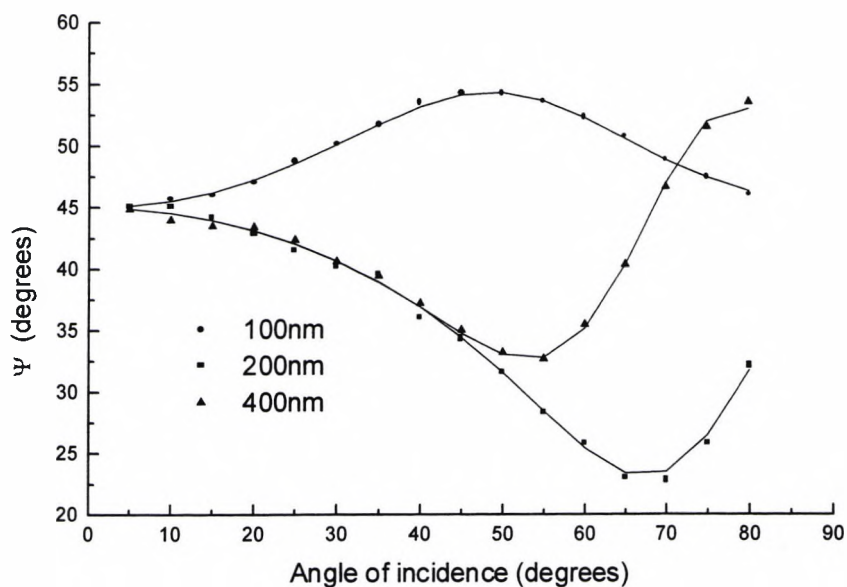


Fig. 7.9 ψ Measurements of three sol-gel films on silica substrate with various thickness at various angles of incidence. Dotted curves represent measured data. Smooth lines are calculated data.

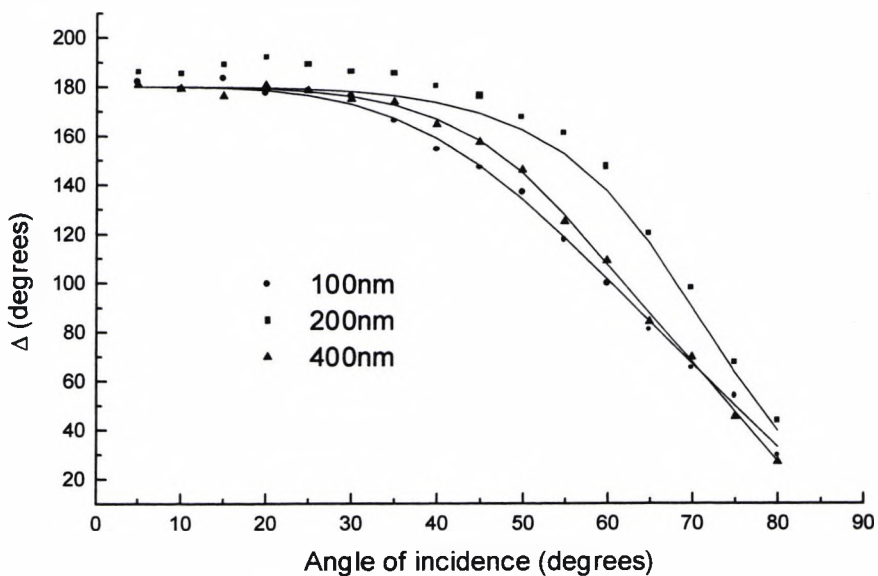


Fig. 7.10 Δ Measurements of three sol-gel films on silica substrate with various thickness at various angles of incidence. Dotted curves represent measured data. Smooth lines are calculated data.

7.9 Summary

A stabilised polarisation modulation ellipsometer has been described. Polarisation modulation is achieved by stretching a HiBi fibre longitudinally. The fibre has both its eigen axes populated equally with a linearly polarised light beam. Environmental and ambient temperature fluctuation effects on the modulated signal have been compensated with a lock-in feedback system. A simple calibration procedure with accuracy of around 0.1% and a feedback compensation with up to 60dB unwanted signal rejection is achieved. Detection and signal processing is done by using a simple electronic circuitry comprising a LPF for the dc signal detection and two individual lock-in amplifiers for the fundamental and second harmonic signal detection. The simplicity of this detection circuitry can be useful for faster real time measurement applications. ψ and Δ measurements of absorbing and non-absorbing samples as well as thin films have been carried out. The results in general showed improvement over the previous PCMCSA arrangement and the overall system simplicity and ease of signal processing is considered superior to the original configuration. In the next chapter a summarised conclusion of the work is given.

References

1. Azzam, R. M. A. and Bashara, N. M. (1977) "*Ellipsometry and polarized light*" (Amsterdam: North Holland)
2. Gerrad, A. and Burch, J. M. (1975) "*Introduction to matrix methods in optics*" (John Wiley & sons Ltd.)
3. Longhurst, R. S., (1973) "*Geometrical and Physical Optics*" (London, Longman.)
4. Hect, E., Zajac, A. (1979) "*Optics*" (Addison-Wesley Publishing company, Inc.)
5. Chitaree R., Weir K., Palmer A. W. and Grattan K. T. V. (1994) "*HiBi fibre polarization modulation scheme for ellipsometric measurements*" Meas. Sci. Technol. 5, p. 1226 - 1232.
6. Grattan, K. T. V and Meggit, B. T. (1995) "*Optical Fibre Sensor Technology*" (Chapman & Hall)
7. Schilling, D. L. and Taub, H. (1986) "*Principles of Communication Systems*" (McGraw- Hill Book Co.)
8. Jaspersen, S. N. and Schnaterley, S. E. (1969) "*An improved method for high reflectivity ellipsometry based on a new polarization modulation technique*" Review of scientific instruments, vol. 40(6), p. 761-767.
9. Gerald, E., Lellison, Jr. and Modine, F. A. (1990) "*Two channel polarization modulation ellipsometer*" Applied optics vol. 29, No. 7, pp 959-974.
10. Jackson, D. A, Priest, R. Dandridge, A. and Tveten, A. B. (1980) "*Elimination of drift in a single mode optical fibre interferometer using piezoelectrically stretched coiled fibre*" Applied Optics, Vol. 19, No. 17, p. 2926-2929.
11. Shadaram, M., Medrano, J., Papert, S. A. and Berry, M. H. (1995) "*Techniques for stabilizing the phase of the reference signals in analog fibre-optic links*" Applied optics, Vol. 34, No. 36, p. 8283-8288.
12. Corke, M. Jones, J. D. C., Kersey, A. D. and Jackson, D. A. (1995) "*All single-mode fibre optic holographic system with active fringe stabilisation*" J. Phys. E: Sci. Instrum. Vol. 18, p. 185-186.
13. Tatam, R. P., Jones, J. D.C., Jackson, D. A. (1986) "*Optical polarisation state control schemes using fibre optics or Bragg cells*" J. Physics E. Sci. Instrum. vol. 19, p. 711-717.

14. Meade, M. L. (1982) "*Advances in Lock-in amplifier*" J. Phys. E: Sci. Instrum. Vol. 15, p. 395-403.
15. Clayton, G. and Newby, B. (1992) "*Operational amplifiers*" (Butterworth-Heinmann Ltd)
16. McCrackin, F. L. and Colson, J. P. (1969) "*Computational Techniques for the Use of the Exact Drude Equations In Reflection Problems*" Symp. Proc. On Ellipsometry in the Measurement of Surfaces and Thin Films

Chapter 8

Conclusions and future work

8.0 Summary of achievements

The main purpose of the work has been to review the present state of ellipsometry and to develop new configurations and measurement techniques for fibre-based ellipsometry in measurement and sensing applications. To this end, fibre based polarisation modulated ellipsometry (FPME) has been thoroughly investigated both theoretically and experimentally. The key benefits of such a system have been outlined and can be summarised as follows [1].

- Small and compact system with a potential for further miniaturisation by replacing polarising optical components with their fibre equivalents.
- All the advantages associated with using optical fibres. These include, light weight, non-contact, non-evasive, immune to electromagnetic interference, low cost etc.

- No mechanically moving parts, which allow faster measurements and greater mechanical stability.

The progress of the work and the specific achievements can be summarised as follows:

- The performance of the FPME has been analysed thoroughly and important steps have been taken to minimise errors introduced in the measurement system through coherent detection of back reflection interference with the main signal.
- The FPME system has been calibrated and applied for ellipsometric measurements. Both bulk optic substrates (absorbing and non-absorbing) as well as thin film measurements have been carried out. The accuracy in measuring the common ellipsometric parameters, Δ and ψ varied slightly on absorbing and anon-absorbing samples. On average accuracy better than 0.5° has been achieved.
- Potential application of the FPME in monitoring dynamic processes on interfaces such as film growth on liquid surfaces or change of the characteristics of the film due to an external perturbation has been demonstrated. The results obtained were encouraging for using the ellipsometer in chemical or biochemical sensing applications, where specifically sensitised films (e.g. sol-gel based films) are used as sensor heads. Although the sol-gel films tested for humidity and heat effects did not suggest any direct use in sensor application, the possibility is there with specifically designed sensor films. It is concluded from these tests that for an effective and economical sensor use of ellipsometer, the sensor heads have to be specifically tailored so as to respond reversibly as refractive index or film thickness changes to external measurands (e.g. chemical sensing).

- The FPME has also been applied to the observation of variation of ψ and Δ of dynamic thin films on water surface. The results clearly showed real time sensing applications based on thin films. Continuous measurements were taken as the film thickness changes. In the case of oil spreading on water surface, it was impossible to measure the thickness accurately. This is due to the oil film breaking up forming a non-uniform layer, furthermore the refractive index of the oil film and the water substrate changes due to mixing of the two layers. The results are nevertheless useful in environmental applications such as water pollution or oil spillage monitoring. For accurate thickness monitoring such as in the manufacture of LB films, film substrate interaction cannot be tolerated.

Having characterised the performance of the FPME and applied for various measurement applications, a thorough study of the sources and magnitudes of systematic errors has been carried out. The motive of such work is to identify the major sources of errors and devise an approach to eliminate or minimise the effect of such errors on the measuring system. To such end, a mathematical model of the system was developed and the main conclusion of the simulations is that:

- The quarter wave plates (QWP) were found to be the major sources of errors both from component imperfection (retardance tolerance) and also azimuthal alignment errors. Thus eliminating the QWP's would improve the accuracy, reduce the cost of the system and leads to a more compact (less number of optical components) system and would be more convenient for further miniaturisation in an all fibre system.

Based on the above results and conclusions, an alternative configuration is proposed. The new configuration does not employ any QWP's. It consists of linear polariser, analyser and HiBi fibre, PMSA configuration. The main advantages of the PMSA system are:

Unlike the previous PCMCSA system, it does not require any use of QWP's and thus accuracy is improved.

It has less number of optical components, providing cheaper and more compact system with potential for an all fibre system. Signal processing of the new PMSA system as described in Chapter 7, uses a simple ratio of intensities obtained from harmonic analysis of the detected signal. The simplicity of such technique is useful for faster data processing offering cheaper and simpler signal processing hardware/software and also high bandwidth measurements.

Ellipsometric measurements have been conducted on bulk samples (absorbing and non-absorbing) with the new Fibre based PMSA system. The familiar ellipsometric parameters, ψ and Δ can be measured with an accuracy of less than 1° . Thin film measurements were also made.

One disadvantage of the PMSA system is the need to calibrate the system for the Bessel coefficients, $J_0(\phi_A)$, $J_1(\phi_A)$ and $J_2(\phi_A)$ (see Chapter 7) and signal fluctuation due to temperature and other unwanted externally modulation effects acting on the fibre. A feedback stabilisation technique has been applied effectively reducing random signal drift problem.

Although the accuracy of measurement on Δ and ψ is less than that of commercial ellipsometers of round 0.01° , it should be remembered that the present system is a

laboratory prototype which did not necessarily use quality components. Further more, the high data rate achieved in this system with such simple signal processing technique allows reduction of statistical errors by averaging the data. The advantage of such a system is to provide a cheaper, more compact (all fibre system) alternative to the traditionally bulky and expensive ellipsometers with a potential for high bandwidth measurements. The time resolution is at less than 0.1s, which is better than 10 times that of most commercial ellipsometers. The accuracy levels reported here, and further improvement of the present system could be achieved with the steps suggested in the next section.

8.1 Future work

- It is concluded that the advantages of the alternative scheme, PMSA described in Chapter 7, outweigh the problem of signal fluctuation due to temperature changes. Although an electronic feedback system has been effectively applied in laboratory configuration for temperature control, alternative temperature control is more practical choice in use for developing the system as an instrument. Careful temperature fluctuation conscious design steps could also be employed, such as making the fibre shorter and placing it in a thermally stable jacket. Further miniaturisation by replacing the polarising prisms and bulk collimating lenses with fibre equivalents would also help in temperature control. A more sound solution would be to use temperature independent birefringent fibres proposed by Wong et al. [2] to reduce thermal drifts.

- Differential configuration method of compensation [3][4] has been demonstrated in the past to simultaneously reduce phase noise and undesired sensitivity to ambient temperature and pressure changes. This was achieved by splicing equal lengths of birefringent fibre after rotating the eigen modes of one half relative to the other by 90° about its axis, thus the fast axis of one section of the fibre is aligned to the slow axis and vice versa. The result is that the polarised light at the output of the fibre has identical propagation times for common mode perturbations such as ambient temperature changes, pressure and light source phase noise, thus not affecting the output polarisation.

This method of compensation can be used for ellipsometric applications. In this configuration, one half of the fibre would be used as a reference section, and the other half would be used for longitudinal modulation. Using this simple differential technique, the electronic feedback technique employed in this work for thermal phase drift compensation could be avoided improving the system accuracy and free of elaborate feedback electronics in an all fibre system.

- The present modulation technique employs low frequency dynamic shaker stretching the fibre longitudinally, for high frequency applications, such as in dynamic film growth monitoring, a high frequency fibre stretcher is required. Thus the dynamic shaker could be replaced by a PZT longitudinal translator, which could provide frequencies in the KHz range.
- A dedicated DSP (digital signal processing) board improves the data acquisition and processing rate of the instrument allowing high bandwidth measurement with

either software on onboard fringe counting possibility for unambiguous phase measurement.

Reference

1. Yoshino, T. and Kurosawa, K. (1984) "*All Fibre Ellipsometry*" Applied Optics (23), p. 1100-1102.
2. Wong, D. and Poole, S. (1993) "*Temperature Independent Birefringent fibres*" International Journal of Optoelectronics (8), p. 179-186.
3. Dakin, J. P. & Wade, C.A., (1984) "*Compensated polarimetric sensor using polarisation-maintaining fibre in a differential configuration*" Electron. Lett. (20), p.51.
4. Turpin, M. Brevignon, M. Le Pesant, J.P., & Gaoditz, O. (1992), "*Intefero-polarimetric fibre optic sensor for both pressure and temperature measurement*" Proceedings of OFS '92, Monterey, p. 362 – 365.

APPENDIX A

Muller and Jones Matrix

Type of device	Muller matrix	Jones matrix
Ideal Linear Polariser at an angle θ	$\begin{bmatrix} 1 & C_2 & S_2 & 0 \\ C_2 & C_2^2 & C_2 S_2 & 0 \\ S_2 & C_2 S_2 & S_2^2 & 0 \\ 0 & 0 & 0 & 0 \end{bmatrix}$	$\begin{bmatrix} C_1^2 & C_1 S_1 \\ C_1 S_1 & S_1^2 \end{bmatrix}$
Quarter wave plate with fast axis at angle θ	$\begin{bmatrix} 1 & 0 & 0 & 0 \\ 0 & C_2^2 & C_2 S_2 & -S_2 \\ 0 & C_2 S_2 & S_2^2 & C_2 \\ 0 & S_2 & -C_2 & 0 \end{bmatrix}$	$\begin{bmatrix} C_1^2 - i S_1^2 & C_1 S_1 (1+i) \\ C_1 S_1 (1+i) & -i C_1^2 + S_1^2 \end{bmatrix}$
Linear Retarder, retardation δ .	$\begin{bmatrix} 1 & 0 & 0 & 0 \\ 0 & 1 & 0 & 0 \\ 0 & 0 & C_\delta & S_\delta \\ 0 & 0 & -S_\delta & C_\delta \end{bmatrix}$	$\begin{bmatrix} e^{i\delta} & 0 \\ 0 & 1 \end{bmatrix}$
Isotropic optical material	$\begin{bmatrix} 1 & -C_{2\psi} & 0 & 0 \\ -C_{2\psi} & 1 & 0 & 0 \\ 0 & 0 & S_{2\psi} C_{2\Delta} & S_{2\psi} S_{2\Delta} \\ 0 & 0 & -S_{2\psi} S_{2\Delta} & S_{2\psi} C_{2\Delta} \end{bmatrix}$	$\begin{bmatrix} r_p & 0 \\ 0 & r_s \end{bmatrix}$

$$C_1 = \cos(\theta)$$

$$S_1 = \sin(\theta)$$

$$C_2 = \cos(2\theta)$$

$$S_2 = \sin(2\theta)$$

$$C_\delta = \cos(\delta)$$

$$S_\delta = \sin(\delta)$$

$$S_{2\psi} = \sin(2\psi)$$

$$S_{2\Delta} = \sin(2\Delta)$$

$$C_\psi = \cos(\psi)$$

$$C_{2\psi} = \cos(2\psi)$$

$$C_\Delta = \cos(\Delta)$$

Where r_p and r_s are the Fresnel reflection coefficients such that the ratio of which gives a relation for ψ and Δ in the form of:

$$\rho = \frac{r_p}{r_s} \equiv \tan \psi \cdot e^{i\Delta} \quad (\text{A.1})$$

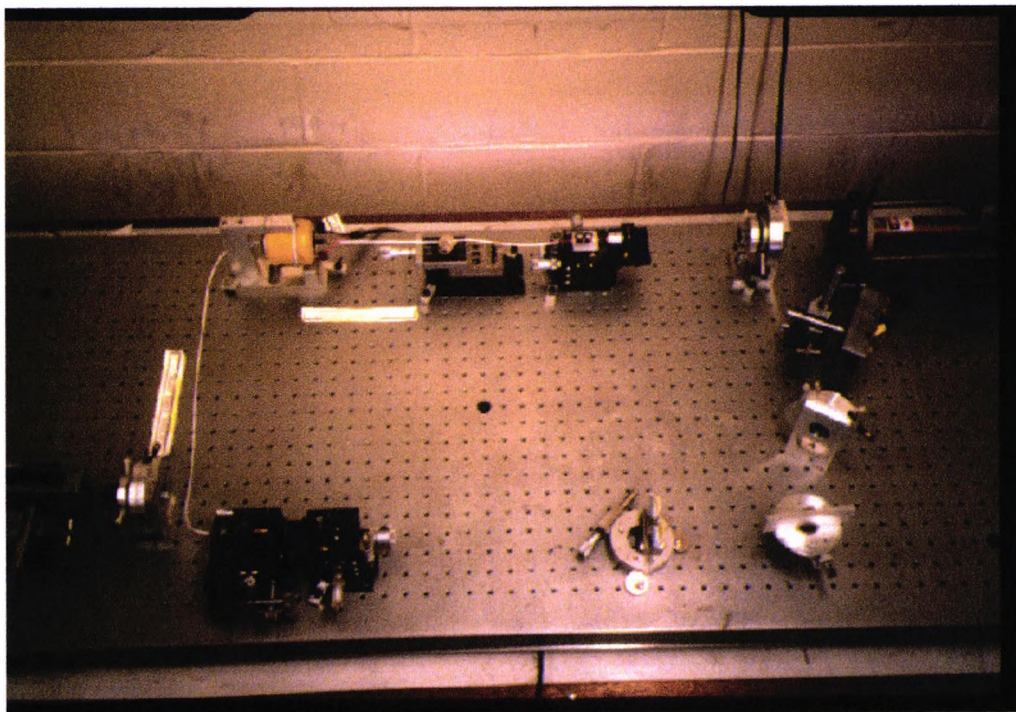
APPENDIX B**Experimental Configuration, Two Channel HiBi fibre Ellipsometry**

Figure B1: Laboratory Set-up, HiBi Fibre Ellipsometry



Figure B2: Laboratory Set-up, Polarised Light into the fibre

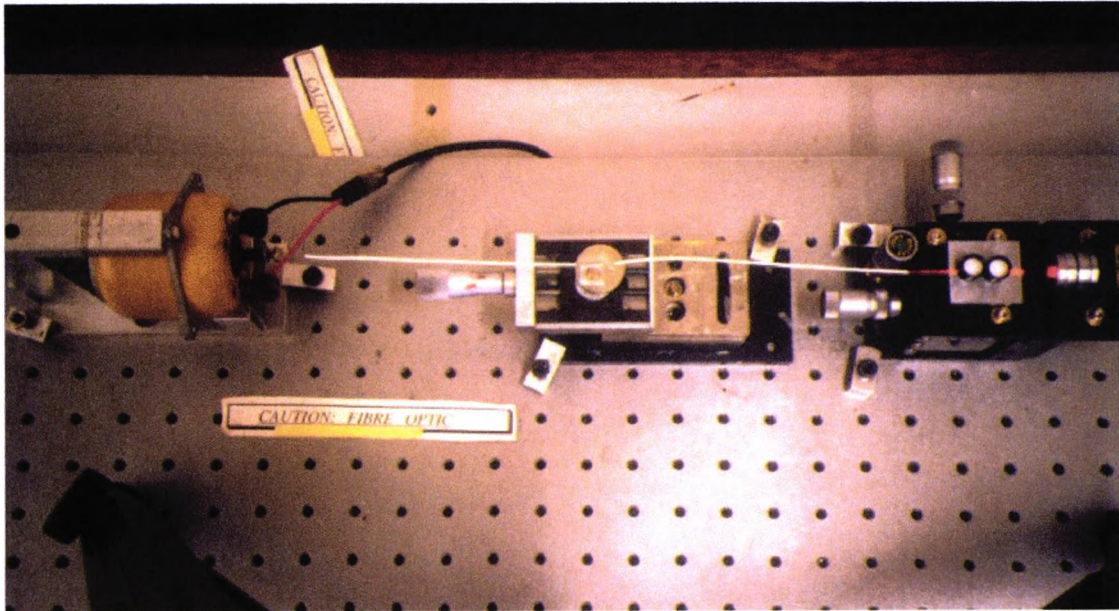


Figure B3: Laboratory Set-up, Longitudinal fibre stretching

List of publications

1. Gebremichael, Y. M., Palmer, A. W. Grattan, K. T. V., and Weir, K. “*Dynamic Oil Film Thickness Measurements using a HiBi Fibre Optic based Polarisation Modulation Ellipsometer*”, Divisional conference of the institute of physics, 16–19 March, 1998, Brighton UK. Proceedings of applied optics, p. 169-174.
2. Gebremichael, Y. M., Tedeschi, G., Palmer, A. W. Grattan, K. T. V., and Weir, K. “*Fibre Optic Ellipsometer in a Thin Film based Sensor System Application*” International Conference on Applications of Photonic Technology. 27-30 July 1998, Ottawa, Canada. Proceedings of SPIE/ICAPT98T279.
3. Gebremichael, Y. M., Palmer, A. W. Grattan, K. T. V., and Weir, K. “*Characterisation of oil films on water surface using fibre optic ellipsometry*” International Conference on Applications of Photonic Technology. 27-30 July 1998, Ottawa, Canada. Proceedings of SPIE/ICAPT98T278.
4. Gebremichael, Y. M., Tedeschi, G., Palmer, A. W. and Grattan, K. T. V. “*HiBi fibre-based birefringence modulated ellipsometry*” International symposium on Lasers, Optoelectronics and Micophotonics. 16-19 September 1998, Beijing, China. Proceedings of SPIE, Vol. 3555 (83).
5. Gebremichael, Y. M., Tedeschi, G., Palmer, A. W. and Grattan, K. T. V. “*Birefringence modulated ellipsometry*” To be submitted for publication in Sensors and Actuators Journal, 2001.